HEAT TRANSFER BY THE CONDENSATION OF STEAM ON A ROTATING DISC

by

HANS ROGER ESPIG

B.Sc.(Eng.), A.C.G.I., S.I.Mech.E.

Beit Scientific Research Fellow

Imperial College,

London, S.W.7.

This work has been carried out in the Mechanical Engineering Department of the Imperial College of Science and Technology on behalf of the Director General Ships, Admiralty.

ABSTRACT

Local heat transfer coefficients were measured experimentally when steam condensed on a cooled disc rotating on a horizontal axis when the surface of the disc was non-isothermal.

A theoretical analysis was made for laminar film condensation on a cooled rotating disc with an isothermal surface in an infinite medium, using the integral form of boundary layer equations, and the theory was extended to include a non-isothermal surface also. From this theoretical analysis an expression was devised which can be used for calculating a theoretical value of the heat transfer coefficient.

Ratios of the experimental to the theoretical values of heat transfer coefficient were studied and were found to be a function of the temperature drop across the film and the rotational speed but not of the radius.

The theoretical solution for an isothermal surface was also compared with the more exact analysis by Sparrow and Gregg using the partial differential form of the boundary layer equations. The two sets of results show good agreement for the conditions under which steam usually condenses.

To gain some knowledge of conditions in the condensate layer, an investigation was made of the flow of a thin film of water on a disc rotating on a vertical axis. This investigation showed that the film was not in plane laminar motion but had waves and vortices visible on its surface. Measurements of the maximum thickness were made for a range of disc speeds and Reynold's Numbers. Due to the waves the maximum film thicknesses were as much as 2.5 times the thickness predicted by a theoretical analysis based on plane laminar flow. These maximum film thicknesses show good agreement with Kirkbrides' measurements on wave flow on a thin film flowing down a vertical tube, and also with results derived from a theoretical formula given by Kapitsa.

Due to the presence of waves, the measured heat transfer coefficients do not agree with those predicted by laminar film theory. An empirical formula derived from the experimental results is suggested for use in calculating heat transfer coefficients.

CONTENTS

		Page No.
1.	Abstract	1
2.	Index to Figures	5
3(a)	Nomenclature	7
(b)	Definitions	9
4.	Introduction	10
5.	Review of Literature	13
6.	The Flow of a Thin Isothermal Liquid Layer on a Horizontal Rotating Disc	
	(a) Introduction	30
	(b) Apparatus	31
	(c) Results	32
	(d) Conclusions	34
7.	Heat Transfer by Condensation to a Rotating Disc	
	(1) General Design Considerations	36
	(2) Layout	38
	(3) Measuring Equipment	50
	(4) Measurements taken during tests and a specimen set of results	51
	(5) Ventilation Equipment	55
	(6) Setting up Apparatus	55
	(7) Test Procedure	56
	(8) Calculation of Local Heat Transfer Coefficient	59

CONTENTS (continued)

		Page No.
(9)	Heat Balances	64
(10)	Estimation of Errors	70
(11)	Comparison of Theoretical Solutions	73
(12)	Analysis of Experimental Results and Conclusions	76
8.	Applications of the Experimental Data	83
9.	Recommendations for further Research Work	84
10.	Appendices	85
11.	Figures	108 - 127
12.	Bibliography	128
13.	Acknowledgements	135

2. INDEX TO FIGURES

Fig. 1 — Transition from laminar to wave flow.

Fig. 2 — Apparatus used to study the flow of a liquid film on a rotating disc.

Fig. 3 — Mean film thickness as a function of Re.

Fig. 4 — Maximum film thickness as a function of Re.

Fig. 5 — Details of rotating disc apparatus.

Fig. 6 — Flow diagram of apparatus.

Fig. 7 — Interior of rotating drum showing distributor and scoops.

Fig. 8 — Copper disc showing plug unit and spray ring.

Fig. 9 — Details of thermocouple circuits.

Fig. 10 — View of 50-way mercury slip ring unit with cover removed.

Fig. 11 — Thermocouple circuit diagrams.

Fig. 12 — Surface temperature distributions.

Fig. 13 — Local heat flux as a function of radius for N = 200, 505 and 900 r.p.m.

Fig. 14 — Local heat transfer coefficient as functions of radius.

Fig. 15 — Variation of $\frac{\dot{q}''}{\dot{q}''_{isoth}}$ with radius.

Fig. 16 — Variation of $\frac{\dot{q}''}{\dot{q}''_{isoth}}$ with film temperature drop at r = 4.0 inches.

Fig. 17 Variation of $\frac{h_m}{h_{isoth}}$ with ΔT for freon from reference 53.

Fig. 18 Graphical integration of local heat flux.

Fig. 19 Typical heat balances.

Fig. 20 Reynold's Number variation with radius for test number 33.

Fig. 21 Heat balances.

Figs. 22 and 23 Condensation on rotating discs. Comparison of "profile" with "exact" solutions.

Fig. 24 Comparison of the radial velocity used in theoretical solutions.

Fig. 25 Theoretical variation of non-dimensional heat flux with radius after a step-wise surface temperature variation.

Fig. 26 Comparison of experimental results with theory.

Fig. 27 Comparison of results for steam with published data.

Fig. 28 $\frac{\dot{q}''}{\dot{q}''_{isoth}}$ as a function of ΔT for all radii between 2.5" and 4.75" at 250, 500 and 900 r.p.m.

Fig. 29 Correlation of heat transfer results for condensation on rotating discs.

3(a) NOMENCLATURE

A	=	amplification factor
a, b, c, d	=	constants in non-isothermal temperature profile
c_p	=	specific heat B.T.U. $lb^{-1}{}^{o}F^{-1}$
f	=	friction factor
g	=	gravitational acceleration $ft.hr^{-2}$
h_m	=	mean heat transfer coefficient B.T.U. $ft^{-2}hr^{-1}{}^{o}F^{-1}$
h_x, h_r	=	local heat transfer coefficients B.T.U. $ft^{-2}hr^{-1}{}^{o}F^{-1}$
j	=	body force $ft.hr^{-2}$
k	=	thermal conductivity B.T.U. $ft^{-1}hr^{-1}{}^{o}F^{-1}$
L	=	latent heat B.T.U. lb^{-1}
N	=	revolution per minute min^{-1}
P	=	pressure $lb.ft^{-2}$
$\dot{q}$	=	heat flow B.T.U. hr^{-1}
$\dot{q}''$	=	heat flux B.T.U. $ft^{-2}hr^{-1}$
r, Θ, z	=	axes
S	=	dynamic surface tension ft^{-2}
ΔT	=	film temperature drop ^{o}F
t_f	=	film temperature = $t_{sat\ vap} - \frac{3}{4}\Delta T$ ^{o}F
t_{sv}	=	saturated vapour temperature ^{o}F
T_w, T_o	=	disc surface temperature ^{o}F
T	=	temperature ^{o}F

NOMENCLATURE (continued)

U	=	radial velocity drop across the film $ft.hr^{-1}$
v	=	local velocity $ft.hr^{-1}$
V	=	tangential velocity drop across the film $ft.hr^{-1}$
v_r	=	local radial velocity $ft.hr^{-1}$
v_θ	=	local tangential velocity $ft.hr^{-1}$
v_z	=	local axial velocity $ft.hr^{-1}$
w_δ	=	axial velocity at film surface $ft.hr^{-1}$
δ	=	film thickness ft.
ρ	=	density $lb.ft^{-3}$
μ	=	viscosity $lb.ft^{-1}hr^{-1}$
ν	=	dynamic viscosity ft^2hr^{-1}
w	=	angular velocity hr^{-1}
x	=	distance travelled by wave ft.
U_m	=	mean mass flow velocity $ft.hr^{-1}$
Γ, C	=	weight rate of flow per unit breadth $lb.ft^{-1}hr^{-1}$
Re	=	Reynold's Number $= \frac{U_m\delta}{\nu} = \frac{4\Gamma}{\mu}$
σ	=	surface tension $lb_f.ft^{-1}$
Pr	=	Prandtl Number
$\dot{W}$, $\dot{Q}$	=	Flow rate $lb.hr^{-1}$

3(b) DEFINITIONS

The following terms are used in this work:

Local heat flux and local heat transfer coefficient are the values of the heat flux and the heat transfer coefficient at a radius 'r' and any angle 'Θ', the values being assumed constant at all positions on the disc surface at a radius 'r' from the centre because the problem is axially symmetrical.

An isothermal surface is defined as a surface over which the temperature is constant, and over a non-isothermal surface the temperature is a function of radius only.

4. INTRODUCTION

It is economically advantageous to be able to load the turbine of a land-based steam turbo-generator as quickly as possible. In an emergency it is also essential to be able to start a ship's turbine in the shortest possible time. The rate at which a steam turbine can be loaded in an accelerated starting procedure is governed by the thermal stresses that occur in the turbine components. Until a few years' ago, the limiting thermal stresses which occurred during quick starting procedures were in the turbine cylinders and nozzle boxes. However, with the use of double and treble walled cylinders and improved designs (1, 1a) more attention is being devoted to the thermal stresses occuring in the rotor. Cracks have been noticed in the high pressure rotors of old turbines which have been started quickly and these have been attributed to fatigue caused by thermal stresses. Eventually the thermal stresses in the rotor will be the main factor limiting the rate at which the turbine can be started, and it is therefore necessary that the turbine designer should be able to compute the thermal stresses occuring in a particular rotor during any starting procedure so that the best procedure may be determined and designs improved to obtain it if necessary.

The calculation of the thermal stresses in a steam turbine rotor when the turbine is started from cold requires a knowledge of the temperature distribution in the turbine rotor at any time during the starting period (1) (2). The temperature distribution at any time can be calculated from a known initial condition if either the variation of the rotor surface temperature with time is known or the steam conditions and the surface heat transfer coefficients are known. The former method requires measurements to be made on existing steam turbines which is virtually impossible and so the latter method of calculation is used.

During the first few minutes of the starting sequence, the rotor surface temperatures are lower than the saturation temperatures of the steam, therefore the steam will condense on the rotor surface. The surface temperature of the rotor rises until it reaches the saturation temperature of the steam after which no further condensation occurs, the rotor surface becoming dry and heat being transferred to the rotor by forced convection. Heat transfer coefficients are available for the transfer of heat from hot gases to colder rotating bodies but no experimental data is available for condensation of steam on rotating bodies.

The surface of a steam turbine rotor can be considered as a series of rotating planes with vertical and horizontal planes as limiting conditions. When steam condenses on these planes, the condensate will be thrown off the horizontal planes in the form of drops whilst the condensate on the vertical planes will drain away radially under the action of centrifugal and corriolis forces. Because of the two different modes by which the condensate is removed from the rotor surface, the measurements of the heat transfer coeffients for the rotor were determined for the two different surfaces. The determination of heat transfer coeffients for steam condensing on a rotating horizontal surface or drum have been measured by Matthews (3), whilst the condensation of steam on a vertical rotating surface or disc is described in this report.

5. REVIEW OF LITERATURE

When steam condenses on a cooled surface, it condenses in the form of drops, a continuous film or a mixture of the two (4). The type of condensation occuring depends on the steam quality, and the condition of the surface on which it condenses. Generally, if promoters and oil are not present in the steam or on the surface, the surface will be wettable and the steam will condense as a continuous film. In the experiments described the optimum conditions were provided for film condensation to occur.

In deriving theoretical relations for heat transfer by condensation, the total thermal resistance is assumed to be in the film of condensate through which the latent heat of condensation is conducted. The flow of the thin film of condensate on the surface is therefore of prime importance in analysing heat transfer by condensation. The flow of the thin film of condensate on a rotating disc is similar to the flow of a thin film of liquid, under the influence of gravity, on a vertical plate or tube if the film thickness is small compared with the tube diameter. It is therefore useful to compare theoretical and experimental analyses for the flow of thin films and condensation on rotating discs, vertical plates and vertical tubes in order to gain a better understanding of the processes involved.

(a) Condensation on Vertical Surfaces

The first attempt to derive theoretical relations for predicting the coefficient of heat transfer between a pure saturated vapour and a colder vertical surface was developed by Nusselt in 1916 (5). Using simple force and heat balances within the condensate film and neglecting the effects of inertia forces, energy convection and shear forces across the surface of the film, he predicted that

$$\frac{h_m}{k}\left[\frac{\nu^2}{g}\right]^{1/3} = 1.47\ Re^{-1/3}$$

Drew (4) showed that for a linear temperature gradient in the film, if the viscosity varied inversely with the temperature, then the viscosity should be evaluated at the film temperature; T_f.

Investigations (6) (7) into the effect of the thermal resistance across the liquid-vapour interface showed that the temperature drop between the pure vapour and the surface temperature of the condensate was less than $0.04^{\circ}F$ at high rates of condensation and atmospheric pressure. Silver (7) predicted that at very high vacuums, the resistance across the interface may be as large as that across the condensate layer. The experiments of Zozulya (8) do not confirm Silver's predictions, the process of heat transfer being determined by the character of the film flow and the heat resistance of the condensate film under high vacuum.

Nusselt's analysis was further improved by Bromley (9) who allowed for the non-linear temperature distribution in the film and obtained correction factors in terms of $\frac{c\Delta T}{L}$ to allow for the effect of heat capacity. An additional refinement by Rosenhow (10) includes the effect of energy convection. The actual temperature profile is determined from an assumed linear profile by using successive approximations. The analysis is shown to agree with Bromley's if the energy convection terms are included.

The effects of slippage and momentum are reported (11, 11a) to be small and lead to small increases in the heat transfer coefficient compared to that calculated from Nusselt's analysis. The effects of the change in physical constants due to the non-isothermal state of the condensate film are also reported as being not appreciable.

The effects of both convection and inertia were included in an analysis by Sparrow and Gregg (12) using similarity transformations to solve the partial differential boundary layer equations for the film. The heat transfer results are in agreement with Rosenhow and the acceleration terms have little effect for Prandtl Numbers greater than 1.0.

The shear forces at the liquid-vapour interface due to the drag of the initially stationary vapour (13) (14) are shown to be negligible for Prandtl Numbers of 1.0. The results show a significant negative velocity gradient at the surface as the result of vapour drag except for small values of $\frac{c\Delta T}{L}$. The effect of the interfacial shear forces are more pronounced in the condensation of liquid metals when they cause a substantial decrease in the heat transfer coefficient.

Koh (15) used the integral method to reduce the solving of the complicated two-phase boundary layer differential equations to simple algebraic equations. The parameter $\left(\frac{\rho_L \mu_L}{\rho_v \mu_v}\right)^{1/2}$ is removed from the problem leaving only the two parameters Pr and $\frac{c\Delta T}{L}$. The solution is in agreement with the exact solutions of the boundary layer equations over a wide range of conditions.

For Reynold's Numbers greater than 1800 to 2100 Kirkbride (16) showed that turbulence could occur in the condensate film and would cause greater heat transfer rates than would be obtained for viscous flow. Colburn (17) derived a relation for condensation with turbulent flow of the condensate layer by analogy to turbulent flow in conduits. Integrating the laminar differential

flow rate equations in the laminar region below Re = 1600, and using the relation for turbulent flow for Re above 1600, he obtained an expression for the mean heat transfer coefficient which showed a satisfactory agreement with experimental results. Grigull (18) combined Nusselt's procedure with Prandtl's analogy between heat transfer and pressure drop in turbulent flow and using Von Karman's seventh power velocity profile obtained heat transfer coefficients for turbulent condensation. Grigull based his transition from laminar to turbulent flow on Re = 1600 from a survey of different workers. Reported transition Reynold's Numbers vary from 280 to 2500. Katateladze also gives a theoretical analysis for condensation with laminar and turbulent flow in the condensate layer. Using a transition Reynold's Number of 400 he successfully correlates a number of experimental results.

Carpenter and Colburn (19) investigated the effect of vapour velocity on condensation inside tubes. The presence of a high frictional force at the liquid-vapour interface lowered the Reynold's Number at which turbulence first occurred in the condensate layer and caused much higher heat transfer coefficients than predicted by Nusselt's theory. A theoretical analysis including the friction of the vapour, the pull of gravity, the momentum change of

the vapour and using a knowledge of heat transfer to fluids in pipes gave a satisfactory agreement with the experimental results.

The effect of non-condensable gases on film condensation has been examined (20) (21). Othmer (22) showed that 1% by volume of air decreased the heat transfer coefficient to about 40% of the heat transfer coefficient without air.

Experimental measurements of both local and mean heat transfer coefficients for film condensation on vertical surfaces with negligible vapour velocity are reported by McAdams (4). The heat transfer coefficients measured vary from between 80% to 170% of the values predicted from Nusselt's equation. These discrepancies are due to the behaviour of the film in that it differs from that assumed in the theoretical analysis. Examination of the film indicates that the condensate flow is often in ripples which reduce the average thickness of the film and account for its low thermal resistance.

Bacon, Fishenden and Saunders, McAdams, Katateladze, Hampson and Ozisek (23) find that Nusselt's theoretical values are about 20% below the actual values measured and suggest

$$\frac{h}{k}\left[\frac{\nu^2}{g}\right]^{1/3} = (1.76 \text{ to } 1.79)\ Re^{-1/3}$$ as the best correlation,

whilst Gebhart (24) suggests

$$\frac{h}{k}\left[\frac{\nu^2}{g}\right]^{1/3} = 1.88\ Re^{-1/3}$$

Shea and Krase (25) measured local heat transfer coefficients for film condensation of air free steam on a vertical plate. The results were 10% greater than Nusselt's value at the top section and increased to over 25% at the bottom.

Zozulya (26) investigating the condensation of steam and glycerine vapour on vertical tubes measured heat transfer coefficients to an accuracy of 5%. Visual examination of the condensate film showed mixed condensation was possible at atmospheric pressure. However, if the pressure was decreased, the viscosity of the condensate increased and only pellicular condensation occurred. Two types of condensate flow were observed, namely, plane laminar flow and wave flow. The length of the plane laminar flow zone depended on heat load and was determined by $Re_x = 30$. The ratio $\frac{h - \text{experimental}_{mean}}{h - \text{Nusselt}_{mean}}$ increased as the pressure increased because the temperature rise due to the increased pressure causes a decrease in the viscosity which shortened the plane laminar flow region and lengthened the wave flow region which had a higher heat transfer coefficient. The author correlated his work and the measurements of other workers by plotting

$$\frac{h_m}{k}\left[\frac{\nu^2}{g}\right]^{1/3} \quad \text{against} \quad Re_x = \frac{4\dot{q}''x}{L}$$

and recommended various design formulae which depend on the film Reynold's Number.

(b) The flow of thin liquid films on vertical surfaces and rotating discs

In 1910, Hopf (27) measured the thickness of films of water and sugar solutions flowing down a slightly inclined trough using a micrometer. In the high velocity experiments ripples occurred making the measurement of the film thickness uncertain. Classen (28), Willey and Cooper (29) and Warden (30) measured the average film thickness for liquid films flowing down vertical tubes. The average thickness was computed from the drainage and the amount of fluid adhering to the tube wall when the flow was stopped.

Cooper, Drew and McAdams (31) reviewed the above data and correlated the results with measurements of friction factors on horizontal tubes in the laminar region using the equation

$$f = \frac{24}{Re} \quad \text{where } f = \frac{2g\delta^3\rho^2}{c^2} \quad \text{and } Re = \frac{4c}{\mu}$$

Nusselt (5) predicted the same result in his derivation of the film thickness

$$\frac{\delta^3\rho^2 g}{\mu^2} = \frac{3Re}{4} = \frac{3U_m\delta 4}{4\nu} \quad \text{where } Re = \frac{4U_m\delta}{\nu}$$

Kirkbride (16) measured the maximum film thickness for oil and water films flowing down a vertical tube using a micrometer. The results showed that for Reynold's Numbers less than 8, a good correlation is obtained with Nusselt's equation. For Reynold's Numbers between 8 and 1800, the measured film thickness was greater than that predicted by Nusselt's theory. In this range, ripples were visible on the film surface.

Friedman and Miller (32) measured the average film thickness and the maximum film velocity for oil, kerosene, Toluene and water films flowing down a vertical tube. The results correlated well with the previous work and with the equation $f = \frac{24}{Re}$. The flow was characterised by the appearance of waves in the liquid films and by much higher interfacial velocities than predicted from Nusselt's equation for Reynold's Numbers between 25 and 1500. Fallah, Hunter and Nash (33) observed similar waves and give Re = 26 as the transition point for wave flow.

The Reynold's Number at which waves appear was determined for a number of fluids by Grimley (34) and he correlated the results by the equation

$$\frac{\sigma^3 \rho}{\mu^4 g} = 0.3\ Re^8$$

When ripples were present in the film Grimley found it difficult to obtain a continuous film of water below Re = 20 due to chanelling. At Re = 400, the disturbances became less violent until at Re = 1000 no disturbances were visible on the film. Measurements of the maximum velocity were higher than predicted by Nusselt's theory and measurements of the velocity profiles showed a marked deviation from the parabolic profile which characterised the laminar streamline flow. For a water film, waves occurred for Reynold's Numbers between 25 and 800 though a photograph of the ripples at a Reynold's Number of 26 shows pronounced waves to be present.

Measurements of the mean film thickness and wave profiles for a film flowing down a vertical tube using a capacitor are reported by Dukler and Bergelin (35). The film became turbulent at a Reynold's Number of 1080. The mean thickness of the film agreed with Nusselt's equation. The wave profiles were regular for the wave laminar flow region but became irregular when turbulence occurred.

In an analysis by Kapitsa (36), the Reynold's Number for transition from laminar flow to wave flow was given as

$$Re_w = 2.43 \left[\frac{\left(\frac{\sigma}{\rho}\right)^3}{j\nu^4} \right]^{\frac{1}{11}}$$

The wave flow was shown to represent the more stable condition and relations were obtained for wave profiles, phase velocity and amplitudes for long waves only. The mean film thickness was predicted to be 7% lower than Nusselt's analysis but this cannot be verified by the experimental data at present available. The theory explained quantitatively the observations of Grimley and Friedman and Miller. The maximum film thickness was given by

$$\delta \left(\frac{g}{\nu^2} \right)^{1/3} = 1.953 \, Re^{1/3}$$

which was in agreement with Kirkbride's measurements over the range of Reynold's Numbers for which Kapitsa's theory was valid. The results for transition from plane-laminar to wave flow compared with Grimley's and Kapitsa's formulae are given in figure 1.

Photographic measurements of the wave velocity and wave length at Reynold's Numbers where waves were just visible were reported by Binnie (37). Brooke Benjamin (38, 39) in a stability analysis for the laminar flow of a thin film down an inclined plane obtained expressions for the velocity and rate of growth of a small disturbance in the form of a long-crested sinusoidal wave travelling in the direction of the flow. Comparison of Brooke Benjamin's theory and Binnie's measurements shows them to be in agreement. The analysis showed the film was unstable for all values of

Reynold's Number and the amplification factor of a small disturbance increased exponentially with Reynold's Number. The theory gave

$$A = \exp\left(0.1737 \frac{\rho^2 x^3 g}{\mu^2} \frac{\mu^4 g}{\sigma^3 \rho} Re^7\right)^{1/3}$$

as the amplification factor of the most unstable wave. The transition from laminar to wave flow was therefore dependent in a complex manner on $\frac{\sigma^3 \rho}{\mu^4 g}$; Re^7 and $\frac{\rho^2 x^3 g}{\mu^2}$. It is interesting to note that Grimley's experimental results correlated with Re^8 and $\frac{\sigma^3 \rho}{\mu^4 g}$ whilst Kapitsa's theory correlates Re^{11} and $\frac{\sigma^3 \rho}{\mu^4 g}$.

The thickness of the liquid film in two phase flow is studied by Charvonia (40). Surface waves were present and influenced the flow in the same way as the roughness in a rough wall pipe.

Whilst waves caused the maximum thickness of a film on a vertical tube to be greater than the film thickness predicted by plane laminar flow theory, the mean film thickness correlated with Nusselt's analysis as shown in figure 3.

Very little experimental work has been carried out on film flows on rotating discs. Hinze and Milborn (41) injected dye into a film of liquid flowing out of a rotating cup atomiser. Measurements of the radial distance between adjacent dye-paths did not agree with

the theoretical values obtained from a radial flow analysis. This was explained as being due to slip between the dye and the liquid layer. No ripples were reported on the film.

Ashwood (42) measured the film thickness of water and various fuels on a rotating disc with capacitors. The mean film thickness was in agreement with Nusselt's theory assuming radial flow. Visual observation showed waves to be present in the liquid film but it was possible that these were due to the method of supplying the liquid to the disc.

Gregory, Stuart and Walker (43) investigated the instability of the boundary layer on a disc rotating in an infinite medium. The theoretical analysis used perturbation techniques on the three-dimensional boundary layer equations. The experimental results showed vortices to be present on the disc surface, the onset of instability occuring at $\frac{r^2 w}{\nu} \simeq 1.80 \times 10^5$ whilst transition to turbulent flow occurred at $\frac{r^2 w}{\nu} = 2.85 \times 10^5$. The vortex flow was due to the strong instability of the laminar boundary layer due to its three dimensionality. As instability is determined by Tollmien's criterion that velocity profiles with a point of inflexion are unstable at infinite Reynold's Number, a similar vortex motion would be expected in a film flowing on a rotating disc.

(c) Heat transfer by condensation to a rotating disc

The shortage of water in certain regions of the world has lead to a renewed interest in Centrifugal Phase Barrier Recompression Distillation as a means of providing fresh water from brackish or salt water at a reasonable cost (44). Details of the still and performance data (45) include overall heat transfer coefficients for condensation on a thin rotating disc cooled by the evaporation of a thin film of water on the other side. An estimate of the thermal conductance of the condensing layer is given as 12,600 B.T.U. $ft^{-2}hr^{-1}F^{-1}$. The rotors of the still show surface markings after operation which indicates that the flow is nearly radial.

A prediction of the performance of the still was made by Bromley (46). The heat transfer coefficient for the condensing layer is determined by a similar approach to Nusselt's analysis for a vertical wall, the acceleration of gravity being replaced by $4\pi^2 rN^2 \sin \phi$. The overall heat transfer coefficients reported by Hickman range from +71% to -32% of Bromley's theoretical calculations, the greatest deviations occuring at either very low flow rates or low temperature differences which magnify the experimental errors.

Further investigations (47, 48, 49) of the condensate film showed that the condensing film does

not form a smooth sheet but tends to break up into rivulets. The possibility of waves being present is mentioned but no details of any observations are given. Heat transfer coefficients are calculated from the fluid flow equations of Hinze and Milborn. (41).

Hickman (50) measured the thickness of an oil film on a rotating disc and gives the following relation between film thickness and rotational speed:

$$\log.N(r.p.m.) = R\left[\frac{1}{\log \delta}\right]$$

Sparrow and Gregg (51) analysed film condensation on a rotating disc situated in a large body of pure saturated vapour using the partial differential form of the boundary layer equations. Transformation of the variables gave a set of simultaneous ordinary differential equations which were solved on an electronic digital computer for a wide range of Prandtl numbers.

The results show that for Pr numbers greater than 1.0 and values of $\frac{c\Delta T}{L}$ less than 0.1, the analysis is in agreement with Bromley's calculation. In a further analysis, the effect of vapour drag is included and shown to be very small (52).

Measurements of the heat transfer coefficients for methanol, ethanol and freon 113 condensing on a cooled rotating disc (53) are below those predicted by Sparrow and Gregg's analysis. Measurements are reported at atmospheric pressures and speeds of up to 2,500 r.p.m.

Injection of dye into the film showed the flow to be nearly radial and photographs showed that ripples were present on the film surface. No measurements were made with steam as drop-wise condensation occurred and highly erratic performances resulted.

As far as the author knows, no measurements have been made of the heat transfer coefficients for steam condensing on a cooled rotating disc or of the type of film flow which exists on the disc. This research was carried out in order to provide more information on these points, and provide design data for thermal stress calculations.

Summary of the main points in the literature

Heat transfer coefficients for steam condensing on a cooled surface under the action of a body force in the direction of flow are usually higher than those predicted by laminar flow theory. The heat transfer coefficient depends mainly on the type of flow present in the condensate film. Examination of the flow of thin films of water on a vertical surface showed that different types of flow occur in the thin film, the type of flow occuring being dependent on the film Reynold's Number.

The following conditions may occur:

1. Plane laminar flow $Re \leqslant 10$
2. Transition from plane laminar flow to wave flow $10 < Re < 25$

3. Wave flow $25 < Re < 1200$

4. Transition from wave flow to turbulent flow $1200 < Re < 1500$

5. Turbulent flow $1500 < Re$.

The film is unstable for all values of Re and therefore conditions 1 and 2 may not occur in practice. In region 1 the heat transfer coefficient will agree with Nusselt's theory, in region 3 it will be 21% to 80% greater than Nusselt's theory and in region 5 it agrees with Grigull's analysis. This has been verified by Zozulya for condensation on a vertical tube. The wide discrepancy between experimental measurements on laminar film condensation is due to the effect of waves and the neglect of region 1 in correlating heat transfer results. The point of transition from plane laminar flow to wave flow is determined by a critical Reynold's Number which is a function of the surface tension. The surface tension is a function of the film temperature and so the overall heat transfer coefficient varies with film temperature and pressure. On a rotating disc, vortex flow may occur simultaneously with the wave flow.

Investigations of the effect of interfacial shear, subcooling of the condensate, etc., are shown to be small compared with the effects of wave flow and the presence of non-condensable gases on the heat transfer coefficient.

6. THE FLOW OF A THIN ISOTHERMAL LIQUID LAYER ON A HORIZONTAL ROTATING DISC

(a) Introduction

Measurements reported in the literature of heat transfer coefficients for steam condensing on a cooled vertical surface are higher than the values predicted from Nusselt's theory. Measurements of the mean film thickness of a thin isothermal film flowing down a vertical surface show a close agreement with Nusselt's theory (figure 3) but measurements of the maximum film thickness are between two and three times that predicted by laminar flow theory. Observation of the films showed that, for Reynold's Numbers between 10 and 1200, waves may exist on the film surface.

The measured heat transfer coefficients and film thicknesses do not agree with those predicted from Nusselt's theory due to the omission from his theory of the factors causing wave motion in the condensate film. Because of this discrepancy, a series of experiments were carried out to determine the deviation, if any, between the actual film thickness and that predicted by laminar film theory and to observe the flow conditions on a thin liquid film on a horizontal rotating disc. A full review of the literature is given on pages 20 to 25.

(b) Apparatus

A diagram of the apparatus is given in figure 2. Water was supplied from a constant head tank to the centre of a horizontal rotating disc by a distributor cup. The cup and the disc were mounted on the spindle of a variable speed electric motor, the motor speed being controlled by varying the resistance in the armature and field circuits. The distributor cup could be adjusted so that a thin uniform liquid film flowed over the disc surface. The disc was balanced in order to minimise effects due to vibration.

The flow of water to the disc was controlled by a valve below the header tank and by the height of the distributor above the disc surface. The water thrown off the rim of the disc was collected in a tray and the water flow rate was measured by collecting the drainage from the tray over a known time and measuring its volume and temperature.

A probe, consisting of a stainless steel needle attached to the cross bar of a vernier, was mounted above the disc to measure the film thickness. The vernier was attached to an insulated arm which allowed the probe to be traversed radially across the disc, the traverse of the probe being limited by the dimensions of the apparatus and the radial distance needed for the film to become uniform after leaving the distributor cup. A dial

gauge mounted on the vernier cross bar was used to measure the needle movement to 0.0001 inches.

The film thickness was measured by lowering the probe until it touched the film surface, this being determined by connecting the probe in series with a 6 V battery and a microammeter to the constant head tank. The needle completed an electrical circuit through the flowing liquid film when it touched the film surface and the microammeter gave a reading of the current flowing. The probe was then lowered until it touched the disc surface which could be detected by the vibration of the needle. The difference in the readings of the dial gauge at these points gave the film thickness.

The rotational speed of the disc was measured by a stroboscope which also enabled the film flow conditions to be studied visually.

The maximum water flow rate fixed the maximum Reynold's Number to 600 and a continuous film could not be obtained for Reynold's Numbers below 10, the film breaking up into channels. Measurements were only taken when the film flow was axially symmetrical which could be seen by studying the film with the stroboscope. The film thickness could be adjusted so that the flow was symmetrical by tilting the distributor cup.

(c) Results

Readings were taken of the water film thickness on the disc at 1.5 and 2.0 inches radius for a series of

rotational speeds and water flow rates. A theory was developed which predicted the relationship between δ, $\dot{Q}$ and N for plane laminar flow on a rotating disc.

The solution is given approximately by:

$$\delta \left[\frac{rw^2}{\nu 2}\right]^{1/3} = 0.909 \, Re^{1/3}$$

and agrees with Nusselt's solution for the flow of a thin film on a vertical surface if g is substituted for rw^2. (See Appendix 1)

Figure 4 shows the results plotted non-dimensionally in the form $\delta \left[\frac{rw^2}{\nu 2}\right]^{1/3}$ and Re. The measurements made by Kirkbride on thin films flowing down vertical tubes are also shown in the same figure together with the theoretical solutions proposed by Nusselt for plane laminar flow and Kapitsa for wave flow.

Visual examination of the film using a stroboscope indicated that the flow was nearly radial for thin films and that four different types of flow occurred in the film.

At very low flow rates it was impossible to obtain a continuous film on the disc surface, the film breaking up into rivulets leaving the rest of the disc surface dry. Increasing the flow rate enabled a plane uniform film of water to be obtained which appeared to be in laminar flow although, even at low speeds, long circumferential waves were sometimes present. A further small increase in the flow rate caused waves to occur on the film surface.

The waves were in the form of circumferential rings of constant radius, the distance between the waves decreasing and the amplitude increasing as the flow rate was increased. At the highest flow rates, helical waves were also visible, superimposed on the circumferential waves. Addition of a detergent to the water, thus lowering the surface tension, increased the Reynold's Number for the onset of wave formation.

Decreasing or increasing the speed caused a corresponding increase or decrease in the film thickness at a constant flow rate.

The circumferential waves were similar to those which occur when a thin film flows down a vertical tube whilst the helical waves appeared to be similar to the vortices described by Gregory, Stuart and Walker (reference 43). Gregory, Stuart and Walker's experiments can be compared to film flow with an infinite film thickness.

(d) Conclusions

Measurements of the film thickness with a probe when waves are present on the film gives the thickness of the film at the top of each wave and will be called the maximum film thickness. The maximum film thickness depends on the radius, speed and flow rate at which the measurement was taken.

Measurements of the maximum film thickness of a film of water flowing on a rotating disc show that the maximum film thickness is greater than the film thickness predicted by theory assuming plane laminar radial flow for Reynold's Numbers between 10 and 600. Waves similar to those visible on a vertical tube are visible on the film surface. These waves are due to instability in the liquid film. The measurements show a similar trend to Kirkbride's measurements on a vertical tube (see figure 4). If the film is thick or the rotational speed is high, helical vortices also become visible in the film.

From the above measurements, the heat transfer coefficients for steam condensing on a cooled rotating disc are expected to be higher than predicted by Nusselt's theory. The deviation between the experimental and theoretical heat transfer coefficients may be higher than for a vertical tube as vortices are also present on the film on a rotational disc. Waves may occur at any Reynold's Number below 1200 above which turbulence occurs. For Reynold's Numbers below 10 the film may break down into rivulets.

7. HEAT TRANSFER BY CONDENSATION TO A ROTATING DISC

1. General design considerations

The objects of the experiments are to obtain heat transfer coefficients for heat transferred by steam condensing on a cold rotating vertical surface under conditions similar to those occuring in a steam turbine when it is started from cold and to provide a formula which can be used to predict the heat transfer coefficient for a range of given conditions. If the conditions in the turbine during starting cannot be reproduced, then the results should be suitable for extrapolation to the conditions occuring in the turbine.

Dimensional analysis (see Appendix 3) indicates that for an isothermal surface in the absence of high vapour velocities and non-condensable gases

$$\frac{hr}{k} = f\left(\frac{c\Delta T}{L} \quad \frac{c\mu}{k} \quad \frac{r^2 w}{\nu}\right)$$

Experiments with thin film on a rotating disc also indicate that the dimensionless group $\frac{\sigma^3\rho}{j\nu^4}$ will be important in determining the Reynold's Number at which ripples may occur. The experiments are concerned with steam only, and therefore the groups $\frac{c\mu}{k}$ and $\frac{\sigma^3\rho}{j\nu^4}$ will be nearly constant over a wide range of conditions. The main variables affecting the heat transfer coefficient will therefore be the film temperature drop ΔT, and the rotational speed w. To investigate the effect of the other two groups it would be necessary to use a range of different vapours.

A theoretical analysis for condensation on a rotating disc (see Appendix 3) indicated that the heat transfer coefficients would be much greater than those on a vertical tube and at high heat fluxes the film temperature drop would be small, therefore the main design considerations for the apparatus were

1. The cooling system should give very high local heat fluxes; it should be easily adjustable and should be flexible enough to give an isothermal or a non-isothermal disc surface.
2. The rotational speed should be variable over as wide a range as possible. The upper limit is determined by the diameter of the disc and the elastic limit of the disc material; the lower limit being fixed as the point at which gravity affects the film flow.
3. The condensate film should be visible in order to determine if the steam is condensing in a continuous film or in drops and if waves are present in film condensation.
4. The range of $h\left(\frac{\nu}{w}\right)^{\frac{1}{2}}/k$, $c\Delta T/L$ and Re should be the same as those found in the turbine during the starting period.
5. The measurements should be as accurate as possible.

When designing the apparatus, it was found to be impossible to satisfy all these requirements with the result that the condensate film is not visible. A separate study was therefore made of the flow of a thin film on a horizontal rotating disc and the results were given in Section 6. The apparatus for measuring heat transfer coefficients for heat transferred by the condensation of steam to a cooled vertical rotating disc is capable of operating under the following conditions:

Rotational speed	100 - 4,000 r.p.m.
Steam pressure	0 - 100 lb/in^{2}guage
Superheat	up to 50^{o}F superheat
Cooling water	0 - 3,000 lb/hr
Steam flow rate	0 - 250 lb/hr

The tests reported were carried out for rotational speeds of up to 2,000 r.p.m. and with dry and saturated steam. A vertical rotating disc was used as it was easier to use mercury slip rings with a vertical disc and the conditions would be closer to those existing in a steam turbine. Above 200 r.p.m. the effect of gravity was negligible.

2. Layout

(a) General description (see figures 5 and 6)

The apparatus is designed to measure the local heat fluxes when steam condenses on a cooled rotating vertical disc. The disc (C) made from high strength, high conductivity chromium-copper alloy is 15" diameter

by 1½" thick. It forms one vertical wall of a stainless steel drum (B) which is fixed to one end of a hollow rotating shaft. Steam can be admitted and condensate removed from inside the drum through the compound tube (A) which fits inside the hollow rotating shaft. The outer face of the disc is cooled by a system of water sprays. The local heat fluxes are calculated from twenty-four measurements of the disc surface temperatures.

(b) Steam supply and control apparatus

Steam can be supplied to the apparatus in a dry and saturated state or superheated to 50°F from a 200 psig, gas fired boiler. The steam pressure is reduced before the steam is supplied to the apparatus. The reducing valve is operated by a diaphragm, the downstream steam pressure being supplied to one side of it and a known constant control pressure to the other side of it. The control pressure is obtained from a 1,500 psig nitrogen cylinder using a spring loaded variable pressure valve to reduce the pressure to the constant control pressure. The steam reducing valve gives an outlet pressure which remains constant to $\pm$ 0.20 psig. The steam from the valve is admitted to the drum through a stationary compound tube (A) and a distributor (see figure 7) which is designed to prevent steam impinging on the disc surface. Stop valves on either side of the reducing valve are used

for quick shut down and for warming up the apparatus by hand.

Steam pressures are measured before the reducing valve, after the reducing valve, in the compound tube and in the drum. All the control apparatus, with the exception of the stop valves can be operated and read from the control panels.

(c) The rotating drum and supporting shaft

The rotating drum (B) is made from high strength stainless steel and has the copper chromium alloy disc (C) as one vertical wall. The drum is fixed to one end of a hollow stainless steel shaft. The shaft runs in spring loaded deep-groove ball bearings which are designed to keep vibration to a minimum and to allow for expansion. The bearings, and the block which holds the stationary compound tube are supported on a base plate which is bolted to a heavy lathe bed. The hollow shaft is driven by a 4 h.p. variable speed 250 volt D.C. electric motor through a lay shaft. A flat nylon belt (L) is used for the drive between the hollow shaft and the lay shaft to reduce vibration and V belts are used to drive the lay shaft from the motor. The motor speed is controlled by two variable resistances in the field circuit, a 250Ω variable resistance being used as a course adjustment and a 150Ω resistance as a fine adjustment. The pulley

ratios between the motor and the lay shaft can be altered to give a wider speed range. The motor speed is measured by a hand tachometer and the rig speed is measured either by a stroboscope or a tachometer attached to the slip ring unit. The bearings supporting the hollow shaft are lubricated and cooled by oil supplied from a constant head reservoir.

The stationary compound tube (A), which passes through the centre of the hollow rotating shaft, is supported at one end by the block (J) attached to the base plate and at the other end by a water cooled tufnol bearing (G). The tufnol bearing has passages to allow the cooling water to flow through it. The gap between the tube and the shaft is sealed at either end by water cooled mechanical seals (H). The central stationary tube (K) supplies steam to the drum. In the outer ring of smaller tubes, two tubes carry condensate and steam from the disc surface, two tubes carry condensate and steam from the other drum surfaces, two tubes carry cooling water to the mechanical seals and two tubes remove cooling water from the mechanical seals. All the tubes are separated over most of their length from the compound tube by air gaps in order to reduce heat losses. The tubes are arranged symmetrically to keep the temperature distribution uniform and reduce distortion and heat transfer to the steam supply.

The cooling water for the mechanical seals flows in the gap between the rotating hollow shaft and the compound tube and helps to keep the bearings cool besides lubricating the tufnol support bearings for the central tube.

(d) Condensate removal

Scoops attached to the compound tube are used to remove condensate from the inside of the drum. The drum walls are relieved so that the condensate from the disc surface is collected in one channel and the condensate from the other surfaces is collected in the other channels. Two scoops are used to remove condensate from each channel. The scoops also enable any non-condensable gases to be removed from inside the drum. The scoops are designed to prevent the condensate splashing back on the disc face.

The two condensate tubes from the disc face are joined into one tube after leaving the compound tube and the steam-condensate mixture passed through separators. The condensate separated can be weighed and the temperature recorded. A similar circuit is used for the condensate-steam mixture from the other drum faces.

The steam from the two separators is then passed through a single tube and a reducing valve to the condenser. The reducing valve is used to control the flow rate of the steam and the drum pressure. The

condensate flow rate from the condenser is measured by a calibrated orifice tank before the condensate is returned to the boiler hot well. The condenser cooling water flow rate is measured by a calibrated venturi meter and the inlet and outlet water temperatures and the condensate outlet temperature can be measured by Mercury in glass thermometers.

(e) Cooling water system (see Figure 8)

The outer surface of the disc is cooled by means of a system of circular sprays. The sprays used were as follows:-

Spray No. 1	1.65" dia.	No. of holes and diameter varied.
Spray No. 2	4½" dia.	29 holes ½" apart, 0.07" dia.
Spray No. 3	6⅞" dia.	42 holes ½" apart, 0.07" dia.

The flow of cooling water through each spray can be controlled independently and the total cooling water flow rate measured by a calibrated venturi meter. The inlet and outlet temperatures of the cooling water were measured by Mercury in glass thermometers.

The cooling water thrown off the disc was collected in a ½" thick steel drum (D) mounted on the lathe bed round the rotating drum. The drum also acted as a safety guard.

(f) Surface temperature measurements

The disc surface temperature distributions are measured on the condensing and cooling water surfaces by ten copper-constantan thermocouples spaced at radii between 1.5 inches and 5.0 inches on each surface as shown in figure 9. Thermocouples are also mounted at 0.5 inch intervals through the disc thickness at 1.5 inches and 5.0 inches radius in order to measure the temperature distribution through the disc at these radii. The two junctions mounted 180° apart on the disc surfaces at 2.25 inches radius were used to check the symmetry of the temperature distribution.

The thermocouples were made from 30 s.w.g. wires double insulated with varnished fibreglass. The junctions were made by welding the two wires together in an inert atmosphere and were approximately 3/64 inch in diameter. The insulated thermocouple wires were mounted in radial slots up to the junction radius and then in slots cut along arcs of circles for at least 0.75 inch before the junction. For the thermocouples at 1.5 and 1.75 inches radius, there was only 0.5 inches available along a circular arc. Heat conduction along the wires should therefore be negligible as they are mounted in an isothermal region near the junction. The junctions were peaned

into small holes drilled into the disc surface at the end of the slots. The holes were drilled so that part of the junction projected slightly above the disc surface. The wires were then cemented into the slots and the slots filled up to the disc surface with Hidux 1033M. The excess Hidux was removed and the top of the thermocouple junction carefully scraped until it was flush with the disc surface. The disc was then polished to a mirror finish.

Junctions that were broken during this operation were replaced before the disc was attached to the stainless steel drum.

The thermocouple wires were attached to a plug unit mounted on a hollow stainless steel shaft attached to the centre of the disc. The shaft was supported by a water lubricated tufnol bearing which acted as a steady bearing for the overhung rotating drum. The plug unit was used to connect and drive the slip ring unit and also to allow easy removal of the slip-ring unit for cleaning.

It was not possible to position every thermocouple head in the disc surface. After the tests had been completed the junctions were examined and any junctions above or below the surface were noted, their depth of immersion in the disc measured and the temperature reading corrected to allow for the junctions being below the surface.

The thermocouples were calibrated in position using a thermostatically controlled oven. The calibration agreed with the data provided by the manufacturers. The thermocouples, slip-ring units and measuring equipment were also tested by measuring the disc surface temperatures with cooling water inside and outside the drum and with steam inside the drum and no-cooling water on the outside at 500 r.p.m. In both cases the thermocouples measured temperatures within $1^{\circ}F$ of the cooling water or steam saturation temperature on the condensing surface. In the second test, the cooling water surface couples were from $2^{\circ}F$ to $3^{\circ}F$ below the saturation temperature of the steam. This was due to the outer surface of the disc being cooled by forced convection.

Before being assembled on the drum, the disc was cleaned with carbon tetrachloride and dilute sodium hydroxide to remove any surface grease. The surfaces were then washed with distilled water and tested for wettability by allowing a jet of steam to impinge on the surfaces. In all cases, a continuous film of liquid covered the disc surface. Care was taken to prevent any further grease from fouling the disc surface and the drum was kept full of water when tests were not being carried out in order to preserve the surface.

(g) Slip ring units (see Figure 10)

Two types of slip ring units were used. A 50-way mercury slip ring unit was used in tests 0 to 47 and a 12-way brush slip ring unit was used in tests 48 to 63.

(i) The 50-way Mercury slip ring unit

This unit was constructed at Imperial College. Figure 10 shows a view of the unit with the top cover removed.

It consists of 50 copper discs arranged to rotate in baths which were filled with mercury. Each disc and bath unit was completely insulated from the other units.

The copper discs were mounted on a stainless steel shaft covered with a tufnol sleeve for insulation. Tufnol spacers were placed between each disc to separate them and act as insulators. A plug unit was attached to the end of the stainless steel shaft. Insulated copper and constantan wires were attached alternately to each disc and laid in slots in the Tufnol sleeve; the other end of the wires being attached to the plug unit. The plug unit served as a drive for the slip ring unit as well as connecting the copper discs to the thermocouples.

The baths were built in two halves. The top half was clamped on the bottom half after the baths had been filled with mercury. The walls of the baths

were made of $\frac{1}{8}$" thick tufnol and the top and bottom sections were $\frac{1}{4}$" thick copper. The top and bottom sections were assembled on three stainless steel rods covered with tufnol sleeves and clamped together by nuts at the ends of the rods.

The top and bottom halves were then held in an insulated split box which was used to clamp the halves together after the bottom half had been filled with mercury. Copper and constantan wires were attached alternately to the copper bottoms of the baths and connected to a plug unit which was connected to the measuring instruments. The wires were arranged so that the copper wires were all in the copper circuit of the thermocouples and the constantan wires were all in the constantan circuit of the thermocouples.

The baths were filled with mercury by means of a hypodermic syringe. The amount of mercury required was determined by continuity measurements between the disc and the bath walls. A gasket of sellotape was used to seal the top and bottom sections of the baths when they were clamped together.

The thermocouple circuit in circuit diagram 2 was used with this slip ring unit. No parasitic e.m.f.s were measurable at speeds of up to 3,000 r.p.m. and after three hours' operation.

The mercury slip ring unit was difficult to operate and in its present form had a very short life at speeds in excess of 900 r.p.m. After one to two hours' operation, the discs would become dirty and no measurements were possible. If the discs were clean or if alcohol was present after cleaning, the contact resistance between the mercury and the copper was very high. This was lowered when the copper amalgamated and it appears to be necessary for complete amalgamation of the copper to have occurred before a low constant contact resistance can be obtained.

Trouble was also experienced with the discs shorting and with mercury being pumped out of the baths necessitating frequent refilling. Above 900 r.p.m. the life of the unit was too short for practical use and the silver silver-graphite brush ring unit proved to be superior.

(ii) Silver, silver-graphite brush slip ring unit

For the tests 48 to 63, a 12-way silver silver-graphite brush slip ring unit built by I.D.M. Electronics was used. The unit was tested up to 3,000 r.p.m. and no stray em.fs could be detected if the circuit shown in circuit diagram 1 was used. If the circuit shown in circuit diagram 2 was used, large thermal em.fs were generated by the unit due to the heating of the brushes. A movable plug unit was constructed to allow eleven

thermocouple circuits to be used in each test, the plug unit having to be adjusted between each test when the apparatus was stationary to use the other eleven circuits. The unit proved more reliable than the mercury unit and only required maintenance after over fifty hours' operation.

3. Measuring equipment

(a) Thermocouple circuits

The thermocouple circuits were designed so that the resistance of each circuit, including the slip ring unit, could be measured during operation by an Avometer. The surface temperatures could either be recorded on a Honeywell-Brown 20 point recorder or measured by hand. All the hand measurements were taken using a Tinsley Potentiometer in conjunction with a Pye Scaleamp Galvanometer. The resistance of the galvanometer was chosen to give maximum sensitivity and the null point measuring technique used to measure the thermal e.m.fs to I microvolt.

(b) Pressures

All pressures were measured by Bourden Gauges. Gauges reading to I lb/in^2 were used for all measurements except for the drum pressure and the pressure in the compound tube where standard test gauges calibrated to 0.5 lb/in^2 were used.

(c) Flow rate

The cooling water flow rates to the disc surface and the condenser were measured by venturi meters. The venturi meters were calibrated before use. The cooling water to the seals and the condensate flow rates were measured by calibrated orifice tanks.

(d) Temperatures

Measurements of all the temperatures except for the disc surface temperatures, were made with mercury in glass thermometers. The thermometers were calibrated to 0.1°C below 50°C and 0.25°C between 50°C and 110°C.

4. Measurements taken during tests and a specimen set of results

The specimen set of results and all calculations given in the text refer to trial no. 33.

(a) Speeds:	Motor	Hand tachometer	r.p.m.	
	Rig	Stroboscope	r.p.m.	
		Fixed tachometer	r.p.m.	200
(b) Pressures:	Steam pressure from boiler		psig	199
	Steam pressure after reducing valve		psig	37
	Steam pressure at distributor		psig	37
	Steam pressure in drum		psig	37

Air supply to reducing valve — psig 58

Barometric pressure — Mercury thermometer

Inches Mercury 29.65

(c) Flow rates: Disc cooling water by

Venturi Inches mercury H_1 = 15.95

Inches mercury H_2 = 6.15

Condenser cooling water by

Venturi Inches water H_3 = 47.3

Inches water H_4 = 34.2

Seal cooling water by

Orifice tank

Inches water H_5 = 37.4

Condensate from condenser by

Orifice tank

Inches water H_6 = 30.8

Condensate from disc face

Weighed

Condensate from other drum faces

Weighed

} Not recorded in this test

(d) Temperatures:

Twenty-four disc temperatures by thermocouples to 1μV. The surface temperatures are in the order of the following radii:

1.5, 1.75, 2.25, 2.75, 3.25, 3.75, 4.25, 4.75, 5.0

Temperature of cooling water surface - °C -

130.4, 115.5, 151, 181.5, 176.3, 183.7, - ,

199.1, 187.5.

Temperature of condensing surface - °C -

256.6, 244, 262.4, 257.1, 258.4, 264.1, 259,

263.5, 264.1

Check temperatures at 2.25" radius:

(1) on water surface = 146.3

(2) on condensing surface = 251.7

Temperatures ½" below condensing surface at 1.5"

radius = 215°C

Temperatures ½" below condensing surface at 5.0"

radius = 232.2°C

Temperatures ½" below cooling water surface at 1.5"

radius = 183.4°C

Temperatures ½" below cooling water surface at 5.0"

radius = 213.7°C

Inlet temperature of lubricating oil; thermometer

0 - 50°C = 28.7°C

Outlet temperature of lubricating oil; thermometer

0 - 110°C = 36°C

Inlet temperature of disc cooling water; thermometer

0 - 50°C = 20.7°C

Outlet temperature of disc cooling water:-

thermometer 0 - 110°C 58.0°C

Inlet temperature of condenser cooling water:-

thermometer 0 - 50°C 20.7°C

Outlet temperature of condenser cooling water:-

thermometer 0 - 110°C 70.0°C

Outlet temperature of seal cooling water:-

thermometer 0 - 110°C 42.0°C

Outlet temperature of water bearing cooling water:-

thermometer 0 - 50°C -

Temperature of condensate from disc face:-

thermometer 0 - 110°C -

Temperature of condensate from other faces of drum:-

thermometer 0 - 110°C -

Temperature of condensate from condenser:-

thermometer 0 - 50°C -

Rig air temperature:-

thermometer 0 - 50°C -

Panel air temperature:-

thermometer 0 - 50°C -

Air temperature at exit from blower:-

thermometer 0 - 50°C -

Connecting box temperature:-

thermometer 0 - 50°C -

Connecting box temperature:-

thermocouple -

(e) Current:

Armature current to motor:-

Ammeter 0 - 25A -

(f) Resistance:

Thermocouple circuits:-

Avometer 0 - 100Ω -

Measurements of room temperature, connecting box temperature, thermocouple circuit resistance etc. have been omitted as they were only used to check other equipment or circuits or did not apply to this test.

5. Ventilation equipment

Due to the open cooling system for the disc, heat and water vapour had to be removed continuously from the room to keep the room temperature and humidity at reasonable level. The air was removed from a chamber around the disc and bearings by a fan and then blown through a condenser before being readmitted to the room.

6. Setting up apparatus

The apparatus is mounted on a lathe bed which was levelled using an accurate clinometer before the apparatus was assembled. During assembly all nuts were tightened with a torque wrench and the eccentricity of the drum components checked after each component was assembled. The eccentricity of the drum and the steady shaft were less than 0.002

inches at the drum periphery and the water bearing between the copper disc and the slip ring unit before testing and 0.004 and 0.003 inches respectively after the final test.

During assembly all parts were cleaned with carbon tetrachloride, alcohol and distilled water and internal parts of the apparatus kept free of oil. The steam pipes were blown through with steam before connecting to the apparatus to remove dirt and grease. After assembly, when the apparatus was not in use, it was filled with water to prevent undue oxidation of the condensing surface. The disc surface was handled as little as possible and rubber gloves used during assembly to prevent oil getting on the disc face.

The apparatus was balanced after assembly and tested up to 3,000 r.p.m. without steam in the drum. The maximum out of balance detectable after balancing was 0.0015" which was only present over a very limited speed range.

7. Test procedure

Before each test, the thermocouple circuits were checked for continuity and the oil level controls for the oil lubricating the bearings were checked. Steam was then admitted to the reducing valve and after confirming that stop valve (T_1) was closed, the reducing valve was pressurised to the test pressure and the steam traps opened.

Cooling water was admitted to the condenser, water bearings, seal circuits and disc cooling water circuits and adjusted to suitable flow rates. The disc cooling water flow rate was adjusted to the minimum rate which would cover the disc, in order to decrease the warming up period.

The motor was started at its slowest speed and the thermocouple circuits checked for continuity. If at least 80% of the circuits were operating correctly, the temperature recorder was switched on and the apparatus warmed up. The apparatus was warmed up admitting steam in short bursts to the drum by hand using stop valve (T_1) until the valve could be completely opened. If the apparatus was warmed through too quickly, rapid expansion of the compound tube occurred and the scoops touched the drum walls. When the valve was completely open, the pressure in the apparatus was allowed to build up to the test pressure, the valve (T_2) being adjusted if and when necessary. The motor speed was then increased to the test speed and the steam traps closed.

The thermocouple circuits were then checked for continuity and if 80% were still operating, measurements were taken by hand of the thermocouple e.m.fs. Readings were then taken of the other measurements (see Section 4). The recording of all the measurements on the apparatus took between 8 and 10 minutes.

Readings were taken continuously until no further change occurred between the readings of the thermo-couple e.m.fs. The final readings were taken after which the conditions were altered for the next test. When less than 80% of the slip rings were operating, or the steam and water supplies fluctuated and steady conditions could not be obtained, the tests were abandoned.

The slip ring unit could usually be repaired by cleaning the discs, refilling the baths, or by changing the mercury. When the brush slip rings units were used, no trouble was experienced due to faulty circuits.

The first series of tests were carried out at about 20 psig drum pressure, for a range of speeds up to 900 r.p.m. at a constant cooling water flow rate. The effect of the film temperature drop was then investigated at one or two specific speeds. The speed range was extended up to 1750 r.p.m. and down to 150 r.p.m. Below 175 r.p.m. the effect of gravity began to be noticeable and the surface temperature varied with angular position. Therefore no tests were carried out below 150 r.p.m. The pressure range covered was from 0 to 55 psig and the cooling water flow rate varied from about 500 to 2,000 lb/hr. The effect of speed becomes less noticeable at higher speeds because h varies as $\sqrt{N}$ and therefore an increase of

300 r.p.m. at 1,500 r.p.m. has a much smaller effect than at 500 r.p.m. The speed would have to be increased four times to double the heat transfer coefficient and therefore it is more practicable to investigate the effect of speed in the lower speed ranges than at higher speeds.

8. Calculation of the local heat transfer coefficient

In the experiments, the surface temperatures on the condensing and cooling water surfaces of the disc for $1.5 < r < 5.0$ inches and the axial temperature distributions through the disc at 1.5 inches and 5.0 inches radius were measured. Graphs as shown in figure 12 were plotted of radial surface temperatures against radius and internal metal temperature against axial distance from the surface and the temperatures at $\frac{1}{4}$" intervals interpolated from these graphs.

A resistance analogue was constructed to represent an axial section of the disc for $1.5 < r < 5.0$ inches using a $\frac{1}{4}$" mesh size and used in conjunction with the Admiralty resistance-analogue computer. The boundary conditions, measured from the temperature distribution graphs, were set up for each test on the analogue computer and the temperatures computed at the network nodal points. Table I shows the network and a set of computer readings (page 62). The temperature at a network point can be calculated from the analogue computer reading using the following formula

$$T(^{o}F) = 90 + \frac{200 \times (\text{analogue reading})}{1000} \quad \ldots (1)$$

The local heat flux at the condensing surface can be calculated from

$$\dot{q}''_L = k\left[\frac{\partial T}{\partial x}\right] \text{ surface } x = o \quad \ldots (2)$$

$\left[\frac{\partial T}{\partial x}\right]_{x = o}$ can be determined from the nodal temperatures either by plotting the temperatures at a constant radius as a function of the distance from the surface and measuring the slope of the graph at the condensing surface or by assuming a smooth curve to pass through the points and calculating the slope numerically using the formula

$$\left[\frac{\partial T}{\partial x}\right]_{x = o} = \frac{11(T_o - T_1) - 7(T_1 - T_2) + 2(T_2 - T_3)}{6L}$$

where T_o is the surface temperature and T_1, T_2 and T_3 are the temperatures at distance L , 2L and 3L from the surface at a constant radius. The formula is derived in Appendix 2. The numerical calculation method was used for all the tests and was checked graphically for some of the tests.

Example at 3.0 inches radius:

T_o = point 180 = 340 analogue units

T_1 = point 120 = 766 analogue units

$(T_o - T_2)$ = 74 analogue units

T_2 = point 121 = 692 analogue units

$(T_1 - T_2)$ = 74 analogue units

T_3 = point 122 = 619 analogue units

$(T_2 - T_3)$ = 73 analogue units

which gives $\left[\frac{\partial T}{\partial x}\right]_{\substack{x = o \\ r = 3.0}}$ = 59.0°F.inch.$^{-1}$

The conductivity 'k', of the chromium copper alloy of which the disc was made was determined by the National Physical Laboratory on our instructions and the value of k, which is also required for equation (2) was given as

k = 164.5 B.T.U. $ft^{-1}hr^{-1}{}^{o}F^{-1}$

The local heat flux $\dot{q}"_L$ is therefore in the example equal to $k\left[\frac{\partial T}{\partial x}\right]_{\substack{x = o \\ r = 3.0}}$

= 164.5 x 59.0 x 12 = 11.63 x 10^4BTU.$ft^{-2}hr^{-1}$

The local heat transfer coefficient $h_L = \frac{\dot{q}"_L}{\Delta T}$ where

ΔT = the difference between the saturation temperature of the steam and the surface temperature at the radius concerned

T_{sat} = 282.9°F

$T_{surface}$ at r = 3.0 inches = 257.8°F

Therefore ΔT = 25.1°F

and the local heat transfer coefficient h_L is

$\frac{11.63 \times 10^4}{25.1}$ = 4,640 BTU.$ft^{-2}hr^{-1}{}^{o}F^{-1}$

The variations of heat transfer coefficient and local heat flux with radius at 200, 505 and 900 r.p.m. are shown in graphs nos. 13 and 14.

TABLE I Analogue network readings for specimen calculations

r = 5.0"		806	741	681	616	550	
r = 4.75"	868	803	739	676	613	550	490
r = 4.50"	863	799	735	672	609	547	487
r = 4.25"	861	796	731	667	604	543	482
r = 4.0"	856	791	725	661	597	535	474
r = 3.75"	852	786	719	653	589	526	466
r = 3.50"	848	779	711	644	577	513	451
r = 3.25"	844	773	762	633	564	496	430
r = 3.0"	840	766	692	619	547	476	407
r = 2.75"	836	758	681	604	527	453	381
r = 2.50"	831	749	667	586	505	425	348
r = 2.25"	821	736	652	567	479	389	305
r = 2.0"	797	720	637	548	452	313	212
r = 1.75"	774	707	625	535	437	313	129
r = 1.5"		710	619	529	450	340	
X =	0.0	0.25"	0.5"	0.75"	1.0"	1.25"	1.50"

Condensing surface

Cooling water surface

Theoretical analyses of the problem (Appendices 3 and 4) show that for a rotating isothermal disc

$$\dot{q}''_{isoth}\left[\frac{2k^3\rho^2 L w^2 \Delta T^3}{3\mu}\right]^{-\frac{1}{4}} = f\left[\frac{c\Delta T}{L}\right]$$

and for a non-isothermal disc $\dot{q}''$ returns to $\dot{q}''_{isoth}$ a short distance radially downstream of the variation in surface temperature and in this case

$$\dot{q}''\left[\frac{2k^3\rho^2 L w^2 \Delta T^3}{3\mu}\right]^{-\frac{1}{4}} = f\left[\frac{c\Delta T}{L}, \quad r\right]$$

The numerical value for $\frac{c\Delta T}{L}$ measured for steam condensing on a rotating disc was found to be less than 0.05 and under this condition $f\left[\frac{c\Delta T}{L}\right] = 1$. The results were therefore plotted non-dimensionally as a function of radius using $\dot{q}''\left[\frac{2k^3\rho^2 L w^2 \Delta T^3}{3\mu}\right]^{-\frac{1}{4}}$ as the non-dimensional heat flux. (See graph no.15).

For trial no. 33 $\dot{q}''_{isoth}$ at r = 3 inches is computed to be 6.93×10^4 BTU.ft^{-2}hr^{-1}, the viscosity being evaluated at the mean film temperature. Therefore $\frac{\dot{q}''}{\dot{q}''_{isoth}}$ is equal to 1.68.

From the graph, $\frac{\dot{q}''}{\dot{q}''_{isoth}}$ soon becomes constant after the temperature change at r = 1.5" as predicted by theory but instead of being equal to 1.0, it is about 60% greater.

In all the tests, $\frac{q''}{q''_{isoth}}$ was found to be independent of radius for all radii above 2.75 inches, the steady value of $\frac{q''}{q''_{isoth}}$ varying from 1.1 to 3.3. (See Figure 16).

9. Heat balances:

(a) Heat balance for copper-chromium disc

The heat transfer coefficients and heat fluxes calculated in the previous section can be checked by a heat balance into the disc. The heat liberated by the steam condensing on the disc surface is conducted into the disc and transferred to the cooling water. If end losses are ignored, the total heat conducted into the disc at the condensing surface is equal to the heat gained by the cooling water.

Another method of calculating the mean heat-transfer coefficient could have been based on the amount of steam condensed on the disc surface. The apparatus was designed to measure this by collecting the condensate by means of the scoops shown in figure 7. However, due to the pressure drop in the condensate-removal tubes, heat transferred to the seal cooling water and the desuper-heating of the steam in the pipes after throttling, the condensate separated out from the steam-condensate mixture by the separators at S in figure 6 did not represent a true measurement of the steam condensed on the disc surface.

Therefore, this method could not be used and the only heat balance made through the disc was between the heat conducted into the disc at the condensing surface and the heat gained by the disc cooling water.

The heat conducted through the disc at the condensing surface is obtained by integrating the local heat flux graphically and is given by

$$\dot{Q}_c = \int_o^R \frac{2\pi \dot{q}'' r}{12} \, dr \qquad \ldots (3)$$

where R is the effective outer limit of the surface area on which condensation can occur. The maximum radius of the condensing surface is 6 inches but temperature measurements are taken only up to r = 5 inches. The true value of R lies between these two radii as heat is still being conducted through the disc to the cooling water at r = 5" but a thick film of water will cover the disc below the scoops at r = 6", reducing the effective radius of the condensing surface below 6 inches.

The integral was evaluated using both R = 5 inches and R = 6 inches; the local heat flux $\dot{q}''_L$ for the area lying between 5 and 6 inches radius used in the latter integral was determined by extrapolating the results obtained for 1.5 to 5.0 inches radius.

Figure 18 shows $\frac{2\pi \dot{q}'' r}{12}$ plotted against radius for trial 33. Graphical integration of this curve

gives :-

$\dot{Q}_{c1}$ = 52,800 BTU.hr^{-1} for R = 5"

$\dot{Q}_{c2}$ = 77,250 BTU.hr^{-1} for R = 6"

The heat transferred to the cooling water is given by

$$\dot{Q}_{cw} = \dot{W}_{cw} \quad C_p \quad (T_1 - T_o)$$

where $\dot{W}_{cw}$ = cooling water flow rate in lb.hr^{-1}

C_p = specific heat at constant pressure BTU.lb^{-1}^{o}F^{-1}

T_1 = outlet temperature of the cooling water (^{o}F)

T_o = inlet temperature of the cooling water (^{o}F)

for trial 33, $\dot{W}_{cw}$ = 1070 lb/hr, and $T_1 - T_o$ = 67.1^{o}F,

$\dot{Q}_{cw}$ = 71,800 BTU/hr.

Summarising for the above results

Heat transferred to cooling water = 71,800 BTU/hr.

Heat conducted through disc up to 5" radius = 52,800 BTU/hr.

Heat conducted through disc up to 6" radius = 77,250 BTU/hr.

Heat is also transferred to the cooling water by conduction through the end of the disc and at high flow rates, the cooling water gains heat by contact with the cylindrical wall of the drum. Heat is lost from the cooling water by conduction to the guard drum wall, convection, evaporation and boiling at

low flow rates. The heat balance should therefore only be used to verify the magnitude of the heat transfer coefficients. At low cooling water flow rates, the end losses will be a minimum and the heat conducted into the disc at the condensing surface is nearly equal to the heat gained by the disc cooling water. Graph sheet 21 shows the heat conducted into the disc at the condensing surface as a function of the heat transferred to the cooling water. The agreement is closest at low cooling water flow rates. The heat balance using R = 6" is also shown on Graph no. 21 and it can be seen that the heat conducted to the cooling water lies between the two limits of R, namely 5 and 6 inches radius. The integral was only evaluated for a few tests at R = 6 inches in order to determine if this was correct.

(b) Condenser heat balance

An estimate of the heat transferred by condensation on the disc surface can be obtained from the condenser heat balance. The figures given here as an example refer to trial no. 33. The cooling water flow rate which is obtained from the calibration curve for the venturi meter shown at L in figure 6 is $\dot{W}_{c2}$ = 1415 lb/hr. The flow rate of condensate from the condenser is $\dot{W}_{c4}$ = 225 lb/hr. from the condensate orifice tank

calibration curve for the orifice tank at K_1 in figure 6. This is also equal to the steam supplied to the apparatus as the leakage losses are small. The measurement of $\dot{W}_{c4}$ is not accurate as bubbles of steam were entrained in the condensate at high pressures causing the orifice tank level to vary considerably.

Suppose the steam supplied to the apparatus is dry and saturated and that, after condensing on the disc surface, the steam-condensate mixture in the scoops consists of $\dot{W}_s$ lb.hr^{-1} dry and saturated steam and $\dot{W}_c$ lb.hr^{-1} condensate. Then the heat conducted through the disc is $\dot{W}_c \times L_D$ where L_D is the latent heat of the steam at the drum pressure.

The steam $\dot{W}_s$ is condensed by transferring heat to the seal cooling water, the condenser cooling water and by convection and conduction losses in the apparatus and the pipework.

The heat transferred to the condenser cooling water is

$$\dot{W}_{c2} \times (T_3 - T_2) = 1415 \times 90.4 = 125,700 \text{ BTU.hr.}^{-1}$$

The condensate leaves the condenser at $T_4{}^{o}F$ = 159^{o}F. Therefore, the heat transferred to the condenser cooling water due to condensing steam

$$= 125,700 - \dot{W}_{c4} (212 - 159)$$

$$= 125,700 - 11,950 = 113,750 \text{ B.T.U.hr}^{-1}$$

assuming the condenser heat losses to be small.

The heat transferred to the seal cooling water $= \dot{W}_{s1}(T_6 - T_5)$ where $\dot{W}_{s1}$ = flow rate of seal cooling water in $lb.hr^{-1}$ measured in the seal cooling water orifice tank at K_2 in figure 6 , and

T_5 = Temperature of seal cooling water leaving apparatus

T_6 = Temperature of seal cooling water entering apparatus

This is found to be 25,000 $B.hr^{-1}$ in the example.

The amount of heat transferred through the drum walls is therefore equal to $\dot{Q}_D$ =

$$\dot{W}_{c4}H - \dot{W}_{s_1}(T_6 - T_5) - \dot{W}_{c2}(T_3 - T_2) - \dot{Q}_L - \dot{W}_{c4}(T_4 - 32)$$

In the example

$\dot{W}_{c4} \times H$	=	264,000
$\dot{W}_{s_1}(T_6 - T_5)$	=	25,000
$\dot{W}_{c2}(T_3 - T_2)$	=	125,700
$\dot{W}_{c4}(T_4 - 32)$	=	28,500

Therefore $\dot{Q}_D$ = 84,800 - $\dot{Q}_L$

Graph sheet 21 shows $\dot{Q}_D$ compared with $\dot{Q}_{c1}$, $\dot{Q}_{c2}$ and the heat to the cooling water.

$\dot{Q}_L$ depends on the convection, conduction and radiation losses from the condenser and rotating drum. The estimation of $\dot{Q}_D$ is dependent on the condensate flow rate which is measured by an orifice tank. The tank level was unsteady during the tests, particularly at high pressures, and so the accuracy of this measurement is less than for the other flow rates. This is apparent in a few trials where the heat losses were found to be negative. A test carried out with no cooling water

supplied to the disc at 504 r.p.m. showed that the heat losses should be very small.

10. Estimation of errors affecting the measurement of the local heat transfer coefficient:

The accuracy to within which the local heat transfer coefficient is measured depends on

(a) Experimental measurement of the disc surface temperatures, the film temperature drop and the conductivity of the disc material.

(b) The assessment of the surface temperature gradient from the disc surface temperatures.

(c) The computation of the heat transfer coefficient from (a) and (b).

The thermocouples used to measure the disc surface temperatures were inspected before and after tests were carried out. Thermocouples not lying in the disc surface were corrected for their depth below the surface or the readings discounted. The other thermocouples were estimated to lie within 0.01 inches of the disc surface. The maximum temperature gradient is about $100^{\circ}F$ per inch and the maximum error in measuring the surface temperature due to positioning of the thermocouples is about $1^{\circ}F$.

The film temperature drop was computed from the saturation temperature of the steam in the vessel and the measurements of the disc surface temperatures. The steam pressure could be measured to within 0.5 psig but was difficult to control to within 1.0 psig. The saturation

temperature can therefore be measured to within $2^{o}F$, the error being greatest at low pressures.

The accuracy of the film temperature measurements was checked by carrying out a test with no cooling water on the disc face. The disc would therefore only be cooled by forced convection and conduction and the reading of the condensing surface thermocouples should be close to the saturation temperature of the steam. The cooling water surface thermocouples should be slightly lower than the condensing surface thermocouples as a small amount of heat will be conducted through the disc. The condensing surface thermocouples measured a temperature approximately $1.5^{o}F$ to $2.0^{o}F$ below the saturation temperature of the steam and the cooling water thermocouples measured a temperature between $2^{o}F$ and $3^{o}F$ below the condensing surface thermocouples. The error between the condensing surface thermocouples and the saturation temperature of the steam is thought to be due to the combined errors in the pressure measurements, thermocouple and slip ring circuits and the small amount of heat conducted through the disc.

The film temperature drop varied from $4^{o}F$ to $50^{o}F$. The results will be most accurate for high film temperature drops. The mean film temperature drop was approximately $18^{o}F$ and the temperature measurements are estimated to be accurate to within 10% for this film temperature drop.

The disc conductivity was measured by the National Physical Laboratory and they estimated that the measurement was accurate to within 5%.

The axial temperature profiles at 1.5 and 5.0 inches radius are not measured to the same accuracy as the surface temperatures as the thermocouples used to measure the axial profiles had to be mounted in the large axial temperature gradient. A trial computation of the condensing surface temperature gradients in which an error was introduced into these axial profiles showed that the affect of the error was small and only affected the value of local heat flux close to 1.5 and 5.0 inches radius. A similar calculation showed that a small error in the surface temperature measurement has little effect on the heat flux calculations.

The condensing surface temperature gradients assessed from the analogue measurements will vary in accuracy according to the axial temperature distribution. In the region between 1.5 and 2.5 inches radius, where the water is sprayed on the disc, the surface temperature varies with radius and the axial temperature distribution is non-linear. The accuracy to within which the gradient has been computed under these conditions is estimated to be 1%. However, over the remainder of the surface, the axial temperature distribution was nearly linear and the surface temperature gradient is estimated to be accurate to within 0.2%. The relaxation technique used

to determine the nodal temperatures also tended to reduce any errors in calculating the local heat flux caused by errors in the surface temperature measurement. It is estimated that $\dot{q}''_L$ was measured to an accuracy within $\pm 6\%$ and the accuracy to within which 'h_L' was determined is estimated to be within $\pm 15\%$ for the tests where the film temperature drop was approximately $20^{\circ}F$.

However, for the tests where the film temperature drop was much less than $20^{\circ}F$, the heat-transfer coefficients were measured with less accuracy. It is estimated that for a film temperature drop of $5^{\circ}F$ the heat transfer coefficients were measured to within an accuracy of 50%.

11. Comparison of various theoretical solutions for calculating heat transfer by condensation to rotating discs with isothermal and non-isothermal surfaces:

(a) Theoretical solution for condensation on a rotating disc having an isothermal surface

Graph sheets 22 & 23 show plots of $\frac{h\left(\frac{\nu^2}{w}\right)^{\frac{1}{3}}}{k}\left(\frac{c\Delta T}{LPr}\right)^{\frac{1}{4}}$ against $\frac{c\Delta T}{h_{fg}}$ for the solution obtained by Sparrow and Gregg by solving the "partial differential" form of the equations expressing the conservation of mass, momentum and energy in the condensate film. On the same graphs are plotted the solution obtained by solving the "Integral" form of the equations and the solution assuming radial flow.

The solution of the "Integral form" of the conservation equations is approximate and the accuracy of the solution depends on assuming the correct velocity and temperature profiles in the film. A comparison of the radial velocity profiles calculated by Sparrow and Gregg with the profiles used in the integral solution is shown in figure 24 and indicates that for thick films, i.e. $\delta\left[\frac{W}{\nu}\right]^{\frac{1}{2}} = 5.0$ the radial velocity profile cannot be represented by a parabolic profile. However, for thin films i.e. $\delta\left[\frac{W}{\nu}\right]^{\frac{1}{2}} = 0.50$, the velocity profiles are very nearly parabolic. Therefore, the two solutions will not agree for thick films, that is for large Prandtl numbers and large values of $\frac{c\Delta T}{L}$.

For steam condensing under normal conditions, L is of the order of 1,000; the Prandtl number is between 1 and 10, and the factor $\frac{c\Delta T}{L}$ is less than 0.1. Under these conditions there is no significant difference between the two solutions based on boundary layer theory and the solution assuming radial flow. It will be seen later that the calculation of the local heat transfer coefficient for heat transfer from steam to a cooled non-isothermal surface can be radically simplified if radial flow approximations can be used. From the above comparison of the three solutions, it is confirmed that radial flow approximations predict the heat transfer coefficient to the same degree of accuracy as the more complex theories based on the boundary layer equations for the condensation of steam.

(b) The theoretical solutions for condensation on a horizontal rotating disc having a non-isothermal surface

Equations 7, 8, 9 and 10 in Appendix 4 are too complex for an analytical solution to be attempted and therefore a standard numerical solution has to be adopted to solve these equations in their present form. However, comparison of the theoretical solutions for condensation on a horizontal rotating disc having an isothermal surface indicates that, for steam, radial flow theory predicts the heat transfer coefficient to a similar degree of accuracy as solutions using the boundary layer equations. For this reason, radial flow theory was used and equations 7, 8, 9 and 10 reduce to the much simpler equations 12, 13, 14 and 15 which can be easily solved for any given surface temperature distribution.

The solution for a step-wise surface temperature profile given in figure 25 and Appendix 5 indicates that the local heat flux approaches the value predicted from isothermal surface theory a very short distance radially downstream of the surface temperature disturbance. The effect of a large error in the surface temperature measurement at 1.5 inches radius is also shown in figure 25 and this indicates that any effects due to the error only affect the solution close to the error

and the solution approaches the isothermal surface theoretical solution a short distance radially downstream of the error. From these analyses, it appears that neglect of the heat flow occuring at radii less than 1.5 inches and any errors in the temperature measurements close to the spray, which were slightly unsteady, will only affect the local heat flux in the proximity of 1.5 inches radius and the heat flux over the remainder of the disc surface should be predicted from isothermal theory.

Figure 26 shows a theoretical calculation of the local heat flux and the local heat transfer coefficient from the measured surface temperature distributions. The theoretical analysis does not agree with the experimental results and this is discussed in more detail in the next section.

12. Analysis of experimental results and conclusions

Some typical experimental surface temperature measurements are shown in figure 12 for tests at 200, 505, and 900 r.p.m. The cooling water was sprayed on the disc by a series of sprays at approximately 1.65 inches radius. After impinging on the disc surface, the water flows radially outwards across the disc surface in a thin film under the action of the centrifugal force.

Due to the high velocity scrubbing action of the water jets at 1.65 inches radius, the cooling water surface temperature is low at this radius and the heat transfer coefficient between the cooled surface and the cooling water is high. The surface temperature then increases with radius due to the film thickness decreasing and the cooling water temperature increasing as it flows across the disc gaining heat from the disc surface. The condensing surface temperature profiles are similar in shape to the cooling water surface temperature profiles but the temperature variations with radius are much smaller and more gentle due to the higher heat transfer coefficient between the steam and the disc surface and the effects of radial heat flow. The saturation temperature of the steam is constant for all practical purposes, the effect of the centrifugal force being negligible.

The variations of the local heat fluxes with radius, calculated from the surface temperature measurements in figure 12 are shown in figure 13. The heat flux rises close to the spray as explained in the last paragraph and then falls as the film temperature drop decreases. The local heat flux increases as the speed increases.

The local heat flux and the film temperature drop at any pressure depend on the speed, the cooling water flow rate and the temperature of the cooling water supplied to the disc. Increasing the speed also

increases the local heat transfer coefficient as can be seen from figure 14. The local heat flux and local heat transfer coefficient rise and then become constant a short distance radially downstream of the variation in the condensing surface temperature. The slight rise near 5.0 inches radius in the local heat flux and local heat transfer coefficient are probably due to the scoops and errors in the axial profile at 5.0 inches radius. Examination of the axial temperature profiles shows that the heat flow is axial except near the sprays and at either end where radial heat flow also occurs.

The laminar flow theories for an isothermal surface given in Appendix 3 and for the non-isothermal surfaces in Appendices 4 and 5 assume the condensate film to be free from waves and predict that the local heat flux should be given by

$$\dot{q}''_{isoth} = \left[\frac{2k^3\rho^2 L w^2 \Delta T^3}{3\mu}\right]^{\frac{1}{4}}$$

for an isothermal surface and that $\frac{\dot{q}''}{\dot{q}''_{isoth}}$ is purely a function of radius for a non-isothermal surface. Therefore, the results should be correlated by plotting $\frac{\dot{q}''}{\dot{q}''_{isoth}}$ against radius if the results obey laminar flow theory. The correlation is shown in figure 15 for the three test results shown in figure 12. The results should vary where the film temperature drop

varies appreciably as in the neighbourhood of the sprays but, according to Appendix 5, $\frac{\dot{q}''}{\dot{q}''_{isoth}}$ should approach 1.0 a short distance radially downstream of the temperature variation. This appears to be so from figure 15 and it also appears that the results are correlated after 3.0 inches radius but are about 1.6 times greater than predicted by the laminar flow theories. However, an examination of the results for the other tests at 4.0 inches radius, where the factor $\frac{\dot{q}''}{\dot{q}''_{isoth}}$ is nearly constant, indicates that $\frac{\dot{q}''}{\dot{q}''_{isoth}}$ is a function of film temperature drop and rotational speed. $\frac{\dot{q}''}{\dot{q}''_{isoth}}$ is shown as a function of the film temperature drop for various speeds in figure 16.

At this point it is useful to examine the other experimental data for condensation on a rotating disc. The only data published in the literature [53] relates to the condensation of methanol, ethanol and freon 113 on a 5" diameter rotating disc. The results are for overall heat transfer coefficients and as such they would not be expected to be correlated to the same empirical relationship as the results for the condensation of steam because the Reynold's Number of the condensate film at the outer radius is low enough for the possibility of plane laminar flow to exist over part of the disc surface. However, examination of the set of results for freon 113 shows that $\frac{\dot{q}''}{\dot{q}''_{isoth}}$ mean

is also possibly a function of film temperature drop and speed. For steam and freon 113, $\frac{\dot{q}''}{\dot{q}''_{isoth}}$ decreases as either the speed or the film temperature drop are increased. (See figures 16, 17 and 27).

If $\frac{\dot{q}''}{\dot{q}''_{isoth}}$ is plotted logarithmically against the film temperature drop for various speeds as shown in figure 27, it can be seen that at any particular speed, $\log \frac{\dot{q}''}{\dot{q}''_{isoth}}$ varies as $\log \Delta T$. The slope of the lines AB on the graph are - 0.6 and therefore $\frac{\dot{q}''}{\dot{q}''_{isoth}} = M\Delta T^{-0.6}$ where M is a function of speed and the fluid properties. The results for freon 113, methanol and ethanol at 200 and 2,000 r.p.m. are also plotted on the graph and it can be seen that they show a similar trend. Not all the results reported in the literature are plotted for clarity.

Figure 28 is a plot of the results from 2.5 inches to 4.5 inches radius and it appears that the ratio of $\frac{\dot{q}''}{\dot{q}''_{isoth}}$ is not a function of radius over this range and depends purely on the film temperature drop and the rotation speed for any particular condensing vapour.

Figure 29 shows the effect of speed on the factor $\frac{\dot{q}''}{\dot{q}''_{isoth}} \times \Delta T^{0.6}$. The results are correlated to within the accuracy of the experiments by the formula

$$\frac{\dot{q}''}{\dot{q}''_{isoth}} = \frac{113}{N^{0.415}\Delta T^{0.6}}$$

from 250 r.p.m. to 2000 r.p.m. Below 200 r.p.m. the effect of gravity was noticeable in the tests and caused the surface temperatures to fluctuate with angular position, and therefore the results below 200 r.p.m. are based on mean surface temperature measurements.

The results for freon 113, ethanol and methanol are also plotted in figure 29 and it can be seen that these results are correlated better by plotting the relation $\frac{\dot{q}''}{\dot{q}''_{isoth}} \Delta T^{0.6}$ against speed than the plot given in the literature. At high speeds, the curves tend to approach the same slope as the curve for steam. This is to be expected as at high speeds the Reynold's Number is large at the disc periphery and the majority of the condensate film should be in wave flow. The range of film temperature drop used in these tests was rather small and it cannot be stated conclusively that these results obey the same relationship of $\frac{\dot{q}''}{\dot{q}''_{isoth}}$ with film temperature drop and speed as does the data for water but only that a similar trend appears to exist.

Examination of the film Reynold's Number for the experiments on condensing steam shows that for all the tests, the film Reynold's Number is of an order of magnitude such that wave flow is almost certain to exist, that is mainly above 30. The variation of the film Reynold's Number with radius is shown in figure 20 for test no. 33. An attempt to correlate the results

with Reynold's Number was not successful and no trend could be distinguished.

Before a real understanding of the processes involved can be attained it would be necessary to increase the range of the experimental results and investigate the effect of the fluid properties. A detailed study of transition from laminar to wave flow and the occurrence of vortex flow would also be necessary. However, for the condensation of steam on a rotating disc, the author recommends the following formula should be used for calculating the heat transfer data where the Reynold's Number of the film is such that wave motion is occuring

$$\frac{\dot{q}''_L}{\dot{q}''_{isoth}} = \frac{h_L}{h_{isoth}} = \frac{113}{N^{0.415}\Delta T^{0.6}} \qquad \ldots (4)$$

In applying the data to a turbine, it would be necessary to determine the film Reynold's Number. This can be determined by integrating the local heat flux as given in Appendix 6. If the film Reynold's Number is above 10 to 20, the above formula (4) should be used. If it is below these figures it is probably advisable to use Nusselt's relationship until further experimental data is available under these conditions.

8. APPLICATION OF THE EXPERIMENTAL DATA FOR HEAT TRANSFER BY THE CONDENSATION OF STEAM TO A ROTATING DISC

The main application of the experimental data will be its use in conjunction with Matthews' (3) results for heat transfer by condensation to a rotating cylinder for calculating temperature-time relations for steam turbine rotors under specified design starting procedures. This will enable designers to predict the thermal stresses in the rotor with more certainty than at present and also allow the starting procedures to be investigated theoretically with a view to determining the optimum procedure for quick starting the turbine from an ambient condition.

However, the data can also be used in improving the design of vapour-compression distillation apparatus and in designing small light heat exchangers capable of operating under conditions where weight is the limiting factor or the effect of gravity is small or non-existent. It may be possible on a future apparatus to artificially induce vortex flow and wave motion with a view to increasing the heat transfer coefficient under conditions where laminar flow might exist.

9. RECOMMENDATIONS FOR FURTHER RESEARCH WORK

(1) Extension of the present work to cover a wider range of film temperature drop, rotational speed and Reynold's Numbers. Confirmation of the published results for freon 113, ethanol and methanol is required and the range of film temperature drop and Reynold's Number should be increased and, if possible, local heat transfer coefficients obtained. The effect of Reynold's Number on laminar flow, wave flow, vortex flow, turbulent flow and the heat transfer coefficient should be studied in order to provide a better understanding of the physical mechanisms involved.

(2) A visual study of thin film flows should be made and a theory developed for predicting wave amplitudes and wave lengths with a view to correlating the results with heat transfer data.

(3) The effects of drop-wise promoters, surface, finish and composition, artificially induced roughness and non-condensable gases on condensation to a rotating disc should be studied.

10. APPENDICES

1. A solution for the flow of a thin film of liquid on a rotating disc.

2. Numerical calculation of the surface temperature gradient from the temperatures recorded at the analogue network points.

3. A solution for condensation on a rotating disc having an isothermal surface.

4. A solution for condensation on a rotating disc having a non-isothermal surface.

5. A solution for condensation on a rotating disc having a stepwise temperature distribution.

6. The film Reynolds Number and effect on flow characteristics.

APPENDIX 1 A SOLUTION FOR THE FLOW OF A THIN FILM OF LIQUID ON A ROTATING DISC

Theoretical Analysis

The problem to be considered is of a thin liquid film of density ρ, and viscosity μ, flowing in a uniform plane film on the surface of a disc rotating in a horizontal plane with an angular velocity w. The flow is assumed to be axially symmetrical, steady and laminar. The shear force between the surface of the film and the atmosphere is assumed to be small so that the velocity profiles can be represented by parabolic arcs with their vertices in the free surface.

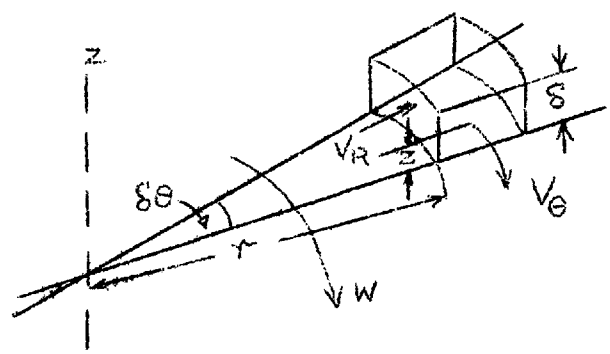

Diagram I

The axes r, θ, z, are as shown in diagram I, the axis z being perpendicular to the disc surface. The axial velocity of the film is denoted by v_r and the tangential velocity of the film by v_θ at a distance

z from the disc surface. The thickness of the film at a distance r from the centre of the disc is δ. The object of the analysis is to determine the relationship between the film thickness δ, the flow rate $\dot{Q}$, the angular velocity w, the radius r and the fluid properties μ and ρ.

(a) Dimensional analysis

For a plane film, δ will be a function of $\dot{Q}$, r, μ, ρ, w.

Dimensional analysis gives

$$\frac{\delta}{r} = f\left(\frac{r^2 w}{\nu}, \frac{\dot{Q}}{r\mu}\right)$$

If ripples are present in the film, the surface tension σ would also be important. In this case

$$\frac{\delta}{r} = f\left(\frac{r^2 w}{\nu}, \frac{\dot{Q}}{r\mu}, \frac{\sigma^3 \rho}{\mu^4 r w^2}\right)$$

or

$$\frac{\delta}{r} = f\left(Re_{rw}, Re_{\delta}, \frac{\sigma^3 \rho}{\mu^4 r w^2}\right)$$

(b) Solution

The equations expressing the conservation of mass and momentum will be set down as the integral form of the boundary layer equations. The flow is assumed to be streamlined laminar flow, and therefore the velocities can be represented by parabolic velocity

profiles. The radial and tangential velocity profiles will be substituted into the equations expressing conservation of mass and momentum and the equations solved for δ in terms of the other variables.

1. <u>The equations expressing the conservation of mass and momentum</u> are

$$\frac{d}{dr}\int_o^\delta \rho\, r\, v_r^2 dz - \int_o^\delta \rho v_\theta^2 dz + \mu\left(\frac{\partial v_r}{\partial z}\right)_{z=0} r = 0 \quad . \ . \ . \ (1)$$

$$\frac{d}{dr}\int_o^\delta \rho\, r^2 v_r v_\theta dz + \mu\left(\frac{\partial v_\theta}{\partial z}\right)_{z=0} r^2 = 0 \quad . \ . \ . \ (2)$$

$$\frac{d}{dr}\int_o^\delta \rho\, r v_r dz = 0 \quad . \ . \ . \ (3)$$

2. <u>The velocity profiles</u> are expressed as

$$v_r = U\left[2\left(\frac{Z}{\delta}\right) - \left(\frac{Z}{\delta}\right)^2\right] \quad . \ . \ . \ (4)$$

$$v_\theta = rw - V\left[2\left(\frac{Z}{\delta}\right) - \left(\frac{Z}{\delta}\right)^2\right] \quad . \ . \ . \ (5)$$

Substitution of (4) and (5) into (1), (2) and (3) gives

$$\frac{2r\rho U\delta}{3} = \text{constant} = B = \frac{\dot{Q}}{2\pi} \quad . \ . \ . \ (6)$$

$$\frac{U}{rw} = \frac{w\delta^2}{2\nu} - \frac{2V\delta^2}{3\nu r} + \frac{4V^2\delta^2}{15\nu r^2} - \frac{4\,r\,\delta}{15\nu r^2 w}\frac{d}{dr}(rU^2\delta) \quad . \ . \ . \ (7)$$

$$\frac{V}{rw} = \frac{\rho\delta}{3\mu r^3 w}\frac{d}{dr}\left[r^3 wU\delta - \frac{4}{5}r^2 UV\delta\right] \quad . \ . \ . \ (8)$$

Equations (6), (7) and (8) can be simplified by eliminating U and rewriting in non-dimensional groups by putting

$$\delta_1 = \frac{\delta}{r}, \quad V = \frac{V_1}{rw} \text{ to give}$$

$$\frac{3}{2}\left(\frac{\dot{Q}}{\pi\mu r}\right)\left(\frac{\nu}{r^2 w}\right)^2 \left(\frac{1}{\delta_1}\right)^3 \left[1 - \frac{2}{5}\left(\frac{\dot{Q}}{\pi\mu r}\right)\delta_1 - \frac{1}{5}\left(\frac{\dot{Q}}{\pi\mu r}\right) r \frac{d\delta_1}{dr}\right]$$

$$= 1 - \frac{4V_1}{3} - \frac{4V_1^2}{15} \qquad \ldots (9)$$

$$V_1 = \left(\frac{\dot{Q}}{\pi\mu r}\right)\left(\frac{\delta_1}{2}\right)\left[1 - \frac{4V_1}{5} - \frac{2}{5r}\frac{dV_1}{dr}\right] \qquad \ldots (10)$$

If $\left(\frac{\dot{Q}}{\pi\mu r}\right)\delta_1$ is considerably less than 1, we can reduce equations (9) and (10) to

$$V_1 = 0$$

$$\frac{3}{2}\left(\frac{\dot{Q}}{\pi\mu r}\right)\left(\frac{\nu}{r^2 w}\right)^2 \left(\frac{1}{\delta_1}\right)^3 = 1$$

or $$\delta_1^3 = \frac{3}{2}\left(\frac{\dot{Q}}{\pi\mu r}\right)\left(\frac{\nu}{r^2 w}\right)^2 \qquad \ldots (11)$$

(c) <u>The range of conditions for which equation (11) is valid</u>

From equation (11), $\frac{r\,d\delta_1}{dr} = \frac{-5\delta_1}{3}$. Substitution of this relation for $r\frac{d\delta_1}{dr}$ in equation (9) reduces the left-hand side to

$$\frac{3}{2}\left(\frac{\dot{Q}}{\pi\mu r}\right)\left(\frac{\nu}{r^2 w}\right)^2 \left(\frac{1}{\delta_1}\right)^3 \left[1 - \frac{1}{15}\left(\frac{\dot{Q}}{\pi\mu r}\right)\delta_1\right]$$

Therefore, if $\left(\frac{\dot{Q}}{\pi\mu r}\right)\delta_1$ is less than 2, $\frac{1}{15}\left(\frac{\dot{Q}}{\pi\mu r}\right)\delta_1$ can be neglected in the solution as the error incurred by neglecting the term at $\delta_1\left(\frac{\dot{Q}}{\pi\mu r}\right) = 2$ is 4% of δ_1. Inspecting the right hand side of equation (9) shows that V_1 can be neglected if V_1 is less than 0.1 and therefore from equation (10) $\left(\frac{\dot{Q}}{\pi\mu r}\right)\frac{\delta_1}{2}$ must be less than 0.1. Therefore, equation (11) is sufficiently accurate for practical purposes if $\delta_1\left(\frac{\dot{Q}}{\pi\mu r}\right)$ is less than 0.2 and therefore from equation (11)

$$\left(\frac{\dot{Q}}{\pi\mu r}\right)^{\frac{4}{3}} \cdot \left(\frac{3}{2}\right)^{\frac{1}{3}} \cdot \left(\frac{\nu}{r^2 w}\right)^{\frac{2}{3}} \ll 0.2$$

The film Reynold's Number $Re = \frac{4U_m\delta}{\nu} = \frac{2\dot{Q}}{\pi\mu r}$ and therefore $\frac{\dot{Q}}{\pi\mu r} = \frac{Re}{2}$

For water at 60°F, it can be shown that

$$\frac{\nu}{r^2 w} = \frac{1.662 \times 10^{-4}}{r_1^2 N_1} \quad \text{where } r_1 = \frac{r}{1''} \text{ and } N_1 = \frac{N}{100}.$$

At N = 100 r.p.m. and r_1 = 1.5 inches, the critical Reynold's Number for equation (11) to be valid is 62.85. In the majority of the tests, N was over 200 r.p.m., r was 1.5 inches or 2.05 inches, and the maximum Reynold's Number was 80. Therefore, the results should be represented by equation (11) if plane laminar flow exists.

APPENDIX 2 NUMERICAL CALCULATION OF THE SURFACE TEMPERATURE GRADIENT FROM THE TEMPERATURES RECORDED AT THE ANALOGUE NETWORK POINTS

Let the temperature of the condensing surface be T_o at a distance r from the centre of the disc. At this same radius let the temperatures be T_1, T_2, T_3, etc. at distance L, 2L, 3L, etc. axially from the condensing surface as in diagram 2.

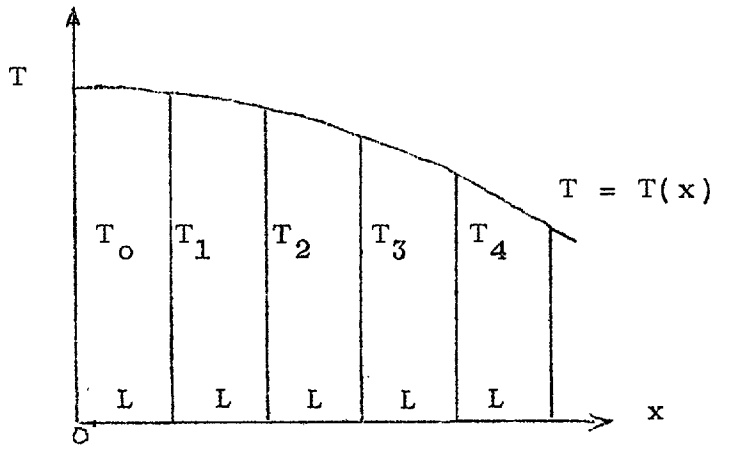

Diagram 2

Let the curve T = T(x) be represented by the series

$$T = a + bx + cx^2 + dx^3 + ex^4 \ldots .$$

Then if four temperature ordinates are used, the surface temperature gradient can be shown to be

$$\left(\frac{\partial T}{\partial x}\right)_o = \frac{11(T_o - T_1) - 7(T_1 - T_2) + 2(T_2 - T_3)}{6L}$$

A more accurate approximation can be obtained by using five temperature ordinates. However, the shape of the curve $T = T(x)$ measured experimentally is such that the accuracy would only be improved by 0.3% over the majority of the disc surface. The formula given above was therefore used to calculate surface temperature gradients.

APPENDIX 3 A SOLUTION FOR CONDENSATION ON A ROTATING DISC HAVING AN ISOTHERMAL SURFACE

(1) Proposed theoretical model

The problem to be considered is of condensation in the form of a plane film on the surface of an infinite disc rotating with an angular velocity w in a large body of pure saturated vapour. The condensate film is assumed to be incompressible and to have a density ρ, viscosity μ, specific heat c and a conductivity k. The film flow is assumed to be axially symmetrical, steady and laminar. The shear forces between the surface of the film and the vapour are assumed to be small so that the velocity profiles can be represented by parabolic arcs with their vertices in the free surface. The axes (r, θ, z) are shown in diagram 3, the axis z being perpendicular to the disc surface.

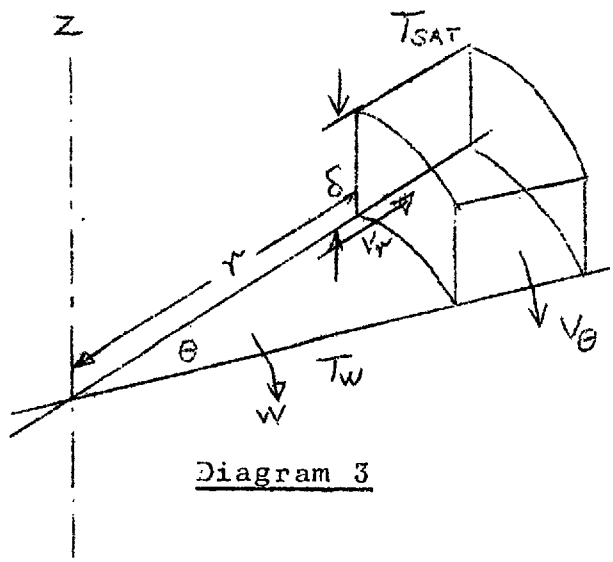

Diagram 3

The axial velocity is denoted by v_r and the tangential velocity by v_θ at a radius r and a distance z from the surface. The thickness of the condensate film at a distance r from the centre of the disc is δ. The disc surface temperature T_w is constant and the saturation temperature of the vapour is T_{sat}.

(2) Required solution

The object of the analysis is to determine the relationship between the heat transfer coefficient h, the angular velocity w, the radius r, the film temperature drop ΔT, the fluid properties c, μ, ρ, and k, and the latent heat of the steam L.

(3) Dimensional analysis

For a plane film condensing on an isothermal surface, the heat transfer coefficient h will be a function of w, ΔT, r, c, μ, ρ, k, L.

Dimensional analysis gives

$$\frac{hr}{k} = f\left[\frac{r^2 w}{\nu}; \quad \frac{c\Delta T}{L}; \quad \frac{c\mu}{k}\right] \qquad \ldots (1)$$

If ripples are present in the film, the effect of the surface tension σ, would be important and the group $\frac{\sigma^3 \rho}{\mu^4 r w^2}$ should be included in (1). For a non-isothermal surface, a function ΔT^1 should be included, where ΔT^1 represents the non-dimensional surface temperature distribution.

Approximate solution

In appendix 1 the thickness of a thin film of liquid on a rotating disc is shown to be given to within 4% by assuming radial flow if the Reynolds Number is below 100. The velocity U is given by

$$\frac{U}{rw} = \frac{w\delta^2}{2\nu} \quad \text{where } v_r = U\left[2\frac{z}{\delta} - \left(\frac{z}{\delta}\right)^2\right] \qquad \ldots (2)$$

The energy equation, neglecting subcooling of the condensate and assuming a linear temperature profile, can be written as

$$\frac{d}{dr}\int_0^{\delta} Lr\rho v_r dz = \frac{k\Delta Tr}{\delta} \qquad \ldots (3)$$

Substituting (2) in (3) gives

$$\delta^4 = 1.5\left[\frac{k\Delta T\nu}{Lw^2}\right]$$

and therefore as $h = \frac{k}{\delta}$ for a linear temperature profile the local heat transfer coefficient is given by the approximate solution

$$\frac{h}{k}\cdot\left(\frac{\nu}{w}\right)^{\frac{1}{2}}\cdot\left(\frac{c\Delta T}{LPr}\right)^{\frac{1}{4}} = 0.904$$

(4) Method of solution

The equations expressing the conservation of mass, momentum, and energy will be set down in the integral form of the boundary layer equations. The radial and tangential velocity profiles represented by parabolas and the temperature profile, assumed to be

linear (see Appendix 4) will be substituted in the boundary layer equations and the equations solved for the condensate film thickness. The heat transfer coefficient will then be obtained from the conduction equation.

(5) Equations expressing the conservation of mass, momentum and energy.

$$\frac{d}{dr}\int_0^\delta r\rho v_r^2 dz - \int_0^\delta \rho v_\theta^2 dz + \mu\left(\frac{\partial v_r}{\partial z}\right)_{z=0} r = 0 \quad \ldots (4)$$

$$\frac{d}{dr}\int_0^\delta r^2 \rho v_r v_\theta dz + \mu\left(\frac{\partial v_r}{\partial z}\right)_{z=0} r = 0 \quad \ldots (5)$$

$$\frac{d}{dr}\int_0^\delta r\rho v_r dz + w_\delta \rho r = 0 \quad \ldots (6)$$

$$\frac{d}{dr}\int_0^\delta c\rho r v_r (T_s - T)dz - w_\delta r\rho L - k\left(\frac{\partial T}{\partial z}\right)_{z=0} r = 0 \quad \ldots (7)$$

Equations (6) and (7) can be combined to form equation (8)

$$\frac{d}{dr}\int_0^\delta c\rho r v_r (T_s - T)dz + \frac{d}{dr}\int_0^\delta Lr\rho v_r dz - k\left(\frac{\partial T}{\partial z}\right)_{z=0} r = 0. \quad (8)$$

(6) Assumed velocity and temperature profiles

$$v_r = U\left[2\left(\frac{z}{\delta}\right) - \left(\frac{z}{\delta}\right)^2\right] \quad \ldots (9)$$

$$v_\theta = rw - V\left[2\left(\frac{z}{\delta}\right) - \left(\frac{z}{\delta}\right)^2\right] \quad \ldots (10)$$

$$T = T_o + \Delta T\left(\frac{z}{\delta}\right) \quad \ldots (11)$$

(7) Solution

Substitution of (9), (10) and (11) into (4), (5) and (8) and solving simultaneously gives U = arw, V = brw, where a and b are constants and δ which is independent of r is given by

$$\delta^4 = \frac{1.5K^2\left(\frac{\nu}{Kw}\right)\left(\frac{3}{5}\frac{Kw}{\nu} + 1\right)\left(\frac{4}{5}\frac{Kw}{\nu} + 1\right)^2}{1 + \frac{4}{15}\frac{Kw}{\nu} + \frac{8}{75}\left(\frac{Kw}{\nu}\right)^2} \qquad \ldots(12)$$

where $K = \frac{k\Delta T}{\rho wL}\frac{1}{\left(\frac{3c\Delta T}{8L} + 1\right)}$ $\qquad \ldots(13)$

(8) Heat transfer coefficients and local heat flux

Fourier's Law gives $\dot{q}'' = k\left(\frac{\partial T}{\partial z}\right)_{z=0} = h\Delta T$ $\qquad \ldots(14)$

From equation (11)

$\left(\frac{\partial T}{\partial z}\right)_0 = \frac{\Delta T}{\delta}$, therefore $\dot{q}'' = \frac{k\Delta T}{\delta}$ and $h = \frac{k}{\delta}$ $\qquad \ldots(15)$

Summary of results

The local heat transfer coefficient $h_L = \frac{k}{\delta}$

The local heat flux $\dot{q}'' = \frac{k\Delta T}{\delta}$

where δ is given by

$$\delta^4 = \frac{1.5K^2\left(\frac{\nu}{Kw}\right)\left(1 + \frac{3Kw}{5\nu}\right)\left(1 + \frac{4Kw}{5\nu}\right)^2}{1 + \frac{4Kw}{15\nu} + \frac{8}{75}\left(\frac{Kw}{\nu}\right)^2}$$

and $K = \frac{k\Delta T}{\rho wL}\left(1 + \frac{3c\Delta T}{8L}\right)^{-1}$

This solution and the approximate solution assuming radial flow given on page 95 are compared with Sparrow and Gregg's solution using the partial differential form of the boundary layer equations in figures 22 and 23.

APPENDIX 4 A SOLUTION FOR CONDENSATION ON A ROTATING DISC HAVING A NON-ISOTHERMAL SURFACE

The theoretical model is similar to the model proposed in Appendix 3 except that the disc surface temperature is a function of the radius.

(1) Method of solution

The equations expressing the conservation of mass, momentum and energy are set out. These are the same as equations 4, 5, 6, 7 and 8 of Appendix 3. The radial and tangential velocity profiles are represented by parabolas, the shape of the profile being assumed independent of radius and variations in the disc surface temperature. The variation of surface temperature with radius has two effects on the condensate film, namely it influences the shape of the temperature profile and the film thickness. The temperature profile is represented by the following equation

$$T = a + bz + cz^2 + dz^3 \qquad \ldots (1)$$

where a, b, c, and d are determined by the boundary conditions and are independent of z.

The velocity and temperature profiles are substituted into the equations representing the conservation of mass, momentum and energy and solved for U, V, and δ, as in Appendix 3. The constants a, b, c, and d in equation (1) being determined separately.

(2) Determination of the constants a, b, c, and d in the temperature profile

The constants a, b, c, and d are determined from the partial differential form of the boundary layer equations expressing the conservation of mass and energy. These equations, for axially symmetrical flow are

$$v_r \frac{\partial T}{\partial r} + v_z \frac{\partial T}{\partial z} = \frac{k}{c\rho}\left[\frac{\partial^2 T}{\partial r^2} + \frac{1}{r}\frac{\partial T}{\partial r} + \frac{\partial^2 T}{\partial z^2}\right] \quad \ldots (2)$$

$$\frac{1}{r}\frac{\partial}{\partial r}(r V_r) + \frac{\partial V_z}{\partial z} = 0 \quad \ldots (3)$$

The boundary conditions for equation (1) can be determined from equations (2) and (3) by differentiating equation (2) at $z = 0$, $z = \delta$.

The boundary conditions are found to be

(a) $z = 0$

$$T = T_o, \left(\frac{\partial^2 T}{\partial z^2}\right)_{z=0} = \frac{-1}{r}\frac{\partial}{\partial r}\left(\frac{r\,dTw}{dr}\right)$$

$$\left(\frac{\partial^3 T}{\partial z^3}\right)_{z=0} = \frac{c\rho}{k}\left(\frac{\partial v_r}{\partial z}\right)_{z=0} \cdot \frac{dTw}{dr} - \left(\frac{\partial^3 T}{\partial z \partial r^2}\right)_{z=0} - \frac{1}{r}\left(\frac{\partial^2 T}{\partial z \partial r}\right)_{z=0}$$

(b) $z = \delta$

$$T = T_s \quad \ldots (4)$$

The constants a, b, c, and d can be determined by differentiating equation (1) and substituting the boundary conditions given in (4). The temperature profile for a non-isothermal surface is then seen to be given by

$$T = T_o + \left[\frac{\Delta T}{\delta} + \frac{\delta}{2r}\frac{d}{dr}\left(r\frac{dTw}{dr}\right) - \frac{\delta^2 c\rho}{6k}\frac{2U}{\delta}\frac{dTw}{dr} + \frac{\delta^2}{6r}\frac{d}{dr}\left(r\frac{db}{dr}\right)\right] z - \frac{1}{2r}\frac{d}{dr}\left(r\frac{dTw}{dr}\right)z^2 + \left[\frac{c\rho}{6k}\frac{2U}{\delta}\frac{dTw}{dr} - \frac{1}{6r}\frac{d}{dr}\left(r\frac{db}{dr}\right)\right] z^3 \quad \ldots (5)$$

where $$b = \frac{\Delta T}{\delta} + \frac{\delta}{2r}\frac{d}{dr}\left(r\frac{dTw}{dr}\right) - \frac{\delta^2 c\rho}{6k}\frac{2U}{\delta}\frac{dTw}{dr} + \frac{\delta^2}{6r}\frac{d}{dr}\left(r\frac{db}{dr}\right) \quad \ldots (6)$$

(3) Solution

Substitution of equation (6) into equations (4) (5) and (8) of Appendix 3 with equations (9) and (10) of Appendix (3) gives the following four equations which have to be solved simultaneously.

$$U = \frac{\frac{3k}{2\rho Lr\delta}\int_o^r rb\,dr}{1 + \frac{27}{20}\frac{C\Delta T}{L} + \frac{11}{40}\frac{c\delta b}{L} - \frac{c\delta^2}{20Lr}\frac{d}{dr}\left(r\frac{dTw}{dr}\right)} \quad \ldots (7)$$

$$\delta^2 = \frac{\frac{2\mu U}{\rho r w^2} + \frac{3}{15}\frac{\delta}{r^2 w^2}\frac{d}{dr}\left(rU^2\delta\right)}{1 + \frac{3}{15}\frac{v^2}{r^2 w^2} - \frac{4}{3}\frac{v}{rw}} \quad \ldots (8)$$

$$V = \frac{\rho\delta w}{3\mu r^2}\frac{d}{dr}\left[r^3 U\delta\left(1 - \frac{4V}{5rw}\right)\right] \quad \ldots (9)$$

$$b = \frac{\Delta T}{\delta}\left[1 + \frac{\delta^2}{2r\Delta T}\frac{d}{dr}\left(r\frac{dTw}{dr}\right) + \frac{\delta^3}{6r\Delta T}\frac{d}{dr}\left(r\frac{db}{dr}\right) - \frac{\delta^2 c\rho U}{3k\Delta T}\left(\frac{dTw}{dr}\right)\right. \quad \ldots (10)$$

It would be possible to solve the equations simultaneously by using numerical techniques for a given surface temperature profile, However, the equations can be radically simplified by considering the order of

magnitude of the various terms. Consider the following experimental data taken from a typical test:

$N \propto$ 150 to 1500 r.p.m.

$L \backsimeq$ 930 B.T.U.lb^{-1}

C = 1 B.T.U.lb$^{-1}{}^{o}F^{-1}$

ρ = 60 lb.ft^{-3}

μ = 0.5 lb.ft^{-1}hr^{-1}

k = 0.4 B.T.U.ft^{-1}hr$^{-1}{}^{o}F^{-1}$

The order of magnitude of the terms in equation (10) are shown in Table 1 for the radial surface temperature profiles measured in the experiments.

TABLE I

Term	Order of Magnitude	Comments
$\frac{\Delta T}{\delta}$	1 x 10^5 to 4 x 10^5	Important term
$\frac{\delta}{2}\frac{d^2Tw}{dr^2}$	1	Negligible
$\frac{\delta}{2r}\frac{dTw}{dr}$	1	Negligible
$\frac{\delta^2}{6}\frac{d^2b}{dr^2}$	1	Negligible
$\frac{\delta^2}{6r}\frac{db}{dr}$	10^{-1}	Negligible
$\frac{\delta c\rho U}{3k}\frac{dTw}{dr}$	0 to 4 x 10^3	Becomes important as speed increases

Therefore, for practical purposes, the equation (10) can be reduced to

$$b = \frac{\Delta T}{\delta}\left[1 - \frac{\delta^2 c\rho U}{3k\Delta T}\frac{dTw}{dr}\right] \quad \ldots (11)$$

and at low values of $\frac{c\Delta T}{L}$ to $b = \frac{\Delta T}{\delta}$

(4) Approximate solution

An approximate solution will be determined using the following equations

$$U = \frac{3k}{2\rho Lr\delta}\int_0^r rbdr \quad \ldots (12)$$

$$V = 0 \quad \ldots (13)$$

$$\delta^2 = \frac{2\mu U}{\rho rw^2} \quad \ldots (14)$$

$$b = \frac{\Delta T}{\delta} \quad \ldots (15)$$

Rearranging the equations and eliminating U and b, gives the following equation for δ

$$\frac{3}{2} r\delta^3\frac{d\delta}{dr} = \frac{3}{2}\frac{\mu k\Delta T}{L\rho^2 w^2} - \delta^4 \quad \ldots (16)$$

This equation can be integrated in the form

$$\delta^4 = \frac{8}{3} r^{-8/3}\int_0^r \frac{3\mu k\Delta T}{2L\rho^2 w^2} r^{5/3}\, dr \quad \ldots (17)$$

for any given surface temperature profile. The local heat transfer coefficient can be obtained, as before, from

$$h_L = \frac{k}{\delta}, \quad \text{and} \quad \dot{q}''_L = h_L\Delta T$$

Graph sheet 26 shows the local heat transfer coefficient and local heat flux calculated from equation (17) for trial no. 33.

When the form $b = \frac{\Delta T}{\delta}\left[1 - \frac{\delta^2 c\rho U}{3k\Delta T}\frac{dTw}{dr}\right]$ is used for equation (10), equation (16) becomes

$$\delta^4\left[1 + \frac{c\Delta Tr}{4L\Delta T}\frac{dTw}{dr}\right] + \frac{3r\delta^3}{2}\frac{d\delta}{dr} = \frac{3\mu k\Delta T}{2L\rho^2 w^2} \qquad \ldots (18)$$

For the tests, $\frac{c}{4L} \doteqdot \frac{1}{4000}$ and therefore the term $\frac{cr}{4L}\frac{dTw}{dr}$ is not important for the values of $\frac{rdTw}{dr}$ found in the experiments. For the conditions in test no. 33 the term $\frac{cr}{4L}\frac{dTw}{dr}$ has a maximum value of 0.03 Numerical solutions would have to be used to include the effect of $\frac{rdTw}{dr}$.

From the graphical integration of equation (17) for test 33, it can be shown that neglect of the heat transferred for radii less than 1.5 inches radius causes a very small effect on the theoretical heat transfer coefficient for radii above 2.25 inches; the effect of any error being quickly reduced as shown in figure 25.

APPENDIX 5 THE FILM REYNOLD'S NUMBER

The critical Reynold's Number for the onset of waves or turbulence in the film is the Reynold's Number based on film thickness and flow velocity. The theoretical analysis assumes laminar flow of the condensate, and for this to be correct the film Reynold's Number must be below 10 to 25, above these figures it is likely that wave flow will exist until the film becomes turbulent at a Reynold's Number of about 1500.

$$\text{Reynold's Number} = \frac{4\, U_m \delta}{\nu}$$

$$\dot{Q} = 2\pi r U_m \delta \rho = \frac{2\pi \int_0^r \dot{q}''r \, dr}{L}$$

$$\rho U_m \delta = \frac{1}{rL} \int_0^r \dot{q}''r \, dr$$

$$\text{Reynold's Number} = \frac{4}{\rho \nu rL} \int_0^r \dot{q}''r \, dr$$

Graph sheet 20 shows the variation of Reynold's Number with radius for test no. 33.

The types of flow which occur on a vertical tube or inclined plane are as follows

Approximate Reynold's Number	Type of flow
Less than 8 to 10	Laminar
10 to 25	Transition to wave flow
25 to 1000	Wave flow
1000 to 1250	Transition to turbulent flow
Above 1250 to 1600	Turbulent flow

APPENDIX 5 A SOLUTION FOR CONDENSATION ON A ROTATING DISC HAVING A STEP-WISE TEMPERATURE DISTRIBUTION

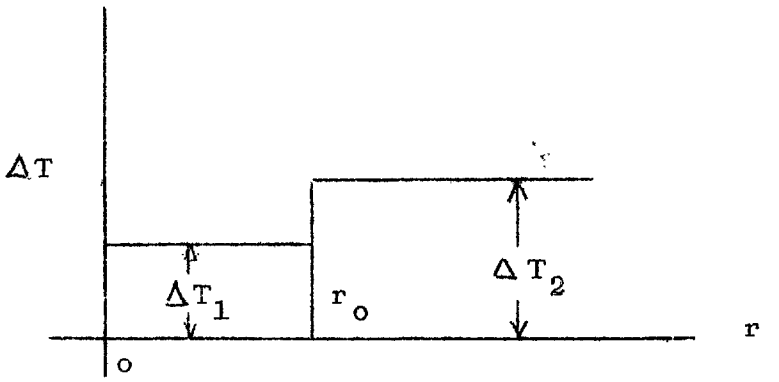

Diagram 4

Let the temperature distribution be as shown in figure 4. The equation for the film thickness for $r < r_o$ using radial flow theory, given in Appendix 4 is

$$\delta^4 = \frac{3}{2} \frac{k\Delta T}{\rho L w^2}$$

For $r > r_o$, the following equation applies (see Appendix 4)

$$\delta^4_{r>r_o} = \frac{8}{3} r^{-8/3} \int_o^r \frac{3\mu k \Delta T \, r^{5/3} dr}{2L\rho^2 w^2}$$

or

$$\delta^4_{r>r_o} = \frac{8}{3} r^{-8/3} \left[\int_o^{r_o} \frac{3\mu k \Delta T_1 r^{5/3} dr}{2L\rho^2 \, 2} + \int_{ro}^r \frac{3\mu k \Delta T_2 r^{5/3} dr}{2L\rho^2 w^2} \right]$$

That is

$$\delta^4_{r>r_o} = \frac{3\mu k}{2L\rho^2 w^2} \frac{8}{3} r^{-8/3} \left[\frac{3}{8} r_o^{\,8/3} \Delta T_1 + \frac{3}{8} \Delta T_2 \left(r^{8/3} - r_o^{\,8/3} \right) \right]$$

or $$\delta^4_{r>r_o} = \frac{3\mu k \Delta T_2}{2L\rho^2 w^2} \left[1 - \left(\frac{\Delta T_2 - \Delta T_1}{\Delta T_2} \right) \left(\frac{r_o}{r} \right)^{8/3} \right]$$

But $\frac{3\mu k \Delta T_2}{2L\rho^2 w^2}$ is equal to the local isothermal film thickness which will be written as δ^4_{isoth}

Therefore $\left[\frac{\delta^4}{\delta^4_{isoth}}\right]_{r>r_o} = 1 - \left(1 - \frac{\Delta T_1}{\Delta T_2}\right)\left(\frac{r_o}{r}\right)^{8/3}$

It can be seen that for $\frac{\Delta T_2}{\Delta T_1}$ equal to infinity, the film thickness is within 10% of the thickness calculated from the isothermal theory for $\frac{r_o}{r} = 0.7$. For example, if $r_o = 1.5"$, as in the experiments, the film thickness, and therefore the heat transfer coefficient, should be within 10% of the isothermal value at $r = 2\frac{1}{4}"$. Also, if $\frac{\Delta T_2}{\Delta T_1}$ does not change appreciably, for example if the change is less than 2, the heat transfer coefficient calculated from isothermal theory is within 16% of that calculated from non-isothermal theory over the total disc surface and is within 5% at 2.25 inches radius.

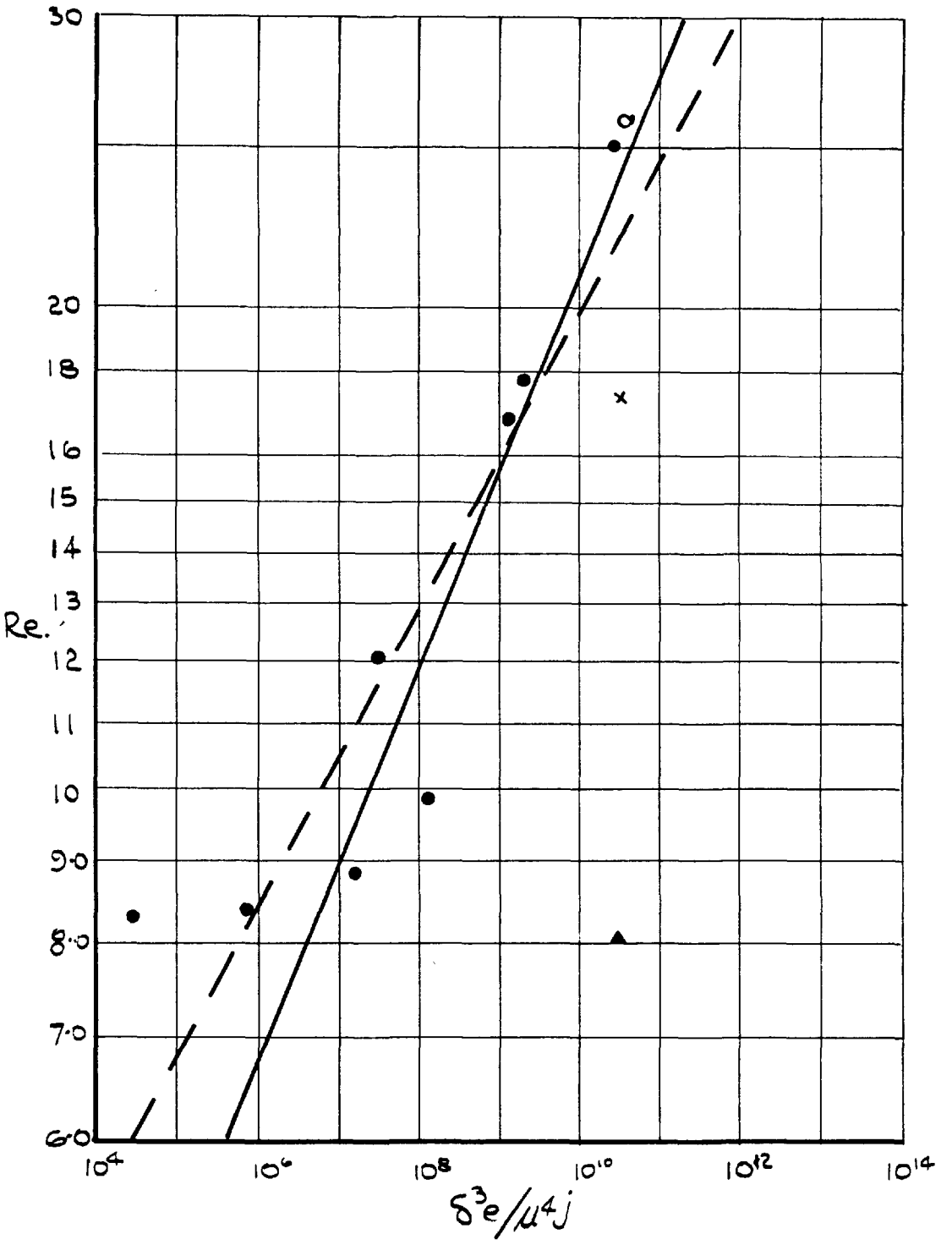

FIG. 1 TRANSITION FROM LAMINAR TO WAVE FLOW

GRIMLEY —— & ●
BINNIE x
KIRKBRIDE ▲
FRIEDMAN & MILLER o
KAPITSA ----

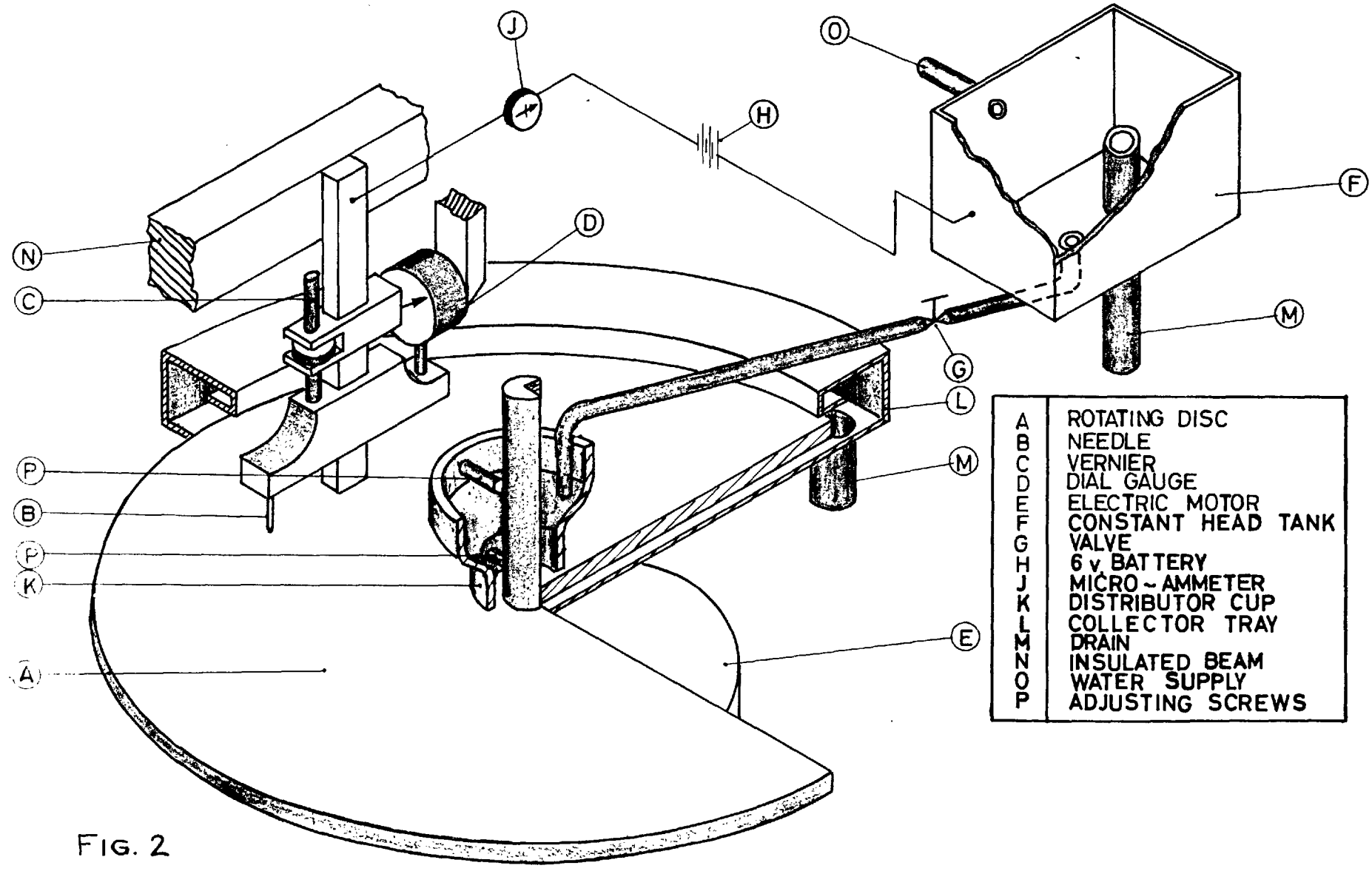

FIG. 2

APPARATUS USED TO STUDY THE FLOW OF A LIQUID FILM ON A ROTATING DISC

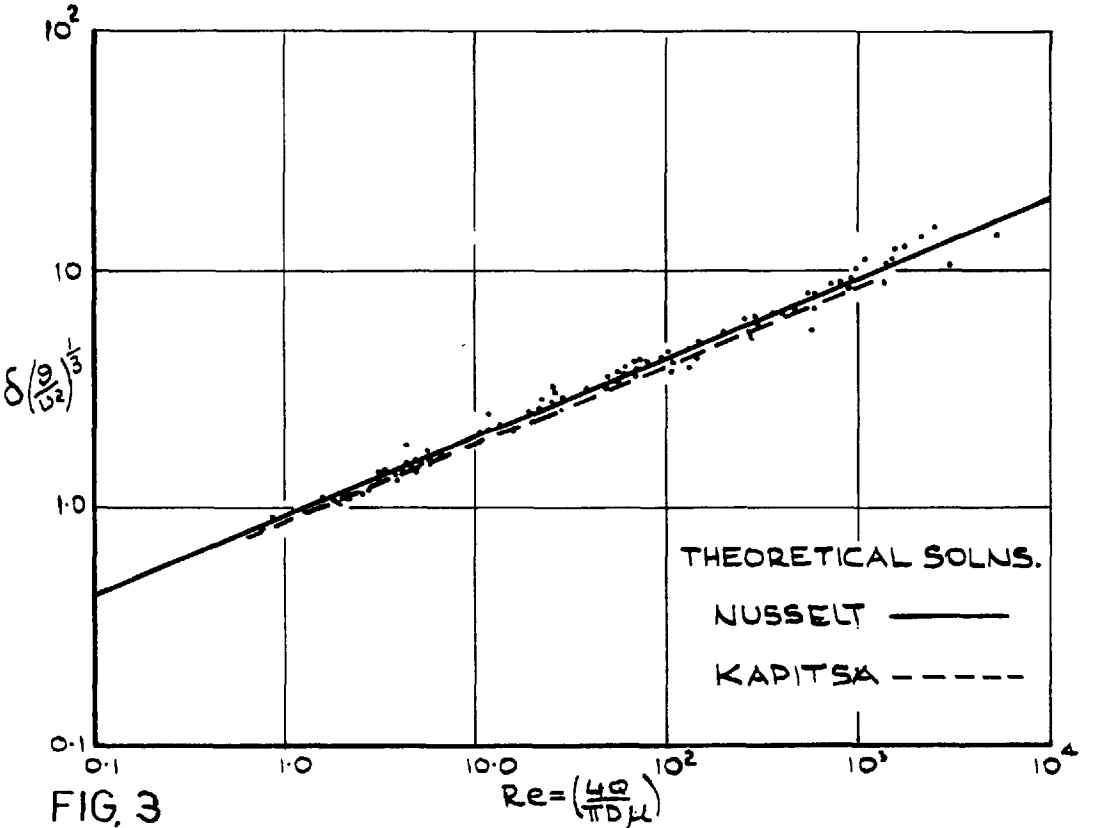

FIG. 3 MEAN FILM THICKNESS AS A FUNCTION OF Re

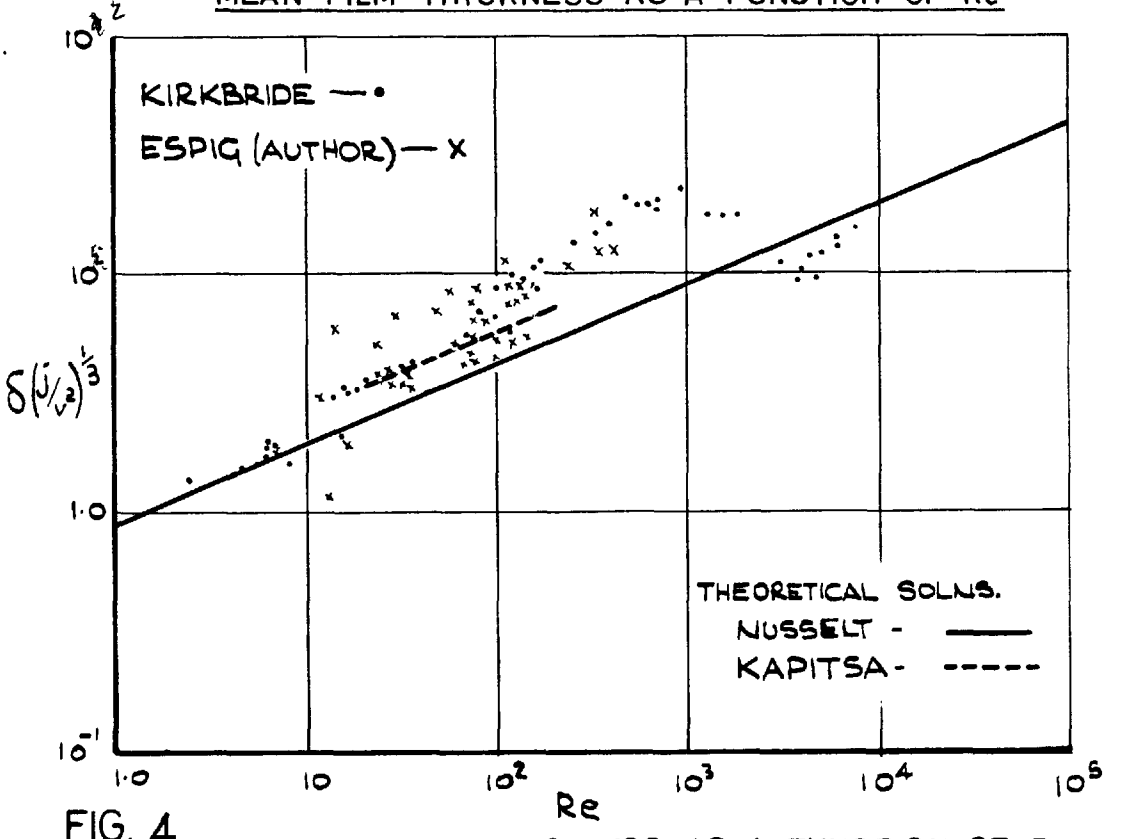

FIG. 4 MAXIMUM FILM THICKNESS AS A FUNCTION OF Re

A	COMPOUND TUBE	B	ROTATING DRUM
C	COPPER DISC	D	GUARD DRUM
E	SPRAY	F	WATER BEARING
G	SUPPORT BEARING	H	SEALS
J	SUPPORT BLOCK	K	STEAM SUPPLY TUBE
L	BELT DRIVE		

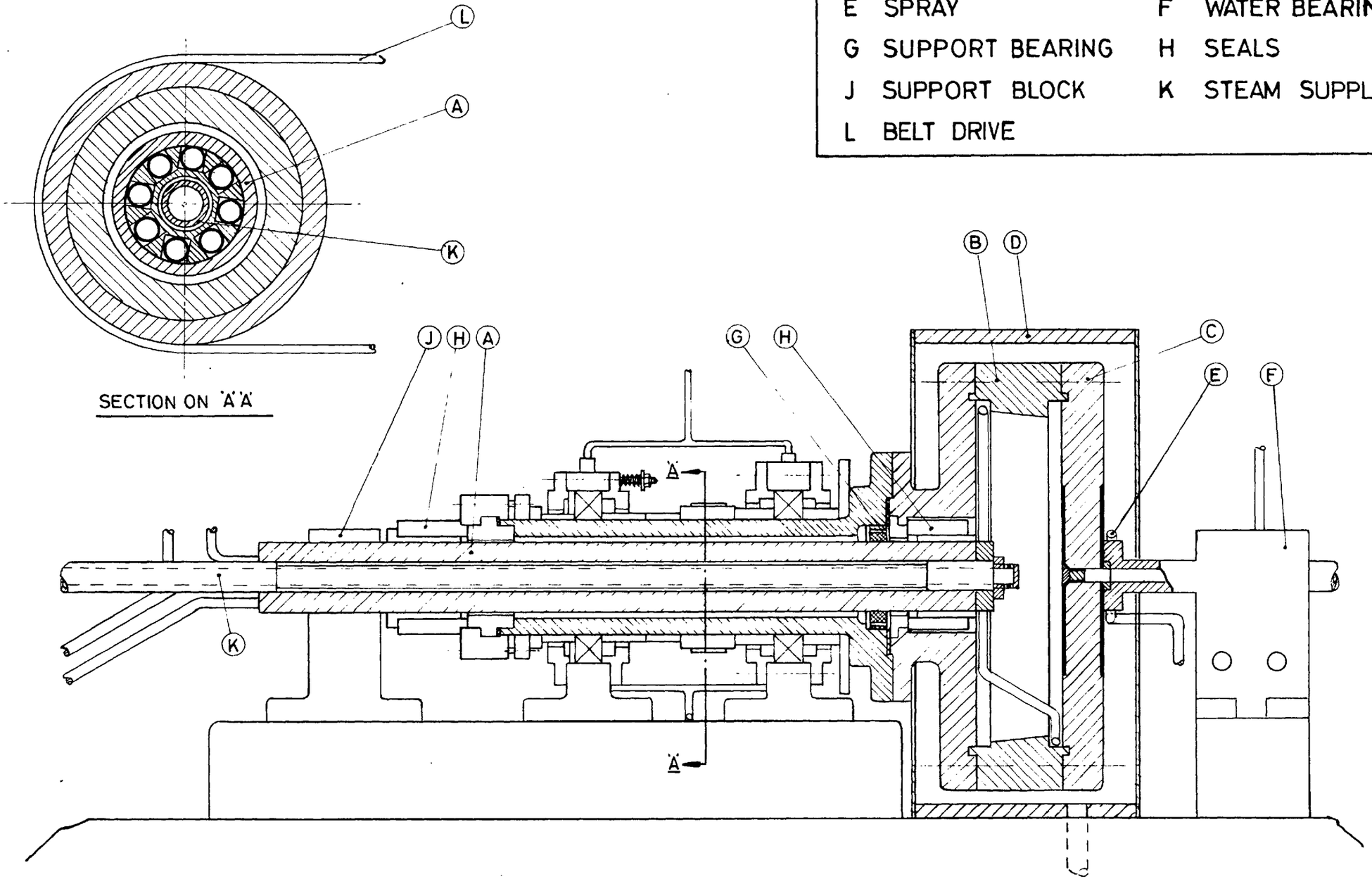

FIG.5 DETAILS OF ROTATING DISC APPARATUS

SCALE 1:4

SECTION ON 'A' 'A' 1:2

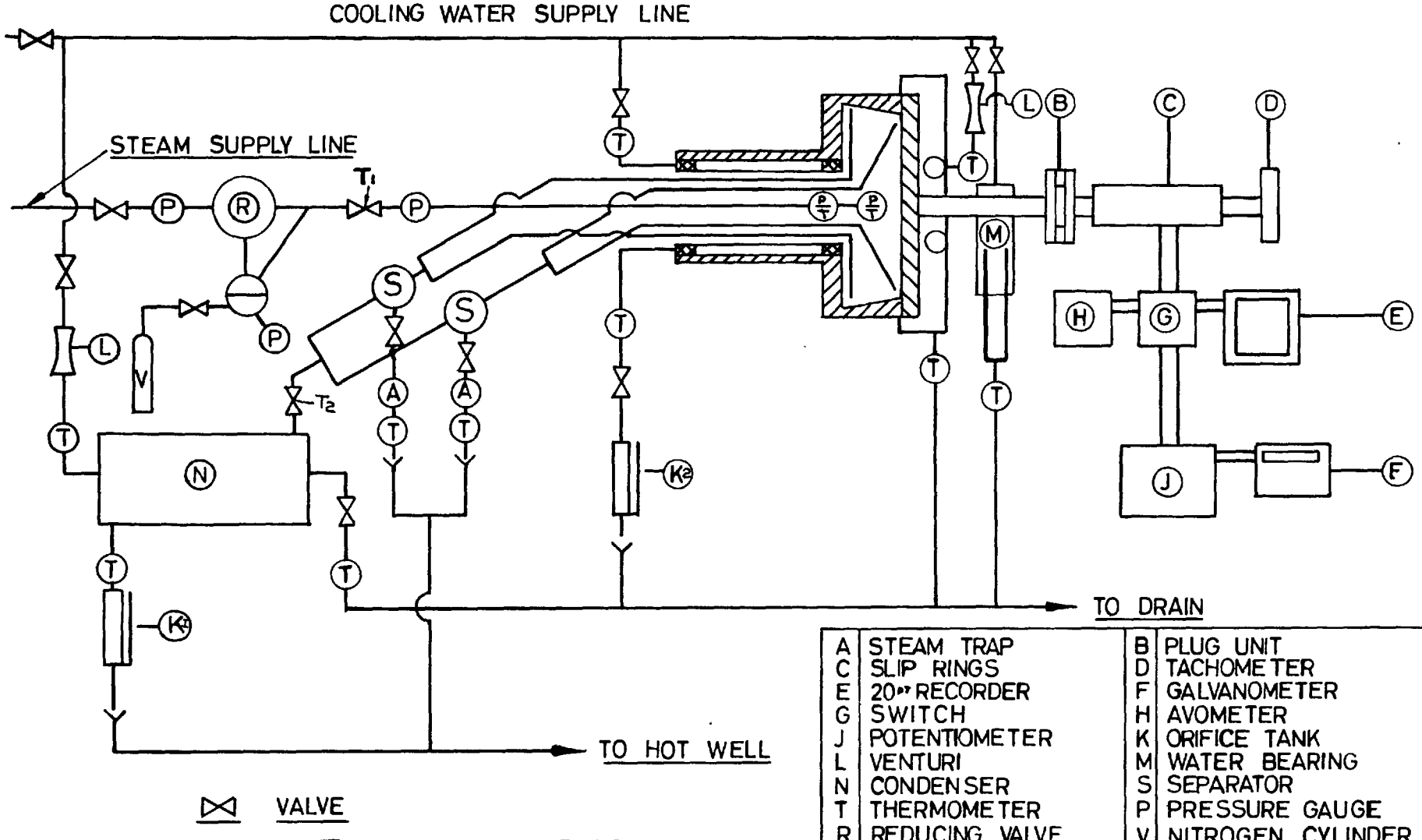

A	STEAM TRAP	B	PLUG UNIT
C	SLIP RINGS	D	TACHOMETER
E	20" RECORDER	F	GALVANOMETER
G	SWITCH	H	AVOMETER
J	POTENTIOMETER	K	ORIFICE TANK
L	VENTURI	M	WATER BEARING
N	CONDENSER	S	SEPARATOR
T	THERMOMETER	P	PRESSURE GAUGE
R	REDUCING VALVE	V	NITROGEN CYLINDER

FIG.6 FLOW DIAGRAM

Figure 7
Interior of Rotating Drum showing Distributor and Scoops

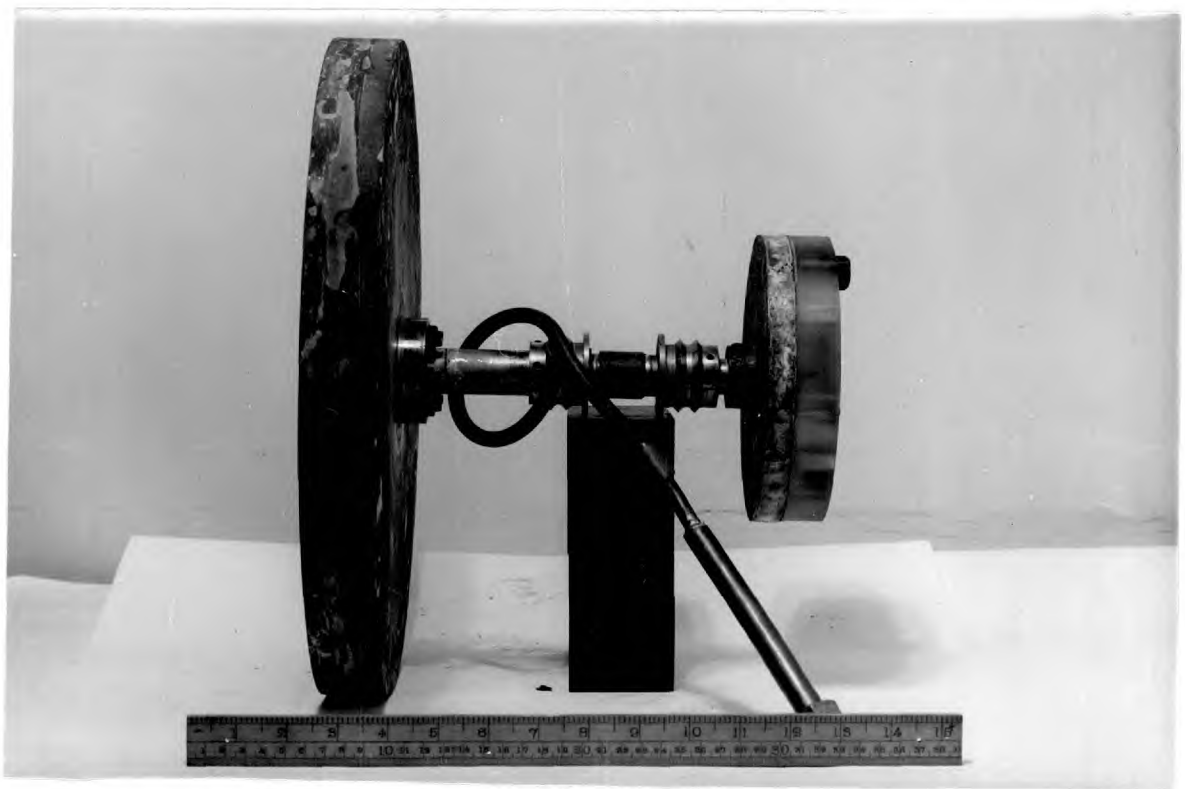

Figure 8
Copper Disc showing Plug Unit and Spray Ring

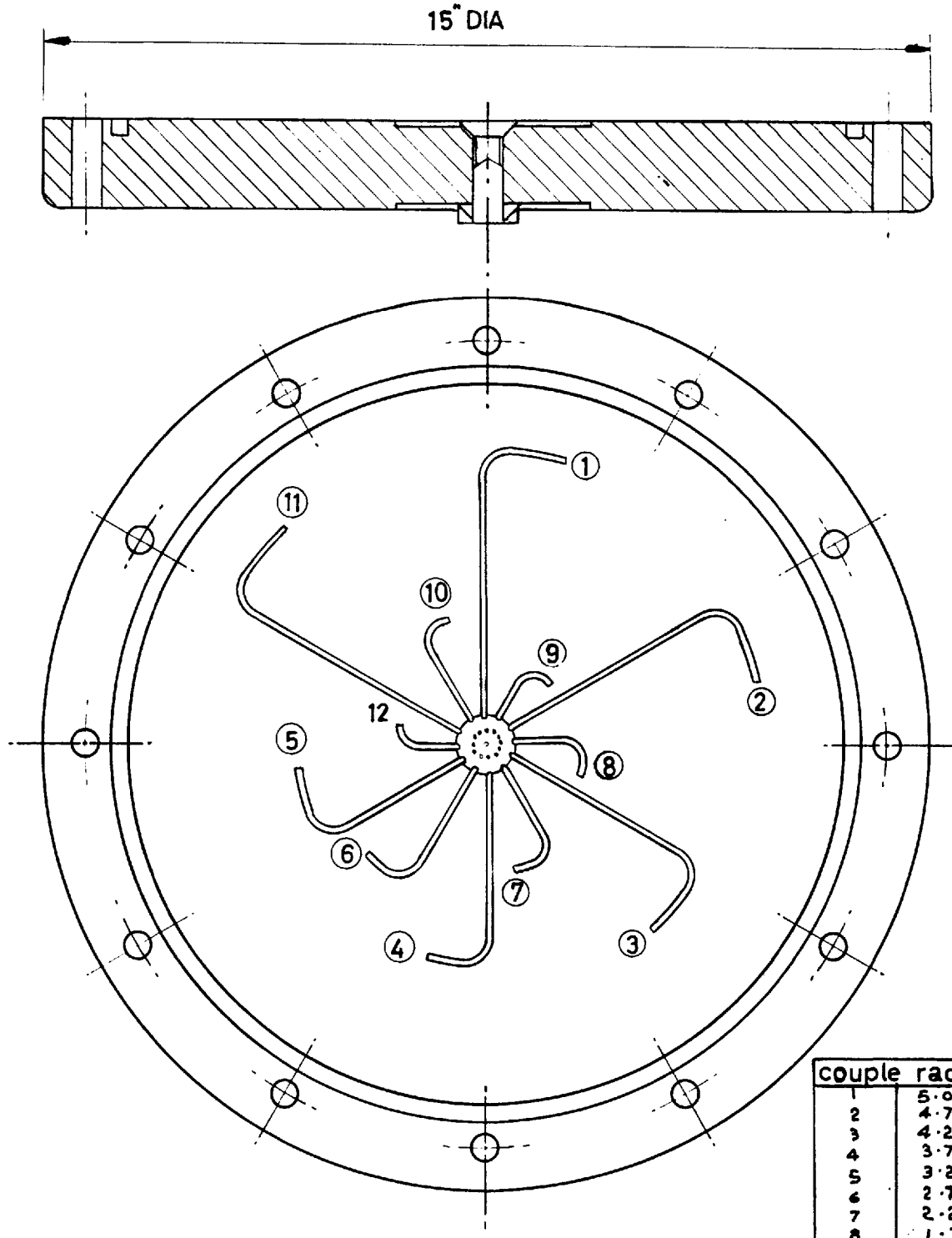

couple	radius
1	5·00"
2	4·75"
3	4·25"
4	3·75"
5	3·25"
6	2·75"
7	2·25"
8	1·75"
9	1·50"
10	2·25"
11	5·00"
12	1·50"

FIG. 9

DETAILS OF THERMOCOUPLE CIRCUITS

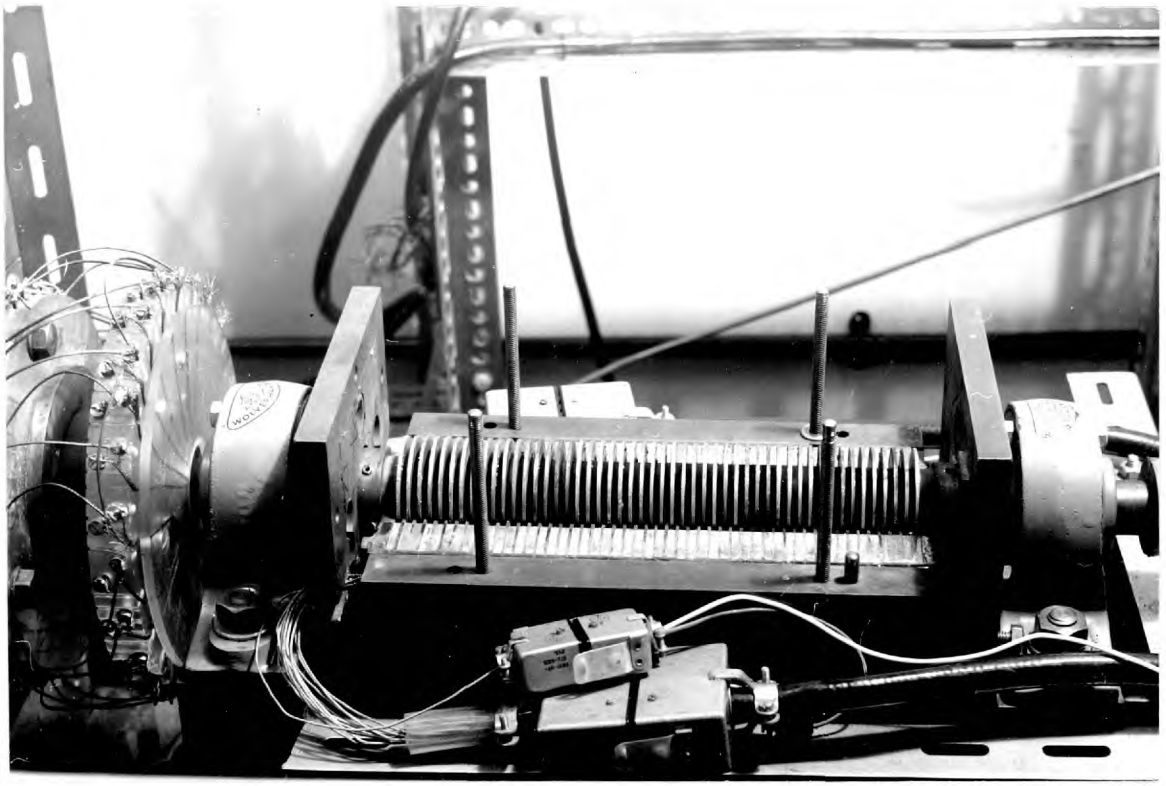

Figure 10
View of 50-way Mercury Slip Ring Unit with Cover Removed

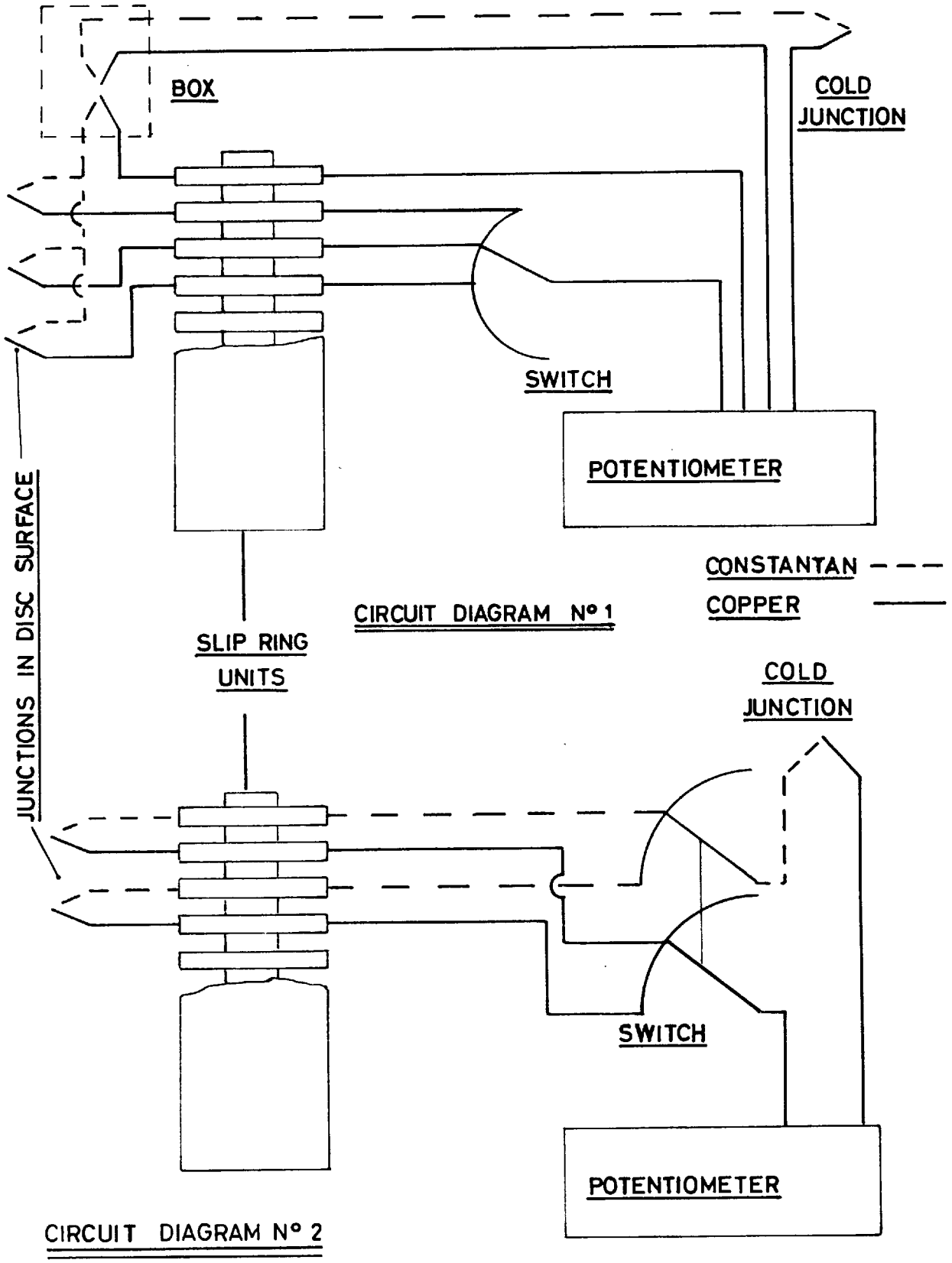

FIG 11 THERMOCOUPLE CIRCUIT DIAGRAMS

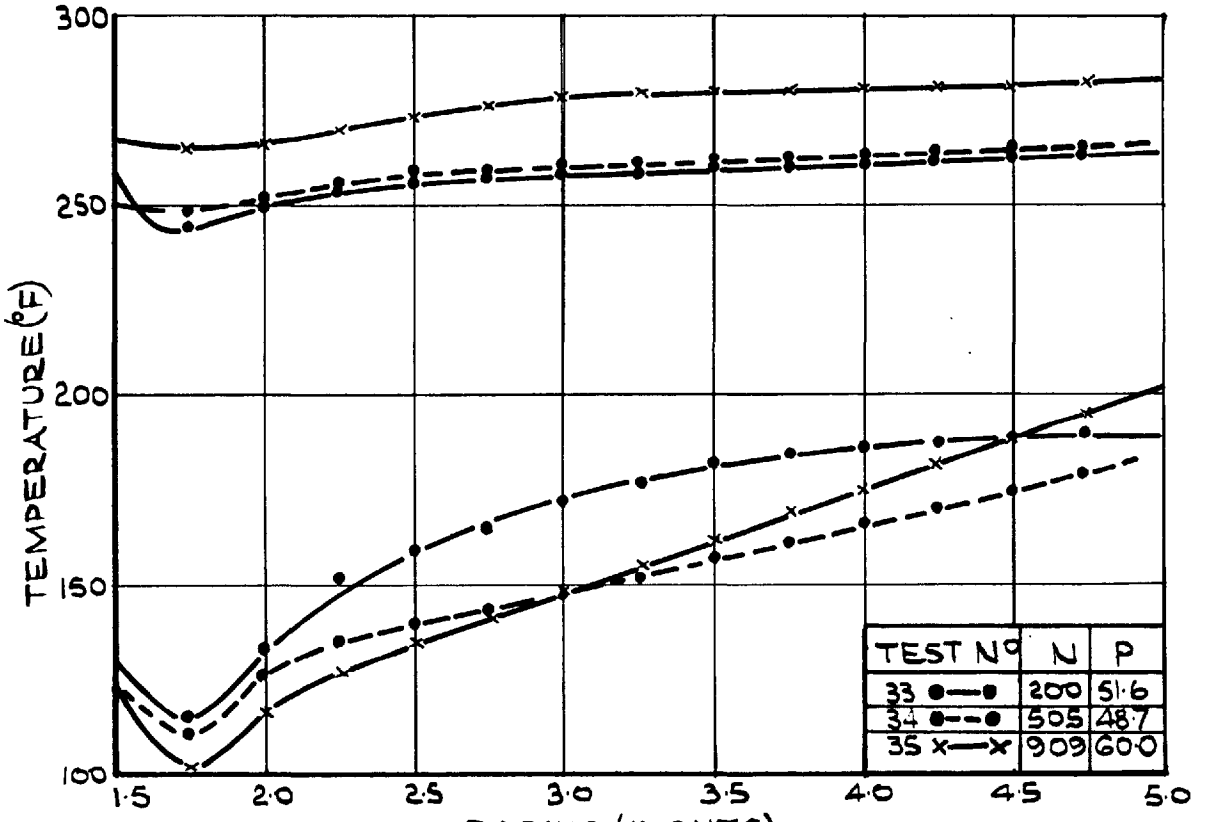

FIG. 12 SURFACE TEMPERATURE DISTRIBUTIONS

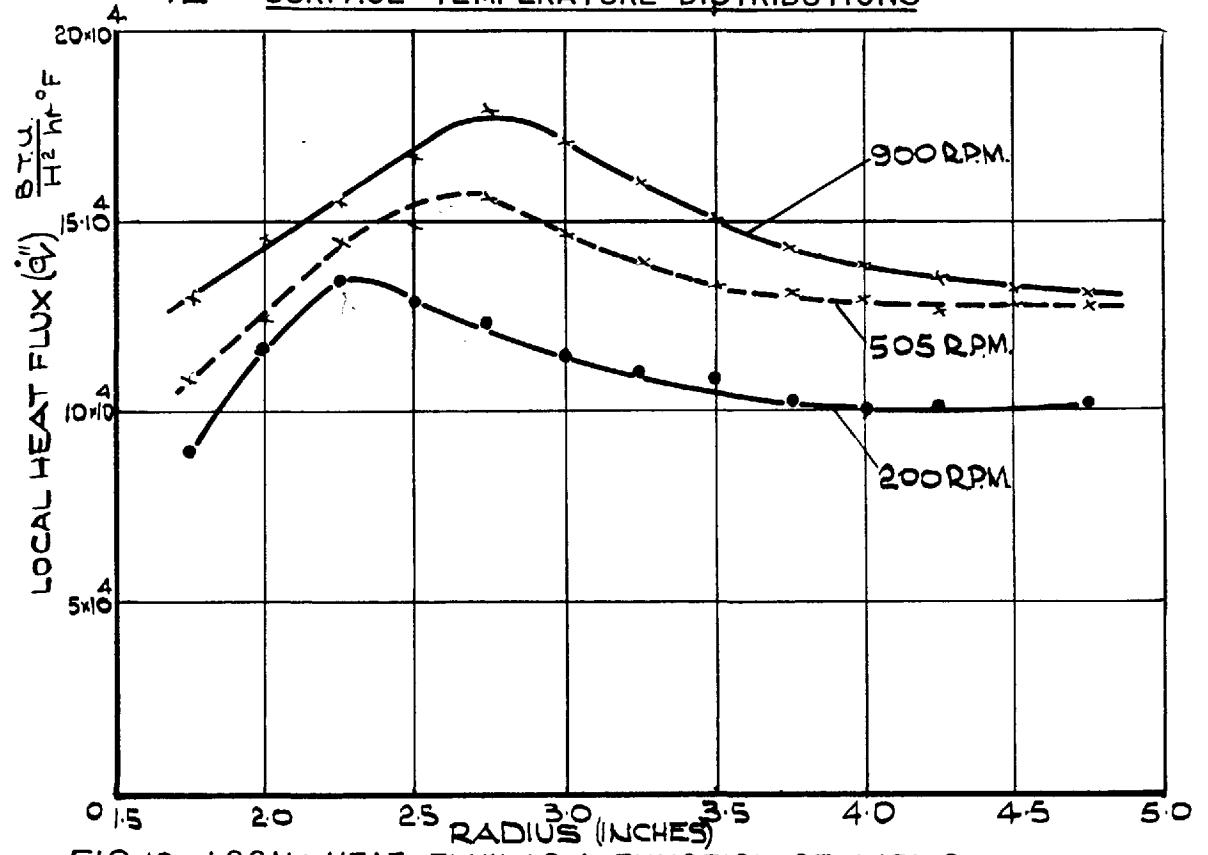

FIG. 13 LOCAL HEAT FLUX AS A FUNCTION OF RADIUS FOR N = 200 505 & 900 R.P.M.

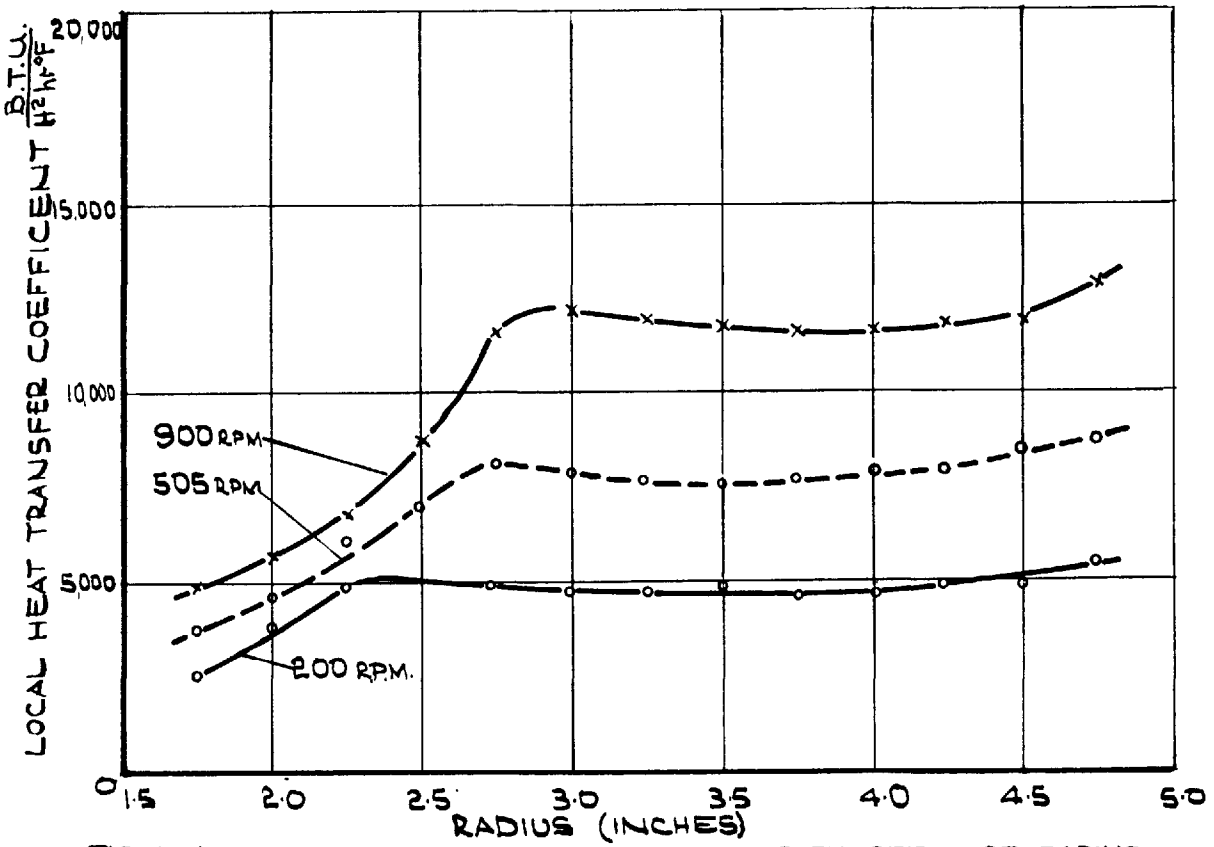

FIG. 14 LOCAL HEAT TRANSFER COEFFICENT AS FUNCTION OF RADIUS

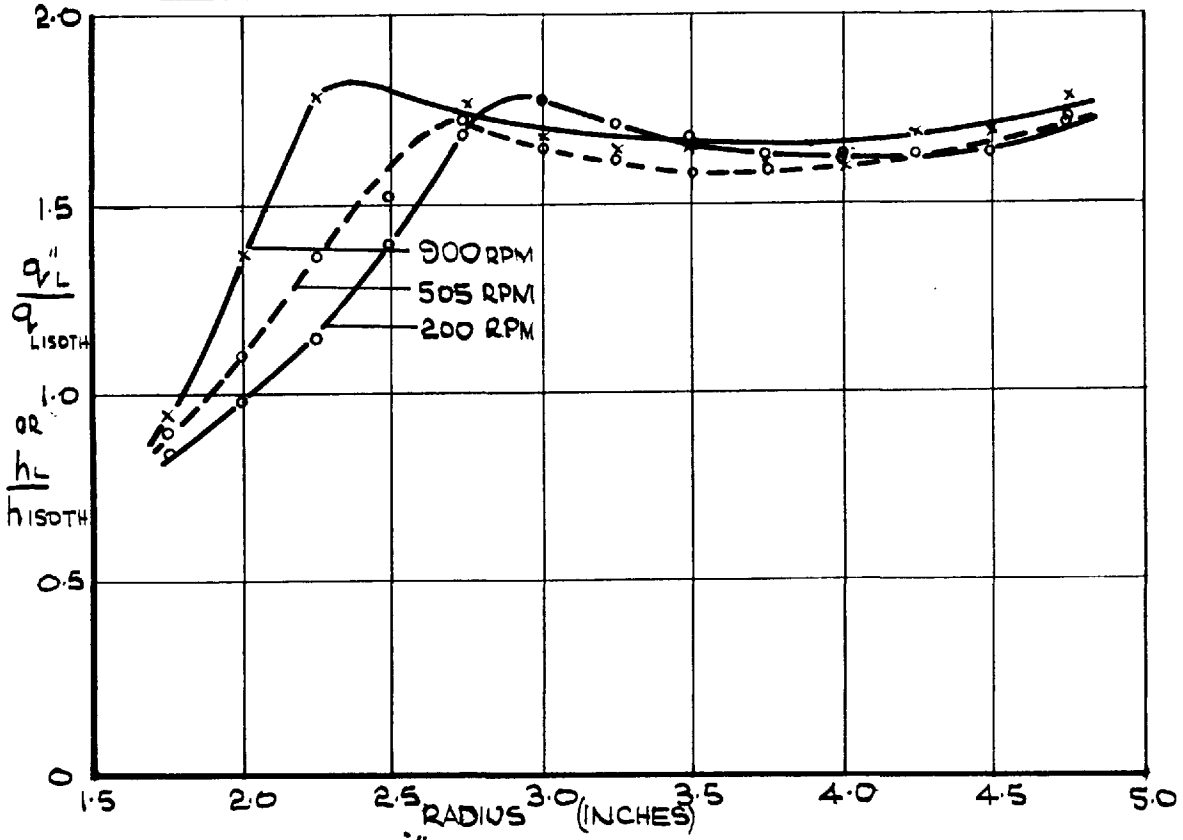

FIG. 15 VARIATION OF $\dot{q}''/\dot{q}''_{ISOTH}$ WITH RADIUS

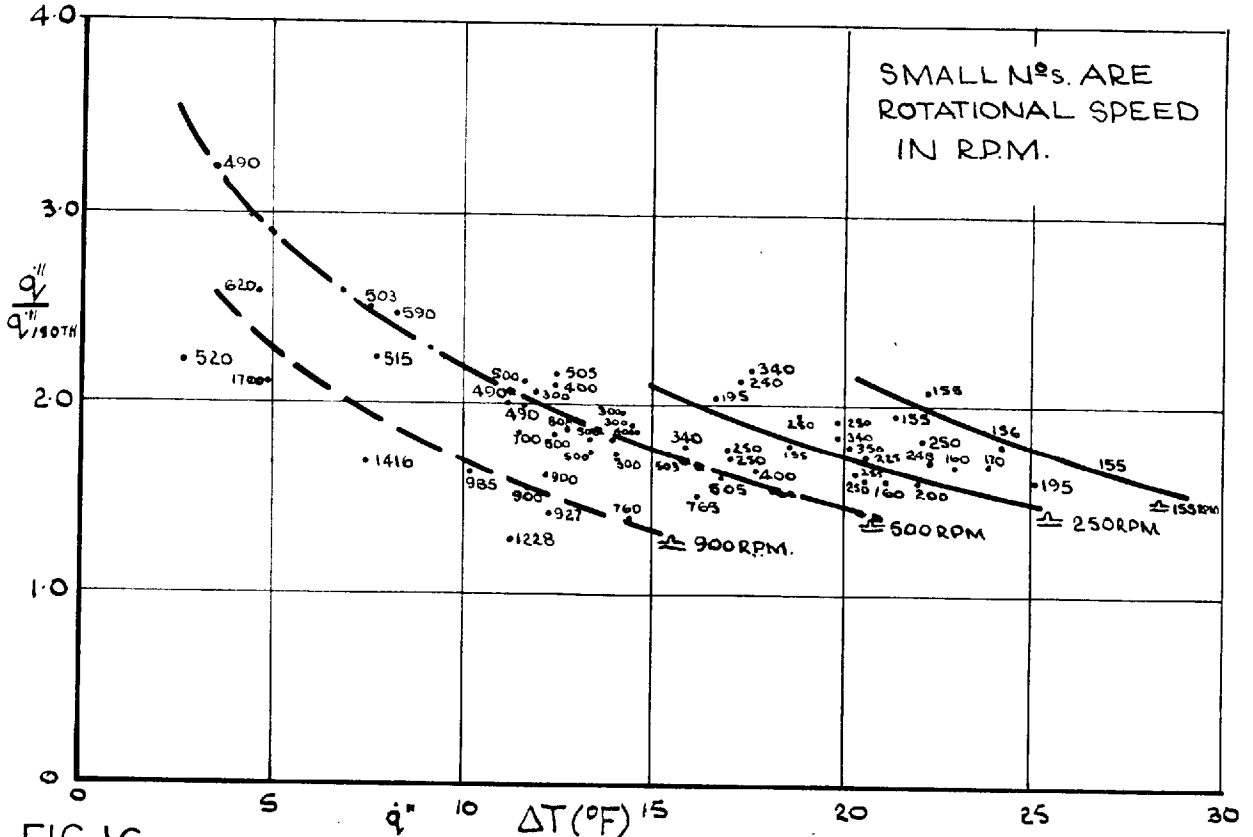

FIG. 16 VARIATION OF $\frac{\dot{q}''}{\dot{q}''_{150TH}}$ WITH FILM TEMP. DROP AT r = 4·0 INCHES

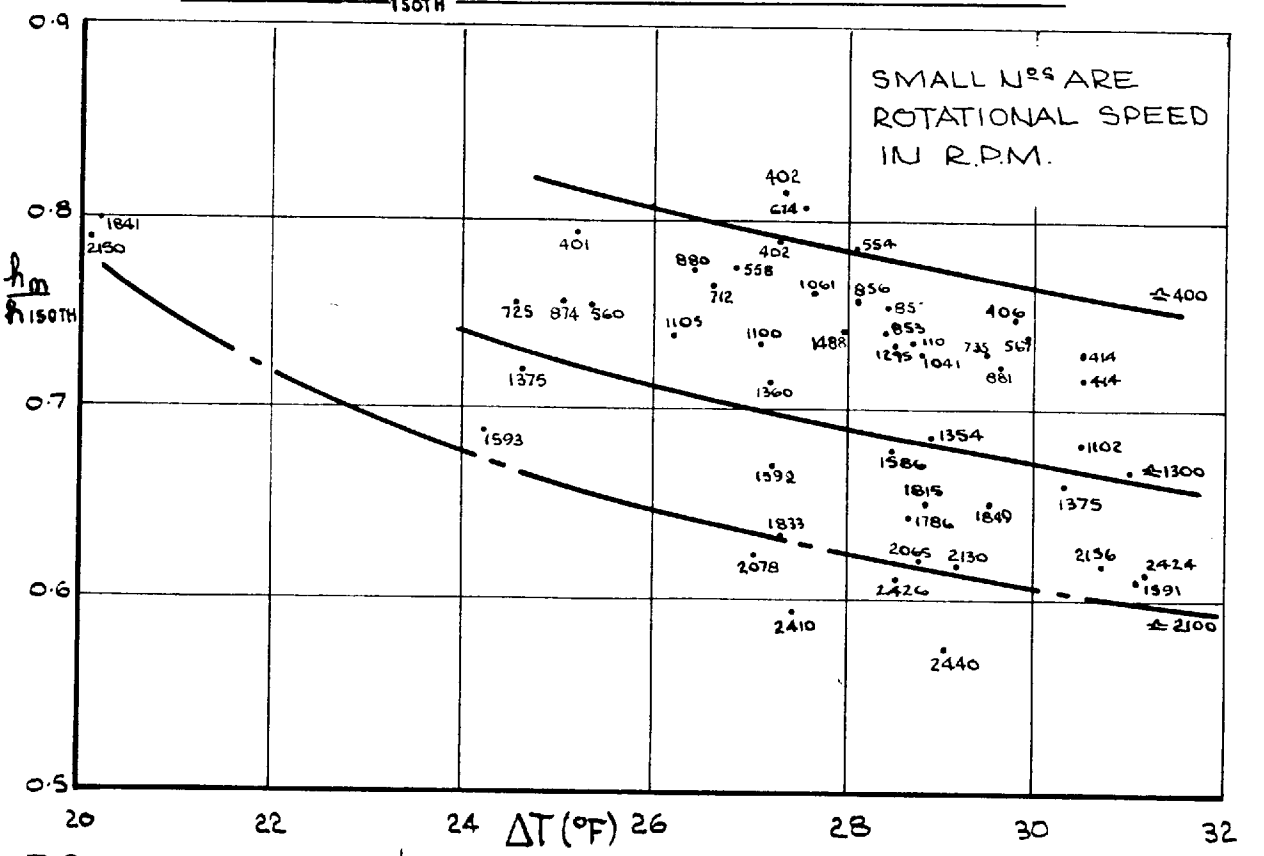

FIG. 17 VARIATION OF $\frac{h_m}{h_{150TH}}$ WITH ΔT FOR FREON FROM REF. 53

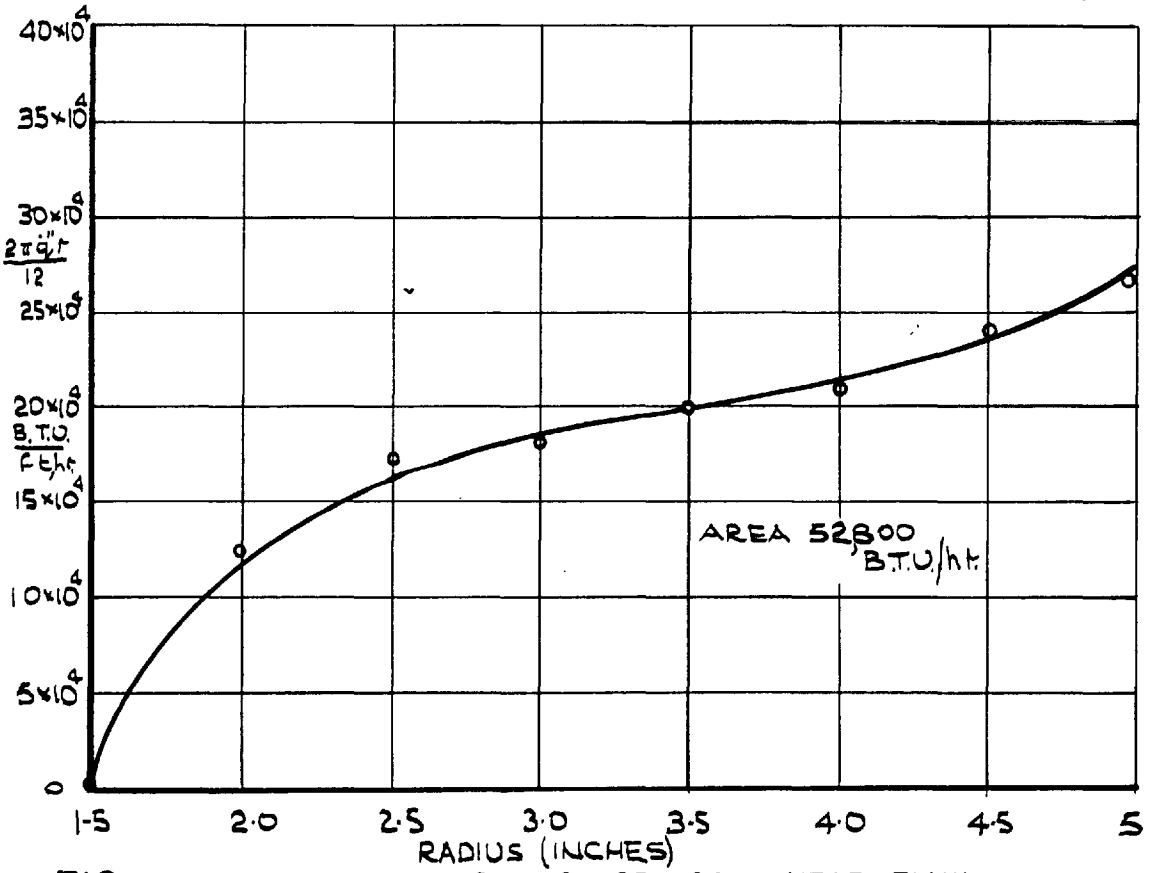

FIG. 18 GRAPHICAL INTEGRATION OF LOCAL HEAT FLUX

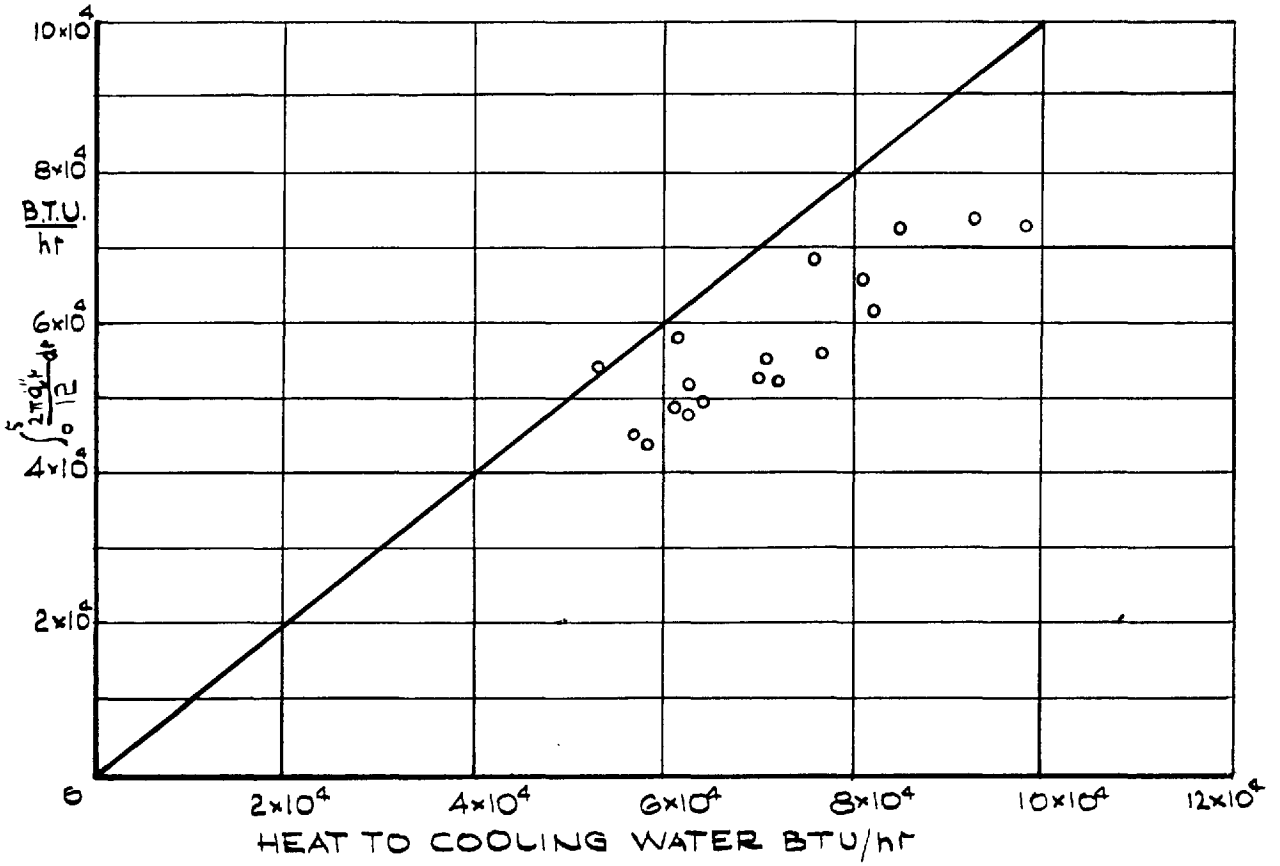

FIG. 19 TYPICAL HEAT BALANCES

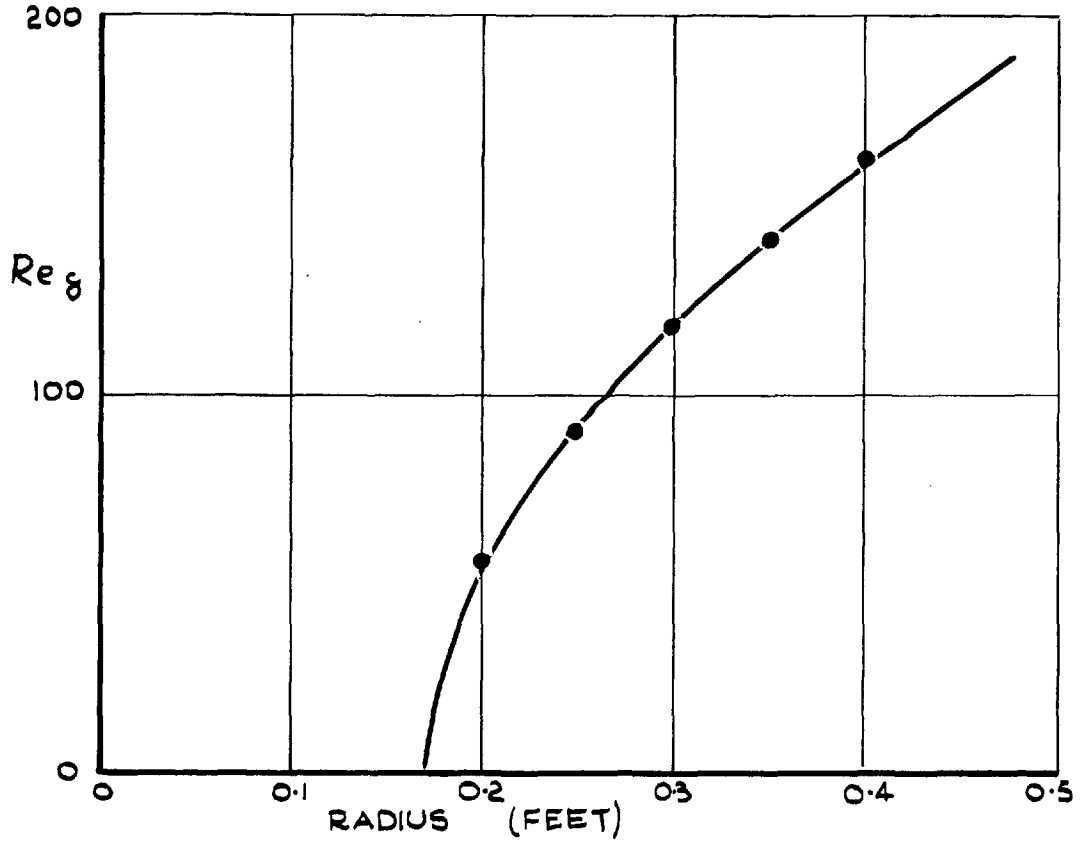

FIG.20 REYNOLDS.NUMBER VARIATION WITH RADIUS FOR TEST N° 33

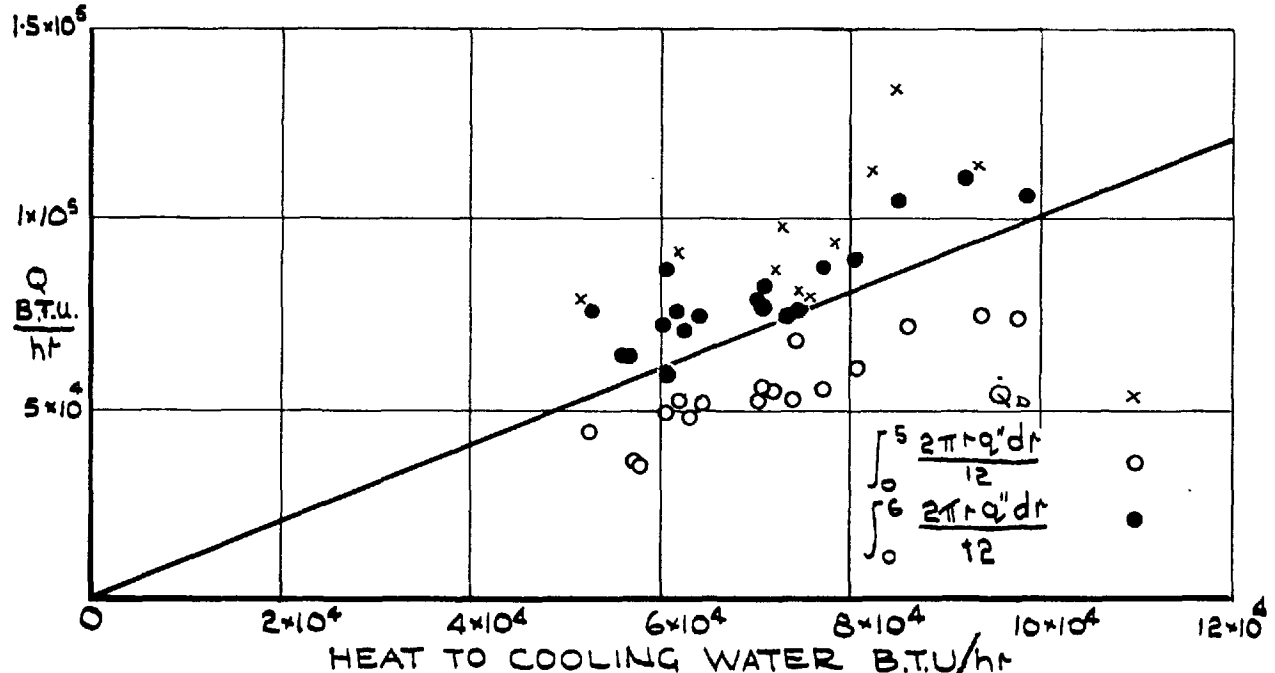

FIG 21 HEAT BALANCES

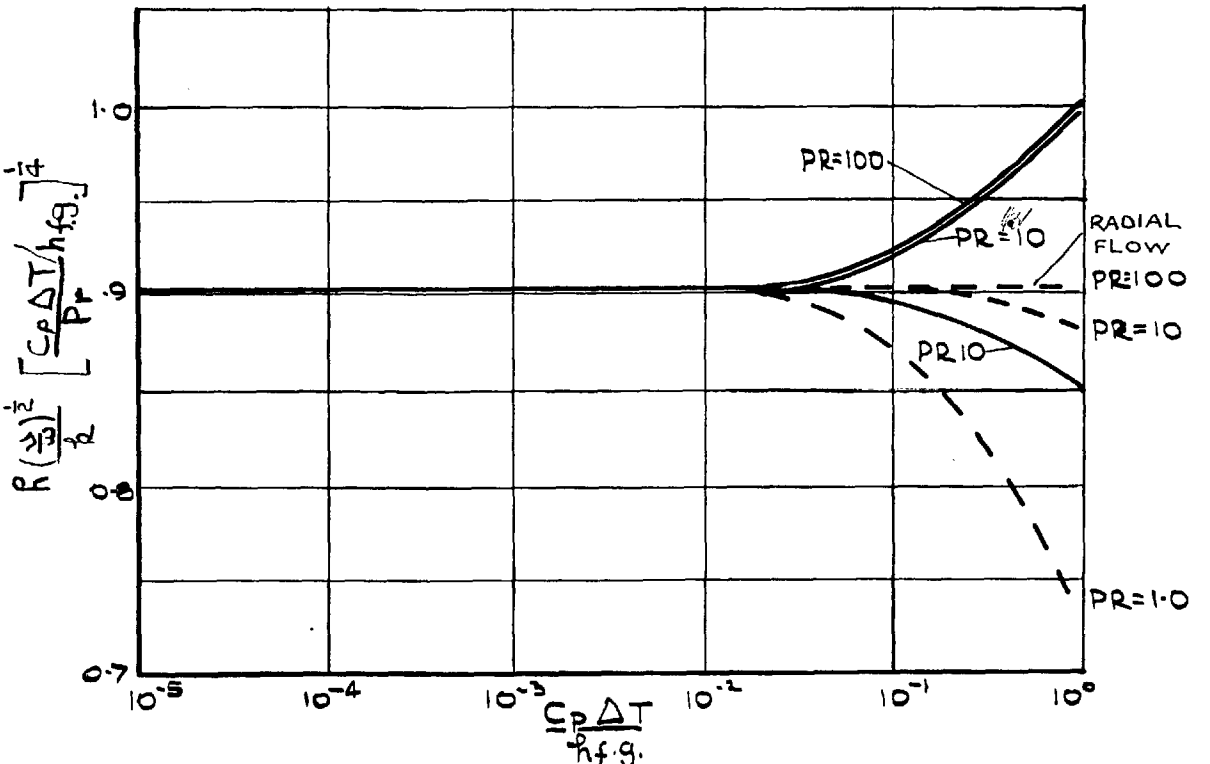

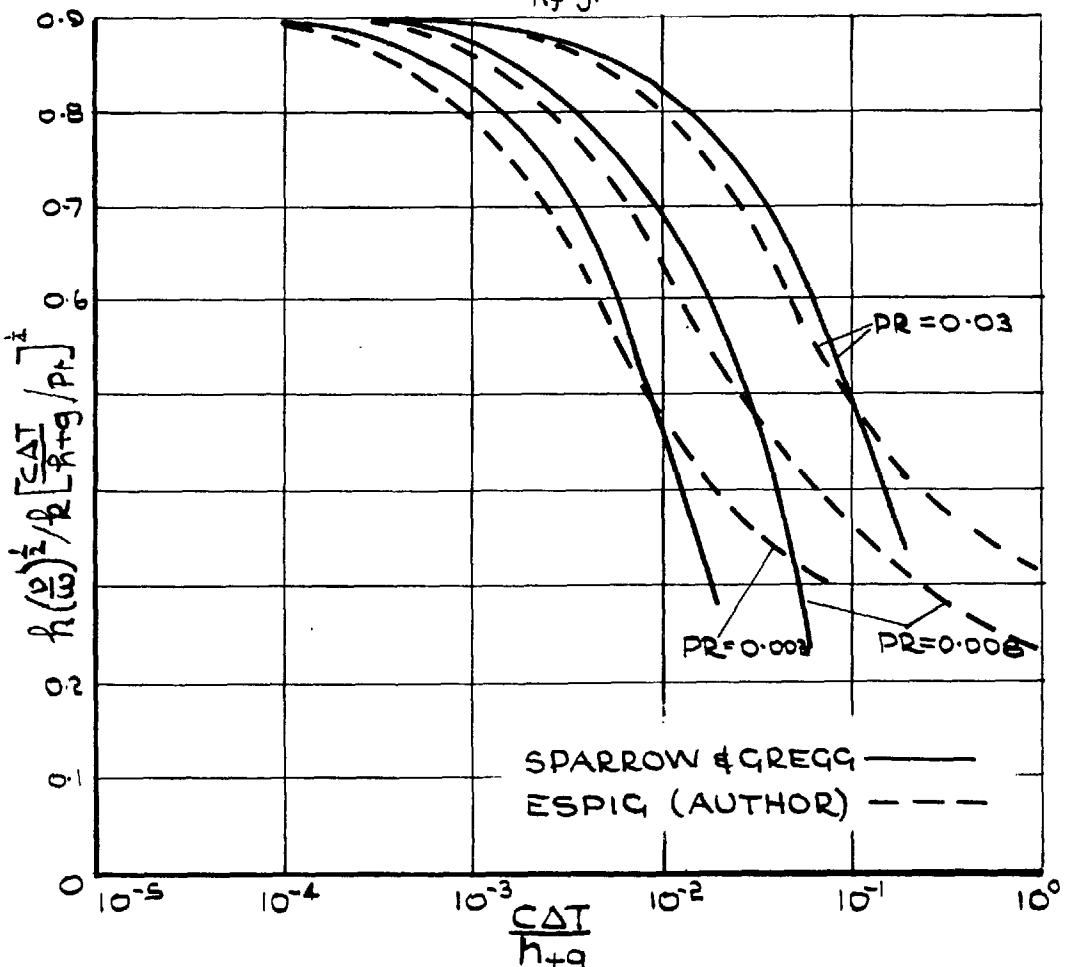

FIGS. 22 & 23 CONDENSATION ON ROTATING DISCS.
COMPARISON OF "PROFILE" WITH "EXACT" SOLUTIONS

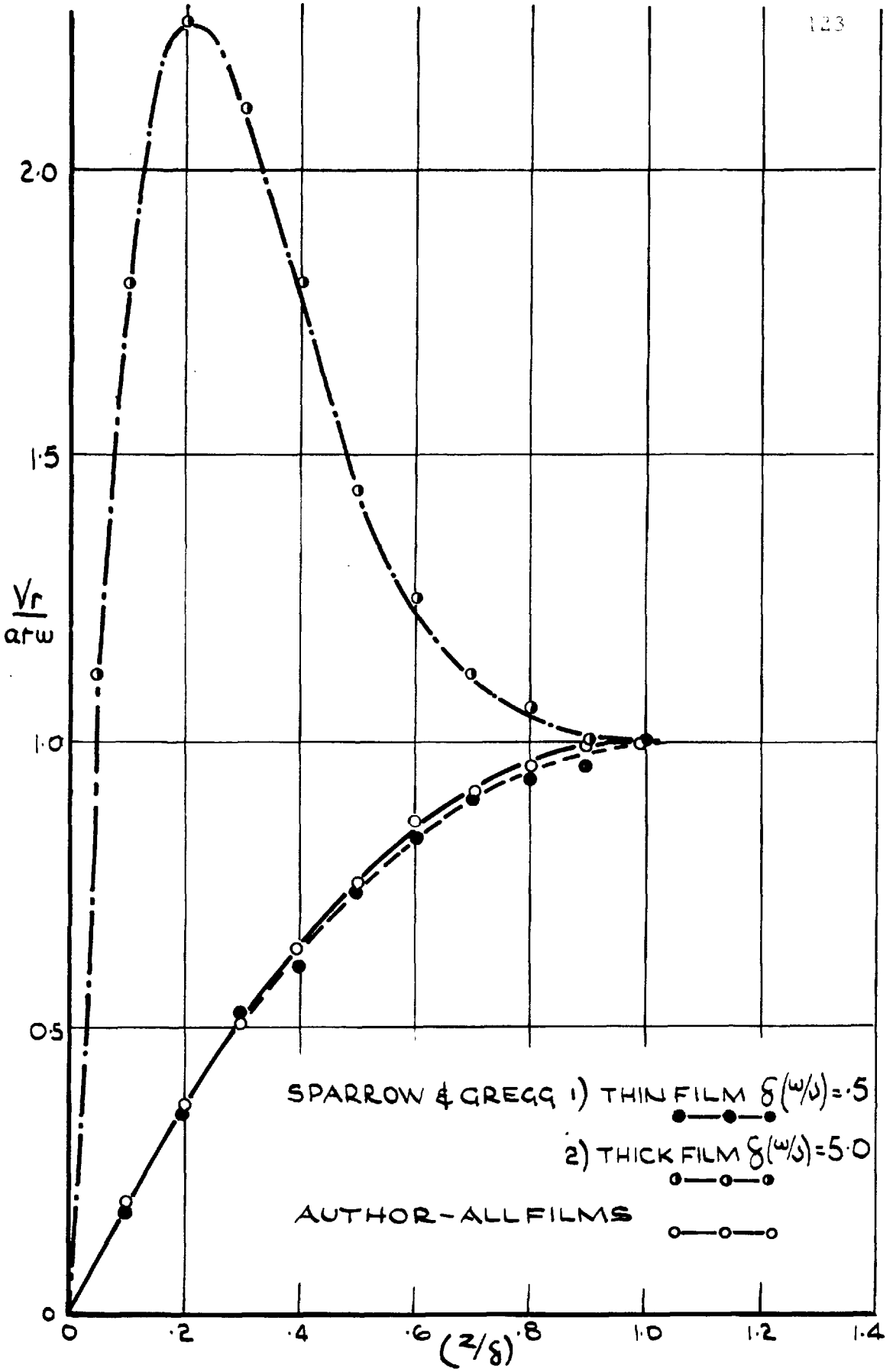

FIG.24 COMPARISON OF THE RADIAL VELOCITY USED IN THEORETICAL SOLUTIONS

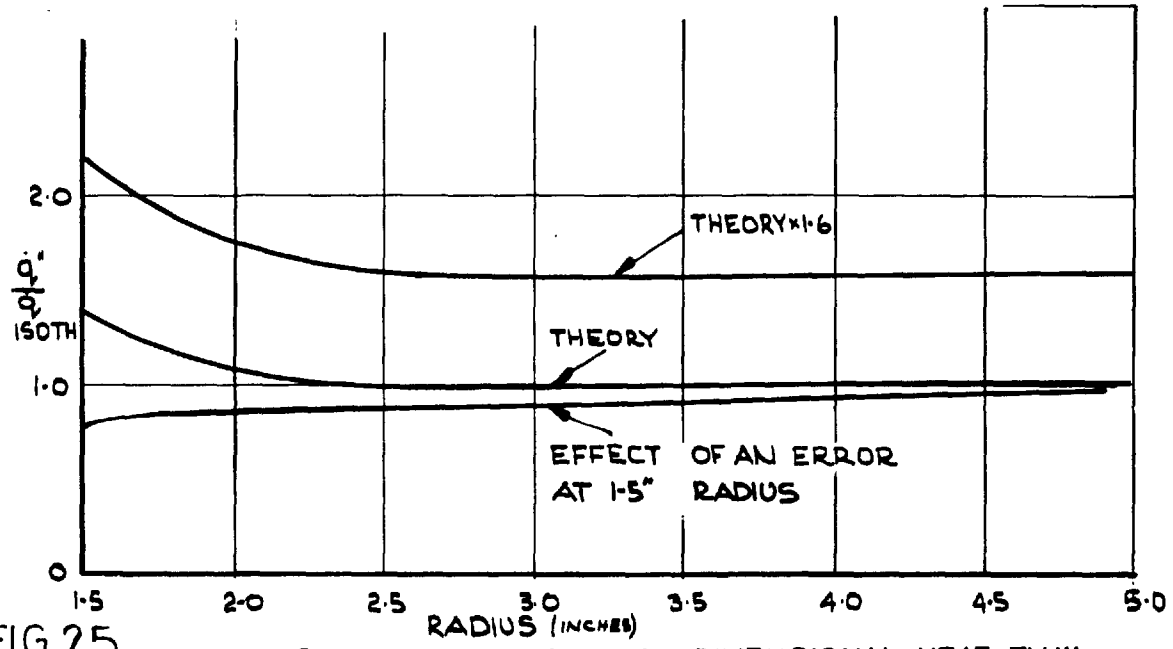

FIG.25 THEORETICAL VARIATION ON NON-DIMENSIONAL HEAT FLUX WITH RADIUS AFTER A STEP-WISE SURFACE TEMPERATURE VARIATION

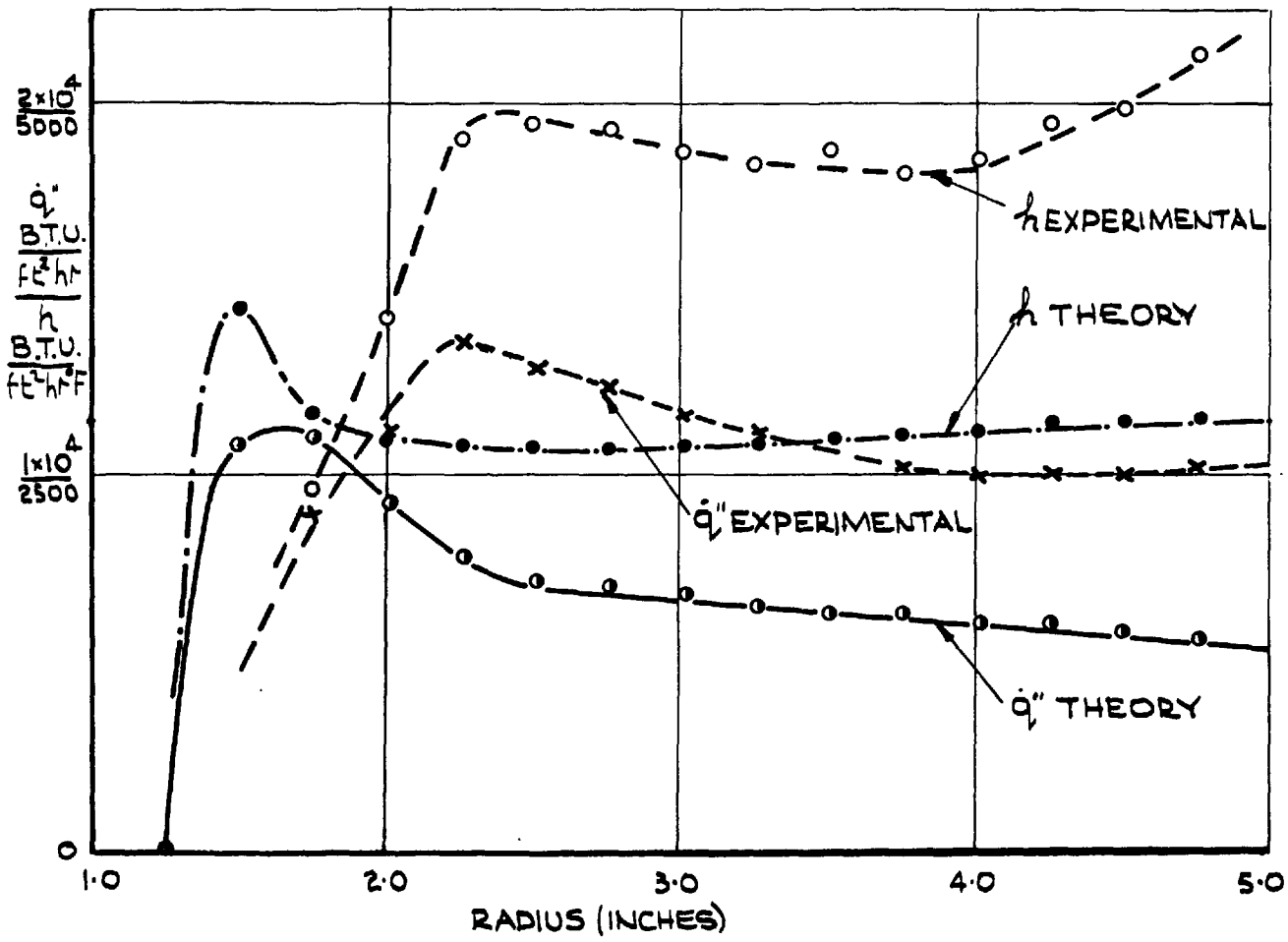

FIG.26 COMPARISON OF EXPERIMENTAL RESULTS WITH THEORY TEST 33

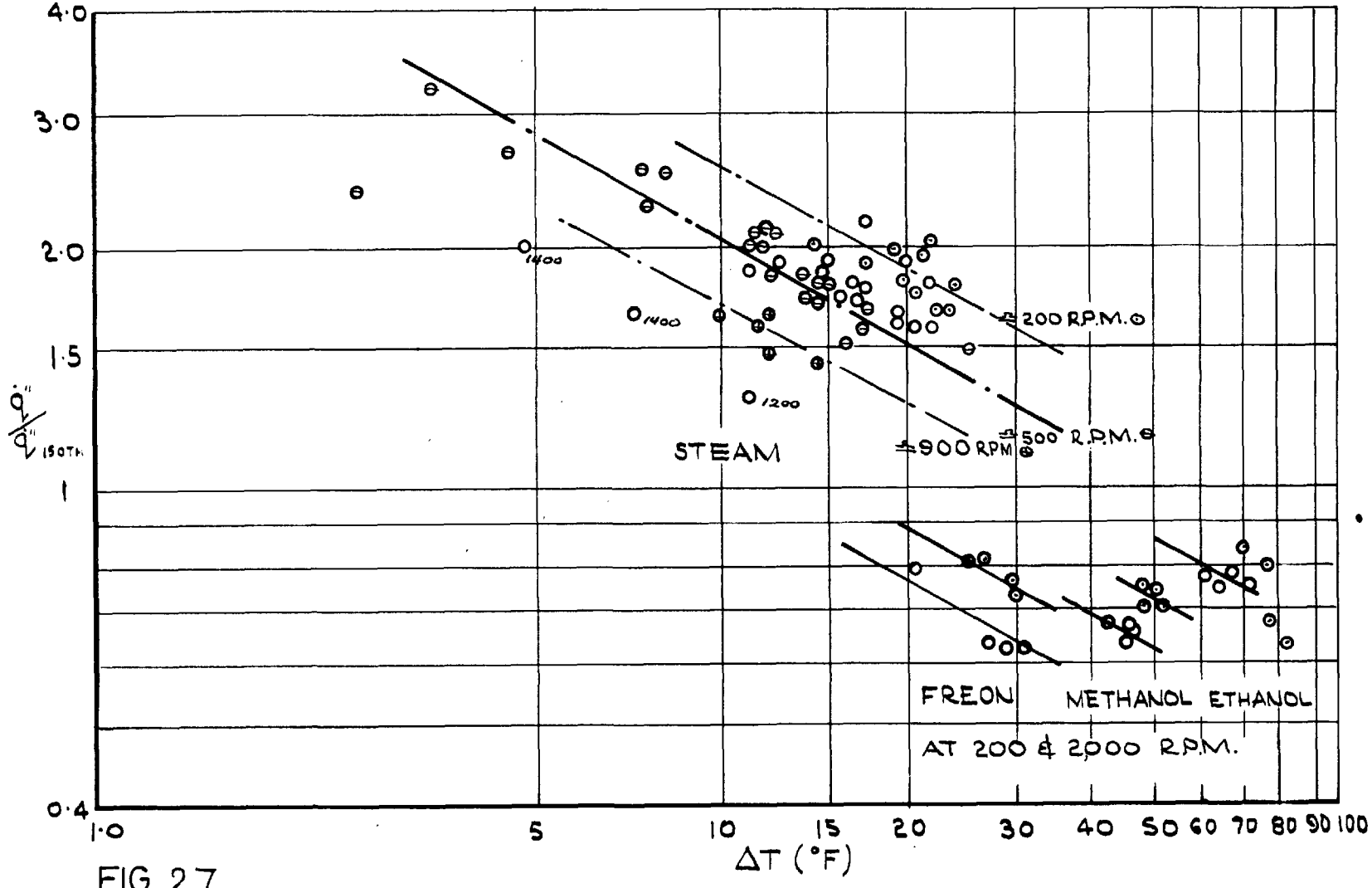

FIG. 27

COMPARISON OF RESULTS FOR STEAM WITH PUBLISHED DATA

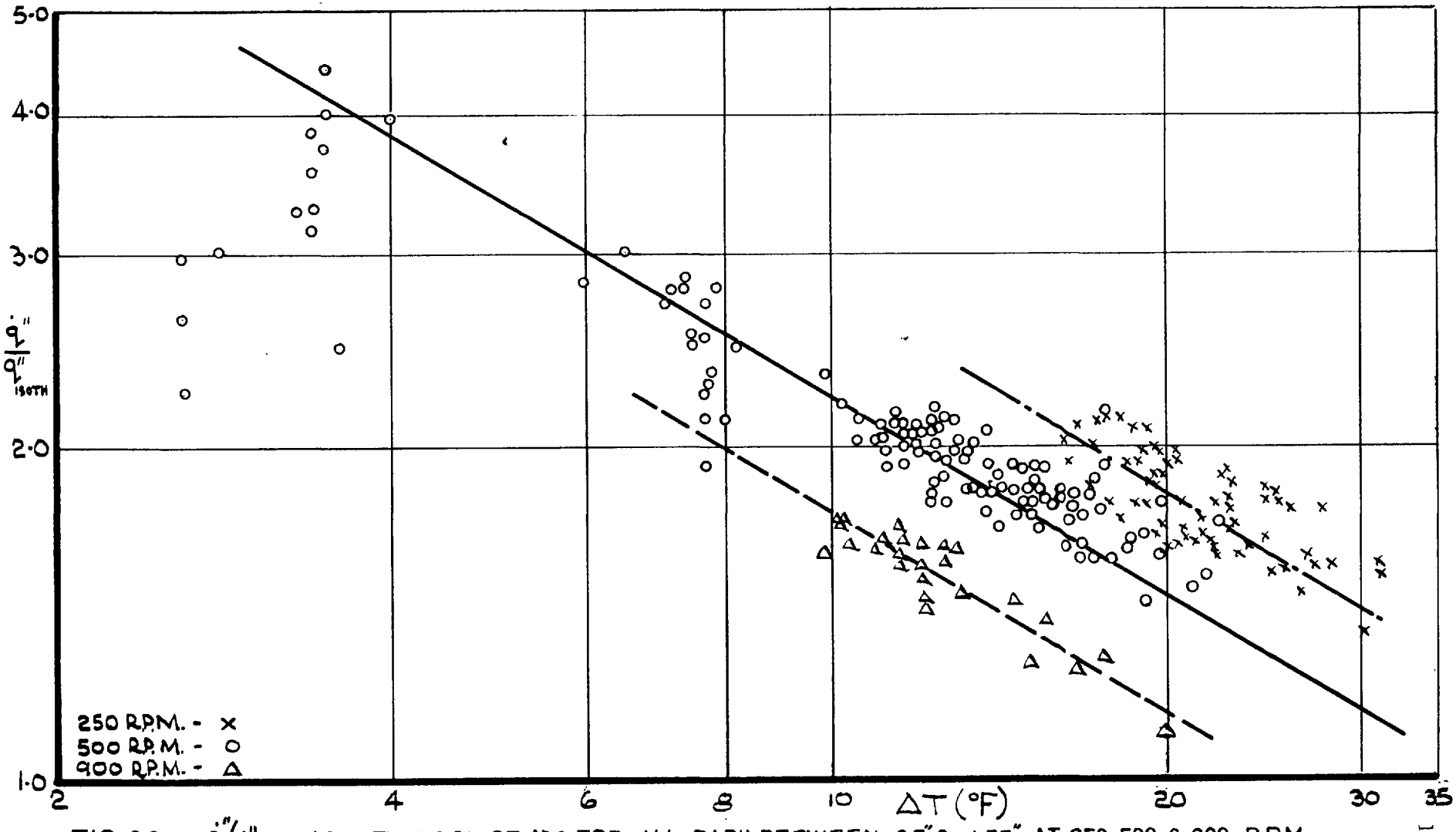

FIG. 28 q''/q''_{ISOTH} AS A FUNCTION OF ΔT FOR ALL RADII BETWEEN 2·5" & 4·75" AT 250, 500, & 900, R.P.M.

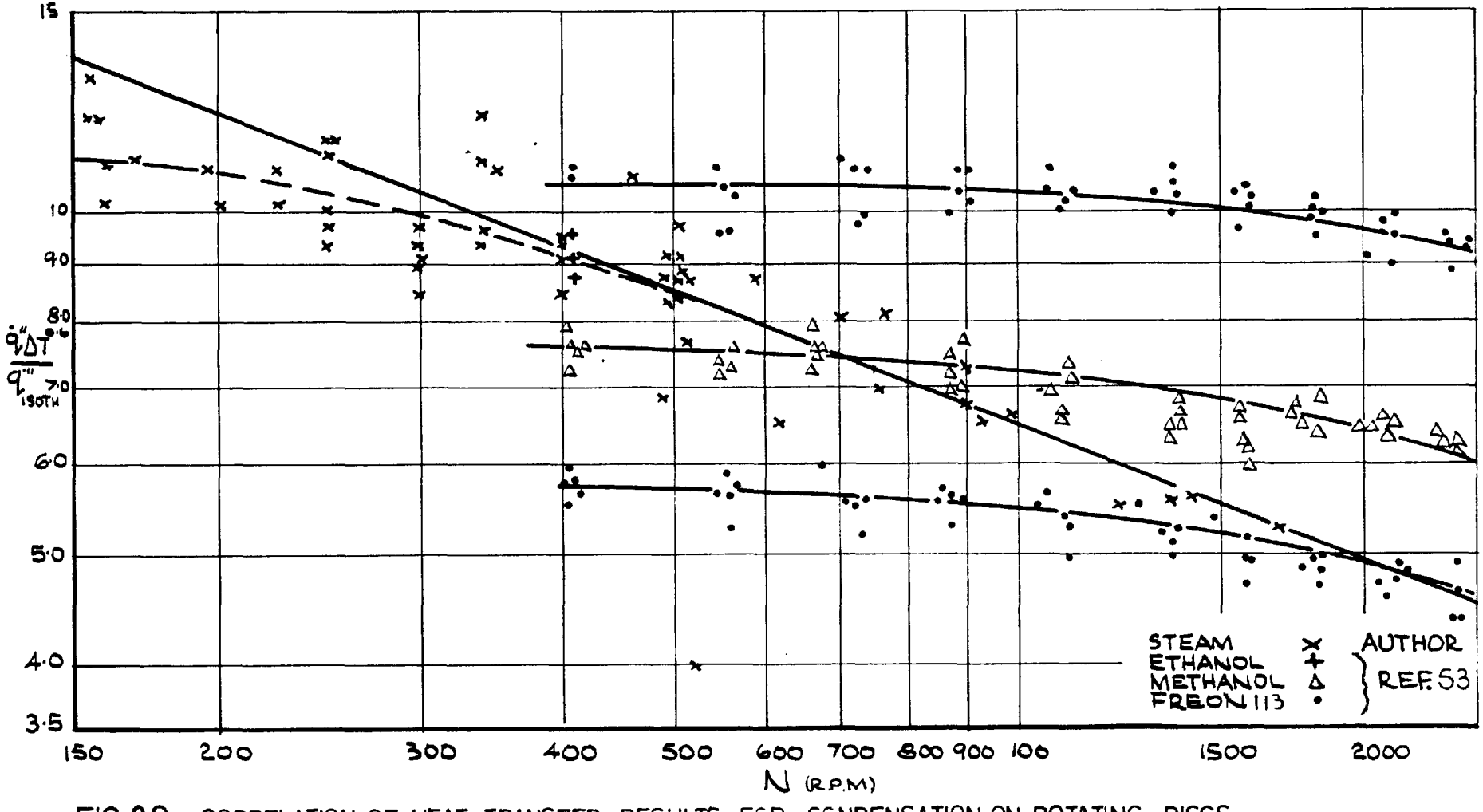

FIG. 29 CORRELATION OF HEAT TRANSFER RESULTS FOR CONDENSATION ON ROTATING DISCS & COMPARISON WITH PUBLISHED DATA

BIBLIOGRAPHY

1. Thermal Stresses in Elastic Axially Symmetrical Bodies. Baines and Hoyle. J. Mech. Eng. Science, Vol. 4, No. 2, June, 1962.

1a. The Role of the Laboratory in the Development of Steam Turbines. Owens and Meyer. Engineering Utility Conference, U.S.A., No. 4, 1958.

2. Transient Temperature Stresses in Axially Symmetrical Systems with Special Application to a Solid Rotor of a Steam Turbine. Hoyle. Proc. I. Mech. E., Vol. 169, No. 31, 1955.

3. Ph.D. Thesis. Matthews. University of London, 1963.

4. Heat Transmission. McAdams. 3rd Edition,

5. Ver Deut. Ing. Nusselt. Vol. 60, pp. 541-569, 1916.

6. Studies in Heat Transmission particularly as applied to Tubular Gas Condensers. Colburn and Hougen. Bulletin 70. Eng. Experiment Station, University of Wisconsin, 1930.
Ind. Eng. Chem. Vol. 26, pp. 1178-1182, 1934.

7. Heat Transfer Coefficients in Surface Condensers. Silver. Engineering Vol. 161, p. 505, 1946.

8. Investigation of Heat Transfer during condensation of vapour on vertical tubes. Zozulya. Teplaperedacha i. teplovoe mo. delirovanie Izelat. AN. USSR. M., pp. 287-297, 1959.

9. Effect of Heat Capacity of Condensate in Condensating. Bromley. Ind. Eng. Chem. Vol. 44, p. 2966, 1952.

10. Heat Transfer and Temperature Distribution in Laminar Film Condensation. Rosenhow. Trans. A.S.M.E., Vol. 78, pp. 1645-1648, paper 54-A-144, 1956.

11. Problems in Design and Research on Condensers of Vapours and Vapour Mixtures. Colburn. Inst. Mech. Engrs and A.S.M.E., Gen. Dis. Heat Transfer, 1951.

11a. Heat Transfer in Condensation and Boiling. Katateladze.

12. A boundary-layer treatment of laminar film condensation. Sparrow and Gregg. A.S.M.E. Paper No. 58. - S.A. - 2.

13. The two phase B.L. in Laminar Film Condensation. Koh, Sparrow and Hartnett. Int. Jour. Heat Mass Transfer, Vol. 2, pp. 69-82, 1961.

14. An Analytical Study of Laminar Film Condensation. Chen. Trans. A.S.M.E. J. Heat Transfer, February, 1961.

15. An Integral Treatment of Two-Phase Boundary-Layer in Film Condensation. Koh. Trans. A.S.M.E. J. of Heat Transfer, Vol. 83, No. 3, Series C., pp. 359-362, August, 1961.

16. Heat Transfer by Condensing Vapour on Vertical Tubes. Kirkbride. Trans. Amer. Inst. Chem. Eng., Vol. 30, p. 170, 1933.
Ind. Eng. Chem., Vol. 26, pp. 425-428, 1934.

17. The calculation of condensation where a portion of the condensate layer is in turbulent motion. Colburn. Ind. Eng. Chem., Vol. 30, pp. 187-193, 1933.
Vol. 26, p. 432, April, 1934.

18. Warmeubergang Bei Der Kondensation mit Turbulenten Wasserhaut. (Heat Transfer by Condensation with Turbulent Flow). Grigull. Forsch. Gebiete Ingenieur. Band 13, No. 2, pp. 49-57, 1942.
Vol. 10, p. 18, 1952.

19. The effect of vapour velocity on condensation inside tubes. Carpenter and Colburn. Gen. Dis. Heat Transfer, 1951.

20. Condensation of Benzure in the Presence of Air. Smith and Robson. A.S.M.E. and I. Mech. Eng., Gen. Disc. on Heat Transfer, September, 1951.

21. Influence of Small Concentrations of Air in Steam on the Steam Film Coefficient of Heat Transfer. Meisenburg, Boarts and Badger. Trans. Am. Inst. Chem. Engrs., Vol. 31, pp. 622-637 (1935) and Vol. 32, pp. 100-104 (1936).

22. The Condensation of Steam. Othmer. Ind. Eng. Chem., Vol. 21, p. 576, 1929.

23. An Investigation into the Condensation of Steam. Hampson and Ozisek. Proc. I. Mech. Eng. (B), Vol. 1B, No. 7, pp. 293-294, 1952.

24. Heat Transfer. Gebhart. 1961.

25. Drop-wise and Film Condensation of Steam. Shea and Krase. Trans. Amer. Inst. Chem. Engrs, Vol. 36, pp. 463-489, 1940.

26. Sb. tr. Int. teploenerg. Zozulya. AN. USSR. (14), pp. 32-42, 1958.

27. Hopf. Ann. Physik, Vol. 32, p. 777, 1910, in Reference 16.

28. Classen. Centralblat f. d. Zucker Industrice, Vol. 26, p. 497, 1918, in Reference 16.

29. Unpublished Memoranda in Reference 16. Milley and Cooper.

30. Thesis M.I.T. in Reference 16. Warden.

31. Isothermal Flow of Liquid Layers. Cooper, Drew and McAdams. Trans. Amer. Inst. Chem. Engrs., Vol. 30, pp. 159-169, 1934.
Ind. Eng. Chem., Vol. 26, p. 428, 1934.

32. Liquid Films in the Viscous Flow Region. Friedman and Miller. Ind. and Eng. Chem., Vol. 33, p. 885, 1941.

33. Isothermal Flow in Liquid Wetted-Wall Systems. Fallah, Hunter and Nash. J. Soc. Chem. Ind., Vol. 53, p. 369 (T), 1934.

34. Liquid Flow Conditions in Packed Powers. Grimley. Trans. Inst. Chem. Engrs., Vol. 23, pp. 228-235, 1945.

35. Experiments on Falling Liquid Films. Dukler and Bergelin. Chem. Eng. Progress, Vol. 48, p. 557, 1952.

36. Volnovoe techenie toukkli sloev vyazkoi zhidkosti (Wave motion of thin layer of a viscous liquid). Kapitsa. Zhurn eksperimental' noi i teoreticheskoi fuzeki (Journal of Experimental and Theoretical Physics), No. 1, 1948.

37. Experiments on Onset of Wave Formation on Film of Water flowing down Vertical Plane. Binnie. J. Fluid Mechanics, Vol. 2, p. 551, 1957.

38. Wave formation in Laminar Flow down Inclined Plane. Brooke-Benjamin. J. Fluid Mechanics, Vol. 2, pp. 554-574, 1957.

39. The Development of three-dimensional disturbances in an unstable film of liquid flowing down an Inclined Plane. Brooke-Benjamin. J. Fluid Mechanics, Vol. 10, Part 3, pp. 401-419, May, 1961.

40. A study of the mean thickness of the liquid film and the characteristics of the interfacial surface in annular two-phase flow in a vertical tube including a review of the literature. Charvonia. L. C. Card MI.C. 59-4129, Ph.D. Thesis.

41. Atomization of Liquids by means of a Rotating Cup. Hinze and Milborn. Trans. A.S.M.E., J. Appl. Mechanics, Vol. 17, No. 2, 1950.

42. Personal Communication. Ashwood.

43. On the stability of three-dimensional boundary-layers with application to the flow due to a rotating disc. Gregory, Stuart and Walker. Symposium of B.L. effects N.P.L., Paper No. 3. Phil. Trans. A. No. 943, Vol. 248, pp. 155-199, 1955.

44. The Water Conversion Problem. Hickman. Ind. Eng. Chem., Vol. 48, part 7A - 18A, April, 1956.

45. Centrifugal Boiler Compression Still. Hickman. Ind. Eng. Chem., Vol. 49, No. 5, pp. 786-800, May, 1957.

46. Prediction of Performance Characteristics of Hickman-Badger Centrifugal Boiler Compression Still. Bromley. Ind. Eng. Chem., Vol. 50, No. 2, pp. 233-236, February, 1958.

47. Centrifugal Phase-Barrier Recompression Distillation. Hickman, Hogan, Bibling and Buckel. Advances in Chemistry. American Chemical Society No. 27, pp. 128-146, 1960.

48. A study and development of the Hickman Sea-Water Still. United States Department of the Interior, Office of Saline Water Research and Development Progress Report, No. 43, September, 1960.

49. An Analysis of Heat Transfer in the Hickman Rotary Evaporator. Putman, Eibling and Buckel. Conf. on Int. Develop. in Heat Transfer, A.S.M.E., 1961.

50. High Vacuum Short Path Distillation. Hickman. Chemical Reviews, Vol. 34, No. 1, February, 1944.

51. A theory of Rotating Condensation. Sparrow and Gregg. A.S.M.E. Paper No. 58-A-70, January 10th, 1959.

52. The Effect of Vapour Drag on Rotating Condensation. Sparrow and Gregg. A.S.M.E. J. Heat Transfer Series C, February, 1960.

53. Condensation on a Horizontal Rotating Disc. Beatty, Jnr. and Nanda Purkar. A.S.M.E. 3rd National Heat Transfer Conference, August, 1959.

ACKNOWLEDGEMENTS

I would like to thank my Supervisor, Dr. R. D. Hoyle, for the unlimited help and advice which he has so readily given to me, and Professor D. B. Spalding for valuable discussions.

I am most grateful to the Admiralty for providing the financial support which has made this work possible, to the Trustees of the Beit Fellowship and to the United Steel Companies Limited for Maintenance Awards.